**ADDIS ABABA UNIVERSTY**

**SCHOOL OF GRADUATE STUDIES**


# SYNTHESIS AND CHARACTERIZATION OF THIENO[3,4-*b*]PYRAZINE-BASED CONJUGATED POLYMERS

**A GRADUATE THESIS SUBMITTED IN PARTIAL FULFILLMENT OF THE REQUIREMENTS FOR THE DEGREE OF MASTER OF SCIENCE IN CHEMISTRY**

**By**

**MESERET ASRAT**

**ADVISOR: WENDIMAGEGN MAMMO (Professor)**

**December 2014**

**DECLARATION**

I, the undersigned, declare that this MSc. research work is my original work and has not been presented for any degree in any other university and that all sources of material used for this MSc. thesis have been duly acknowledged.

Name: Meseret Asrat

Signature: _____

This MSc. Thesis has been submitted for examination with my approval as a university advisor.

Name: Wendimagegn Mammo (Professor)

Signature: _____

Date and place of submission: Department of Chemistry

Addis Ababa University

December 2014

**ADDIS ABABA UNIVERSTY**

**SCHOOL OF GRADUATE STUDIES**

# SYNTHESIS AND CHARACTERIZATION OF THIENO[3,4-*b*]PYRAZINE-BASED CONJUGATED POLYMERS

Submitted by Signature

Meseret Asrat _____

Approved by the Examining Board: Signature

Prof. Wendimagegn Mammo _____
Advisor

Prof. Ermias Dagne _____
Examiner

Dr.Ashebir Fiseha _____
Examiner

**Acknowledgments**

I would like to express my deepest gratitude to my research adviser, Professor. Wendimagegn Mammo, for all his unreserved guidance, technical and moral support, and encouragement during the entire research work and preparation of the paper.

I would like to extend my deepest gratitude to Yadessa Melaku for running NMR spectra of most compounds and Zewdneh Genene for running the NMR spectra of all polymers, encouragements and for always making my work in the laboratory fruitful. My special appreciation goes to my colleagues Dr. Zelalem Abdissa, Kumasser Kusse and Teshome Gonfa for sharing fruitful ideas, experience and encouragement. I express my indebtedness to W/o Weynshet Gebeyehu and Dr. Yonas Chebude for running FT-IR spectra of all the compounds. My gratitude goes to Yisak Tsegazeab for running UV-Vis spectra of all compounds and Hagos Tukue for spin coating all polymers on glass slides. I would also like to thank Ato Sahlemichael Deme, W/o Mihret Gebremeskel and Ato Wodaje Emiru for technical support. I would like to thank my family for encouragement and ongoing support.

Finally, I would like to acknowledge the Department of Chemistry, AAU, for giving me the opportunity to work on this MSc research and Haramaya University for financial support.

**List of Appendices**

**List of tables**

**List of schemes**

**List of figures**

**List of abbreviations**

DHAP: Direct heteroarylation polymerization
$E_g$: Bandgap
HOMO: Highest occupied molecular orbital
LUMO: Lowest unoccupied molecular orbital
DMF: *N*,*N*-Dimethylformamide
DMSO: Dimethyl sulfoxide
NBS: *N*-Bromosuccinimide
HAc: Acetic acid
PLED: Polymer light emitting diodes
PFETs: Polymer field effect transistors
PPVCs: Polymer photovoltaic cells
PSCs: Polymer solar cells
*Voc*: Open circuit voltage
*Jsc*: Short-circuit current
*FF*: Fill factor
*ca*. Approximately
NMR: Nuclear Magnetic Resonance
EDTA: Ethylenediaminetetra acetic acid disodium salt
DMAc: *N*,*N*-dimethylacetamide
br.m: Broad multiplet
br.s: Broad singlet
$^oC$: Degree Celsius
hr: Hour(s)
min: Minutes
%: Percentage
J: Coupling constants
d: Doublet
m: Multiplet
dd: Doublet of doublets
t: Triplet
q: Quartet
ppm: Parts per million
ICT: Intermolecular charge transfer
SWV: Square-wave voltammetry

# SYNTHESIS AND CHARACTERIZATION OF THIENO[3,4-*b*]PYRAZINE-BASED CONJUGATED POLYMERS

**By**

**Meseret Asrat**

**Advisor: Wendimagegn Mammo (Professor)**

**Addis Ababa University, Department of Chemistry**

## Abstract

Seven novel thieno[3,4-*b*]pyrazine-based donor-acceptor polymers, namely, poly[2,3-bis(3-(dodecyloxy)phenyl)thieno[3,4-*b*]pyrazine-5,7-diyl-*alt*-thiophene-2,5-diyl](**52**, **52'**), poly[2,3-bis(3-(decyloxy)phenyl)thieno[3,4-*b*]pyrazine-5,7-diyl-*alt*-thiophene-2,5-diyl] (**53**), poly[2,3-bis-(2,3-bis(3-(octyloxy)phenyl)thieno[3,4-*b*]pyrazine-5,7-diyl-*alt*-thiophene-2,5-diyl] (**54**, **54'**) and poly[2,3-bis(3-(hexyloxy)phenyl)thieno[3,4-*b*]pyrazine-5,7-diyl-*alt*-thiophene-2,5-diyl] (**55**, **55'**) were synthesized and characterized. The polymers were prepared by employing the Stille cross coupling polymerization and the direct heteroarylation polymerization techniques. For the Stille cross coupling polymerization reactions, the monomers used were dibromo derivatives of substituted thieno[3,4-*b*]pyrazines and 2,5-bis(tributylstannyl)thiophene. On the other hand, the monomers used for the direct heteroarylation polymerization reactions were non-brominated thieno[3,4-*b*]pyrazine derivatives and 2,5-dibromothiophene. Monomers and intermediate compounds were characterized by using NMR ($^{1}$H and $^{13}$C), UV-Vis-NIR and IR spectroscopy. The structural, electrochemical and optical properties of the polymers were investigated by using $^{1}$HNMR, UV-Vis-NIR spectroscopy and square-wave voltammetry (SWV).

## 1. Introduction

The use of coal, oil and other combustible raw materials as the main energy sources of today have harmful effects on our planet and their supplies are limited. Therefore, different kinds of renewable energy sources, such as solar energy, must be considered.[1] Solar energy can potentially provide a clean, sustainable alternative to fossil fuels to meet the global growing needs for energy. Solar cells based on the photovoltaic effect are an effective method to convert solar energy into electricity.[2] Conventional solar cells made of inorganic semiconductors (mono- and polycrystalline silicon) require costly and energy-consuming processing.[1]

In order to develop low-cost technologies, organic materials are appropriate alternatives. In particular, semiconducting polymers combine the favorable optoelectronic properties, such as high absorption coefficients, of organic materials with the excellent processing and mechanical properties of plastic materials.[1] Conjugated polymers and their use in polymer photovoltaic offer a great technological potential as renewable energy sources for electrical energy and they are currently one of the most promising approaches for the next generation thin-film photovoltaic devices.[3] With increasing energy demand, polymer-based solar cells are a promising sustainable solar energy converter for their unique advantages, such as low cost, light weight, and potential use inflexible devices.[4,5]

Conjugated polymers are materials which contain alternative double and single bonds along their main chain and are characterized by the presence of delocalized $\pi$ electrons system. Some examples of $\pi$-conjugated polymers include:- poly(*p*-phenylene)[6], poly(*p*-phenylenevinylene)[7], polyaniline[8], polypyrrole[9], polythiophene[10] and polyfluorene[11] (Figure 1).

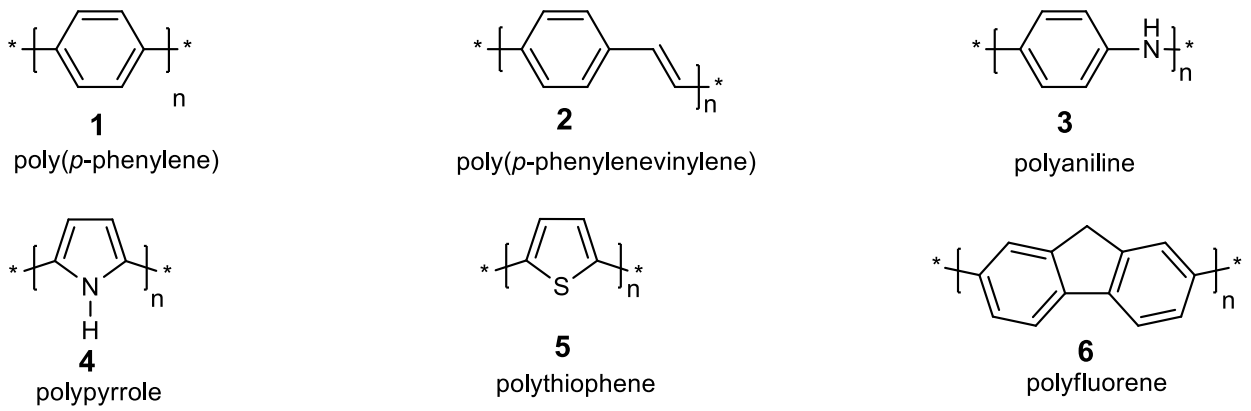


Figure 1: Some conjugated polymers

Conjugated polymers have attracted considerable attention due to their versatile applications in the fields of conducting polymers and conjugated polymer optoelectronic devices. As optoelectronic materials, conjugated polymers are broadly used in polymer light-emitting diodes (PLEDs), polymer field effect transistors (PFETs), sensors, photodetectors, polymer photovoltaic cells (PPVCs) or polymer solar cells (PSCs), etc. In order to get efficient electronic devices, it is necessary to tune their properties, such as bandgap, molecular energy level, solubility, luminescence, absorbance and so on.[12]

The history of conjugated polymers started in the late of 1970s with the discovery of metallic electrical conductivity in oxidatively doped polyacetylene.[13] Even in the late 1970s, researchers understood the potential for having the special combination of optical properties of metals and semiconductors and the processing advantages and mechanical properties of polymers. Polyacetylene (Figure 2), although conceptually simple, is a very complex polymer. It is not soluble, it cannot be processed in any way, and it is in fact unstable. After the discovery of polyacetylene, new classes of conducting polymers based on aromatic precursors such as pyrrole, benzene, aniline, and thiophene have been developed.[13] This discovery led to the 2000 Nobel Prize in chemistry awarded to Alan Heeger, Alan MacDiarmid, and Hideki Shirakawa.[14,15]

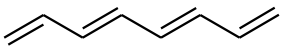

Figure 2: Polyacetylene

The bandgap $E_g$ of a polymer is defined as the energy difference between the highest occupied molecular orbital (HOMO) and the lowest unoccupied molecular orbital (LUMO), and is typically reported in electronvolt (eV). The bandgap can be measured in different ways; the two most important ones are the optical bandgap estimated from UV-vis spectroscopy and the electronic bandgap determined from cyclic voltammetry (CV). The low bandgap polymers are in general defined as polymers with a bandgap below 2eV, i.e., the polymer absorbs light with wavelengths ($\lambda$) longer than 620 nm.[16] Low bandgap polymers have received more attention the in the past few years, since it is believed that they can improve the efficiency of the photovoltaic devices, due to a better overlap between the absorption spectra of the polymer and the solar spectrum.[17,18]

There are several factors that influence the bandgap of a conjugated polymer material. Among these are: (1) intra-chain charge transfer, (2) bond-length alternation, (3) aromaticity, (4) substituents effects, (5) intermolecular interactions and (6) $\pi$-conjugation length.

The most widely used strategy to synthesize a low bandgap polymers involves incorporation of electron-rich (donor) and electron-deficient (acceptor) unit in an alternating fashion in the same polymer backbone.[19] Examples of electron-rich units are thiophene, carbazole, dithienosilole, and dibenzosilole, while electron-deficient units are thieno[3,4-*b*]pyrazine, 2,1,3-benzothiadiazole, and quinoxaline.[45] The substituents on the donor (D) and acceptor (A) units can affect the bandgap. The bandgap of the D-A copolymer is determined by the HOMO of the donor and LUMO of the acceptor. The high energy level for the HOMO of the donor and the low energy level for the LUMO of the acceptor results in a lower bandgap due to an intra-chain charge transfer from donor to acceptor. Planarity along the aromatic backbone results in a low bandgap, due to a high degree of delocalization of the $\pi$ electrons. The alternation between single and double bonds along the polymer chain has a tendency to increase the bandgap. A reduction of the difference in bond length alternation is achieved by the alternation of donor and acceptor units along the conjugated polymer chain thus lowering the bandgap. The alternation between donor and acceptor results in two resonance forms: D–A and $D^+=A^-$.

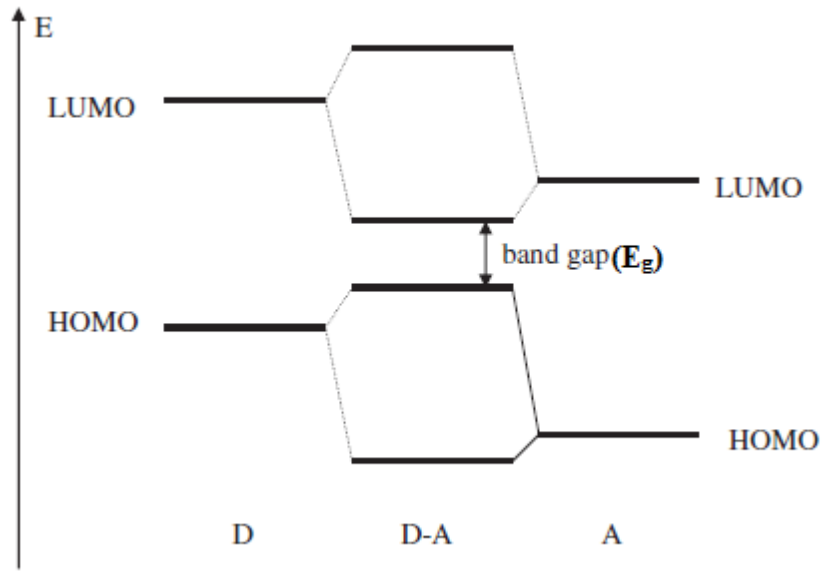


Figure 3: Alternating donor–acceptor units lower the effective bandgap by orbital mixing.

When the HOMO level of the donor and the LUMO level of the acceptor are close in energy, it results in a low bandgap as shown in Figure 3. Therefore, to achieve a lower bandgap the strength of the donor and the acceptor must be increased. This is efficiently achieved by using electron withdrawing groups (EWG) on the acceptor and electron donating groups (EDG) on the donor. EWG such as CN, $NO_2$ on quinoxalines, pyrazines or thiadiazole lower the energy levels (and thereby LUMO) of the acceptor. EDGs such as alkoxy groups on thiophene or pyrrole raise the energy levels (and thereby HOMO) of the donor.[16,20] Besides this, the intermolecular interactions affect the bandgap. The bandgap for certain polymers is lowered in the solid phase due to ordering compared to the observed disorder in solution.

In the development of new materials for polymer solar cells applications, it is central to understand the relationship between molecular structure and device performance. Three properties, i.e., open circuit voltage (*Voc*), short-circuit current (*Jsc*), and fill factor (*FF*), are of great importance in achieving high power conversion efficiency (PCE) of polymer solar cells (PSCs) and evaluating the device performance. The *Voc* is limited by the difference between the electron affinity (the LUMO) of the electron acceptor, and the ionization potential (the HOMO) of the polymer donor. Therefore, the HOMO level is a very important factor to be considered when designing new conjugated polymers. In donor-acceptor (D–A) structured polymers, alkyl

or alkoxy groups are introduced to the conjugated main chain to increase the solubilities of conjugated polymers. But, the electron affinities of the side groups can affect the HOMO and LUMO levels. Therefore, side groups of conjugated polymers play an important role not only in imparting solubility but also in influencing the optical and electrical properties of polymers. For example, the alkoxy group is rarely used as side chain on the acceptor units to increase the solubility as the alkoxy group elevates the HOMO level and therefore decreases the *Voc*. Therefore, attaching an electron-donating or an electron-withdrawing group to the main chain has been largely considered in order to optimize the HOMO/LUMO levels of the conjugated polymers and the *Voc* of the corresponding PSCs.[21]

A donor-acceptor structure reduces optical bandgap, enables absorption down to the near infrared, and may raise power conversion efficiency (PCE) in solar cells through increased photocurrent.[22]

### 1.1. Polymerization methods

Most low bandgap polymers were synthesized by using a variety of transition-metal-catalyzed cross-coupling reactions including Suzuki,[23,24,25] Stille[33,26,27] and Negishi[19] reactions. Compared with these polymerization methods, the ferric(III) chloride ($FeCl_3$) oxidative polymerization is easy and cheap with mild reaction conditions, thereby making it suitable for large scale production of polymers.[28] Recently, the direct heteroarylation polymerization technique has attracted much attention as means of polymer synthesis.

#### 1.1.1. Stille cross-coupling reaction

The Stille cross-coupling reaction also known as Migita−Kosugi−Stille coupling is a coupling reaction between stannanes and aryl halides to form new carbon-carbon bonds. It has become a versatile synthetic methodology and has been widely applied to the syntheses of numerous organic compounds. Despite its great versatility, the Stille reaction involves drawbacks such as the formation of a stoichiometric amount of toxic by-products and in some cases, some instability of the organometallic reagents**.**[29]

The general mechanism of the Stille reaction shown in Figure 4 consists of an oxidative addition step, a transmetallation step, and reductive elimination step, which yields the product and

regenerates the catalyst.[27] Other polymerization methods based on transition metals (e.g. Suzuki cross coupling) used to prepare low bandgap polymers also follow this reaction cycle.

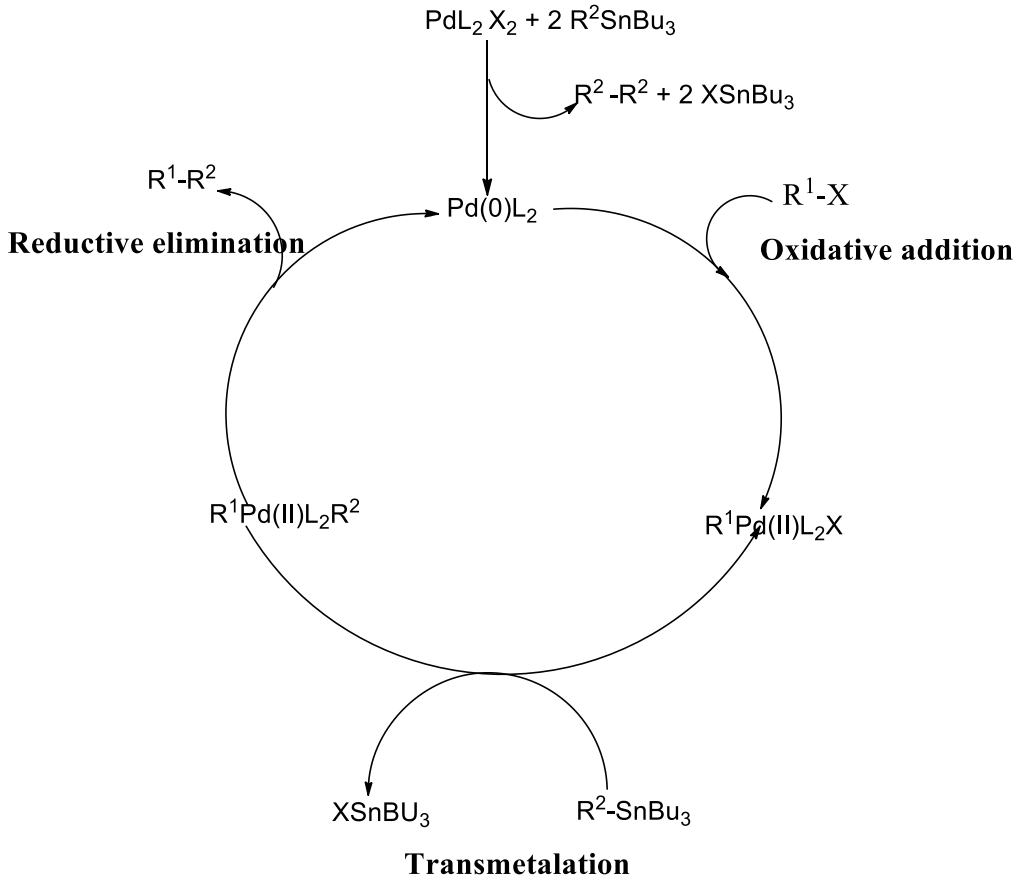


Figure 4: Mechanism of the Stille cross-coupling reaction and the catalytic cycle

### 1.1.2. Suzuki cross-coupling reactions

The Pd-catalyzed Suzuki–Miyaura coupling reaction is a very useful carbon–carbon bond-forming reaction which involves the coupling of organic electrophiles such as aryl or alkenyl halides and triflates, with organoboron compounds in the presence of a base as shown in Scheme 1. Amongst its various applications, the Suzuki reaction is particularly useful as a method for the construction of conjugated dienes and higher polyene systems. Furthermore, tremendous progress has been made in the development of Suzuki coupling reactions of unactivated alkyl halides, enabling $C(sp^2)$–$C(sp^3)$ and even $C(sp^3)$–$C(sp^3)$ bond-forming processes. In addition, the handling and removal of boron-containing by-products is easy when compared to other

organometallic reagents, such as organo-tin compounds in the Stille reaction, especially in a large-scale synthesis.[30]

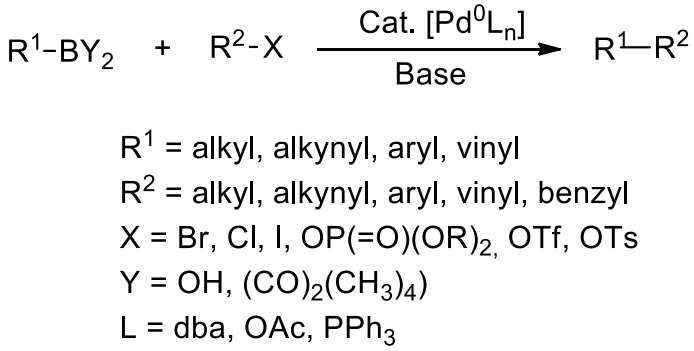


Scheme 1: The Suzuki coupling reaction

### 1.1.3. Negishi coupling

The use of organozinc reagents as the nucleophilic component in palladium-catalyzed cross-coupling reactions is known as the Negishi coupling. Organozinc reagents exhibit a very high intrinsic reactivity in palladium-catalyzed cross-coupling reactions, which combined with the availability of a number of procedures for their preparation and their relatively low toxicity, makes the Negishi coupling very useful alternative to other cross-coupling techniques, as well as constituting an important method for carbon–carbon bond formation as shown in Scheme 2.[30]

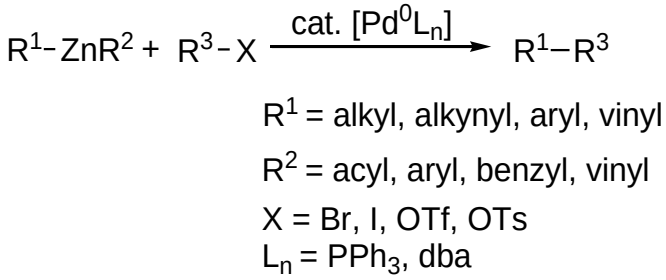


Scheme 2: The Negishi coupling reaction.

### 1.1.4. Direct heteroarylation polymerization (DHAP)

The direct heteroarylation polymerization reaction is a catalytic dehydrohalogenative cross-coupling reaction of non-preactivated arenes or heteroarenes with aryl halides. This technique should be advantageous for the synthesis of π-conjugated polymers with respect to decreasing the number of reaction steps and reducing undesired waste from the organometallic reagents.[31] Despite a lot of attractive merits, direct heteroarylation polymerization has also drawbacks. This synthetic method is difficult to completely avoid a side reaction at unexpected C–H bonds, which leads to formation of branched or cross-linked structures because all aromatic C–H bonds in a monomer have potential for direct arylation reactions. Since the number of expected C–H bonds for direct arylation decreases with increasing degree of polymerization, a reaction for too long time causes overreaction at unexpected C–H bonds. Therefore, appropriate reaction time needs to be determined in direct heteroarylation polymerization to avoid overreactions and to obtain high-molecular-weight polymers.[32]

Abdo *et al.*[33] suggested a reasonable reaction mechanism for the direct heteroarylation of thienopyrazines as shown in Scheme 3. The basic synthesis steps of the reaction involve C–H activation, cyclometallation, oxidative addition and reductive elimination.

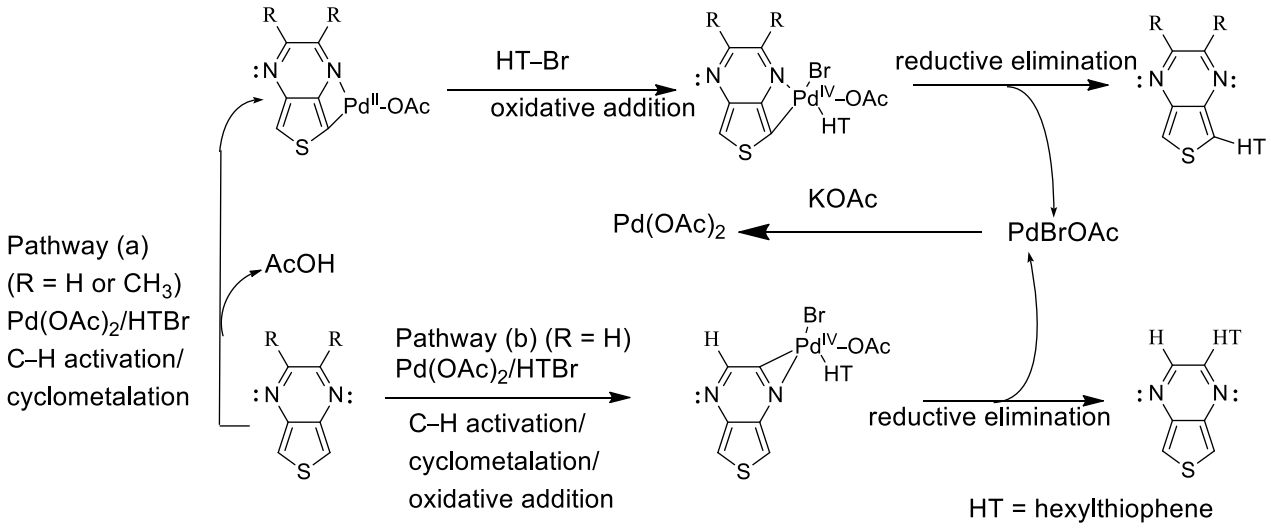


Scheme 3: Mechanistic pathways for the heteroarylation of the thienopyrazine moiety.

## 2. Thieno[3,4-*b*]pyrazines

Thieno[3,4-*b*]pyrazines have been shown to be excellent precursors for the production of low bandgap conjugated polymers.[34,35,36] They are commonly used as acceptors in polymer solar cells. They are advantageous because they allow modification of the pyrazine ring without introducing steric effects directly into the polymer backbone.[22]

### 2.1. Thieno[3,4-*b*]pyrazine-containing monomers

The first report of a thieno[3,4-*b*]pyrazine was the synthesis of 2,3-diphenylthieno[3,4-*b*]pyrazine (**10**) reported by Imoto and co-workers in 1957.[37] In 1981, Binder and co-workers reported a modified synthesis for the dimethyl analogue (**8**).[38] The first attempt at a general route to these compounds was published a year later by Outurquin and Paulmier.[39,40] Their approach applied modifications of the earlier methods to the preparation of thieno[3,4-*b*]pyrazine (**7**) and its 2-substituted and 2,3-disubstituted analogues (where the substituent is methyl or phenyl). In 1992, Pomerantz and co-workers applied the methods of Outurquin and Paulmier to the synthesis of 2,3-dihexylthieno[3,4-*b*]pyrazine (**9**) utilizing tetradecane-7,8-dione prepared by the oxidation of the corresponding alkyne.[41] Subsequently, Kuzmany and co-workers also used these methods to prepare a series of 2,3-disubstituted analogues.[42,43]

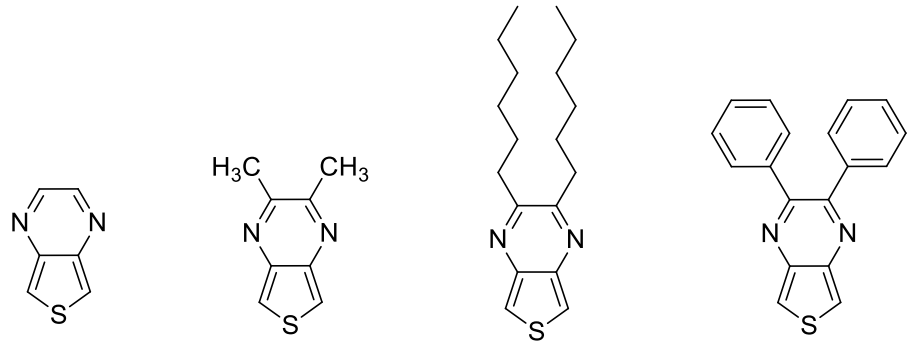


**7** **8** **9** **10**

Thieno[3,4-*b*]pyrazine and its 2,3-disubstituted analogues can be readily synthesized from thiophene as shown in Scheme 4. Thus, compound **12** was readily produced by the nitration of **11** using fuming $HNO_3$ and $H_2SO_4$. Treatment of **12** with Sn and HCl both reduced the $NO_2$ functionalities and removed the Br groups. The resulting 3,4-diaminothiopene (**13**) was

condensed with α-diones (**14**), which were obtained by reaction of organocuprates (derived from Grignard reagents) with oxalyl chloride, to afford thieno[3,4-*b*]pyrazines (**15**). While previous methods utilized short periods of heating (i.e., 50-70 °C for 10-15 min),[40] it was found that by allowing the reaction to run at room temperature for longer periods of time, unwanted polymerization reactions were reduced and the thieno[3,4-*b*]pyrazines were recovered in higher yields.[44]

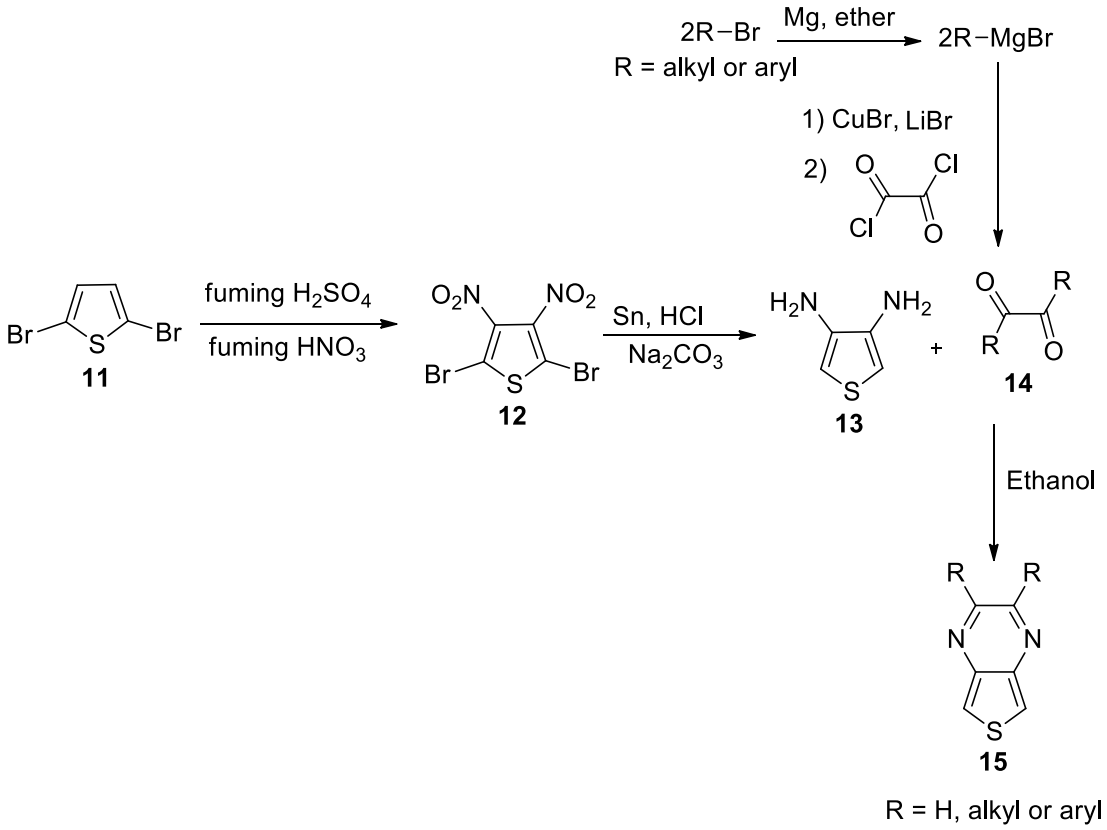


Scheme 4: Synthesis of symmetrically substituted thieno[3,4-*b*]pyrazines.

5,7-Dibromothieno[3,4-*b*]pyrazines (**16**) can be synthesized from thieno[3,4-*b*]pyrazines (**15**) by bromination using NBS in DMF or NBS in $CHCl_3/CH_3COOH$ in the dark under nitrogen (Scheme 5).[12,33]

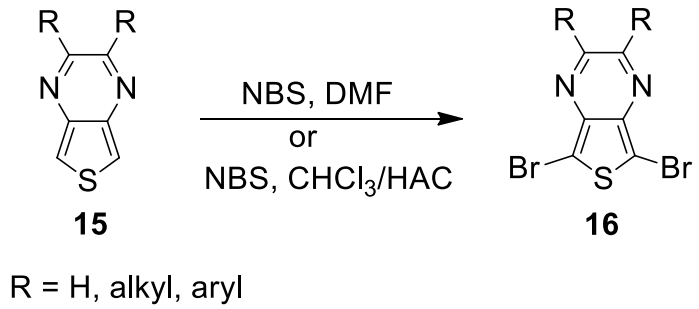


Scheme 5 : Synthesis of 5,7-dibromothieno[3,4-*b*]pyrazines.

### 2.2. Thieno[3,4-*b*]pyrazine-containing polymers

Recently, photovoltaic devices consisting of thieno[3,4-*b*]pyrazine-based low-bandgap polymers as hole-transporting materials have shown improved efficiencies.[33,34,35,36] Thieno[3,4-*b*]pyrazine-based polymers could be synthesized by using transition-metal-catalyzed cross-coupling reactions (e.g., Suzuki and Stille) and direct heteroarylation polymerization. Scheme 6 shows the preparation of **P1**-**P4** via Stille coupling and direct heteroarylation polymerization methods.[33] C–H arylation of 2,3-dimethylthieno[3,4-*b*]pyrazine (**8**) with **17a** or **18a** (1:1 molar ratio) afforded copolymers with identical $^{1}$H NMR spectroscopic data to those of copolymers **P2** and **P4** prepared through the Stille cross-coupling of equimolar ratios of **16b** with 3-hexylthiophene-2,5-diyl)bis(tributylstannane (**17b**) or 3,3'-dihexyl-5,5'-bis(tributylstannyl)-2,2'-bithiophene (**18b**), respectively. However, longer reaction times and/or higher temperatures afforded copolymers that were very sparingly soluble in most common organic solvents. $^{1}$H NMR spectra of the soluble parts of the copolymers **P1** and **P3** obtained through C–H arylation were completely different to those of the copolymers **P1** and **P3** obtained through the Stille-cross-coupling of **16a** with **17b** or **18b**, respectively (Scheme 6). Based on the postulated mechanism of C–H arylation of thienopyrazine (see Scheme 3), it is believed that cross-linking occurred through multiple C–H arylation at positions 2, 5, and 7 of the thienopyrazine moiety.

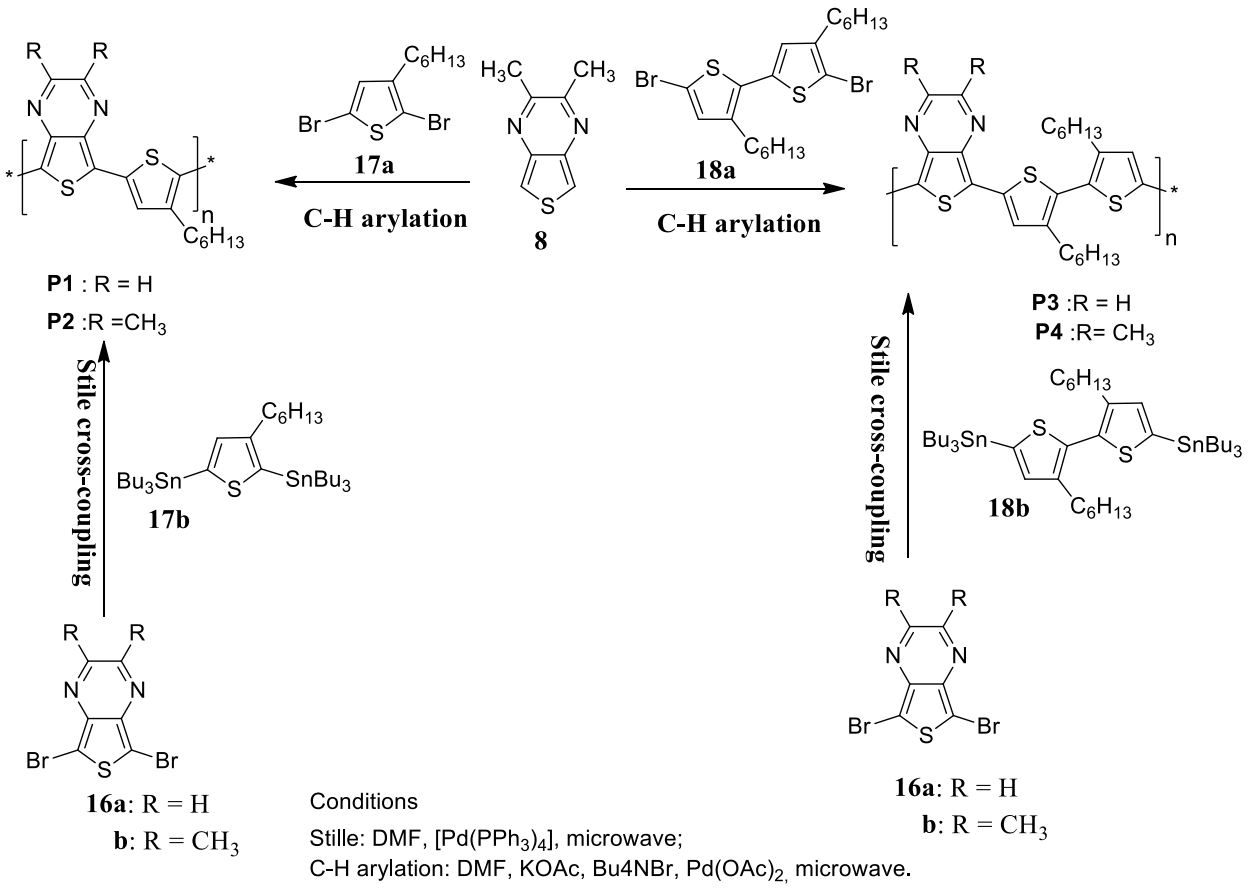


Scheme 6: Synthesis of π-conjugated copolymers **P1**–**P4**.

### 2.3 Thieno[3,4-*b*]pyrazine-containing polymers by using carbazole as a donor

The synthesis of poly(3,6-(*N*-2-ethylhexyl)carbazole-*alt*-2,3-bis(4-fluorophenyl)thieno[3,4-*b*]pyrazine) (**23**, PEC-FTP) is outlined in Scheme 7. Thus, treatment of 3,4-diaminothiophene dihydrochloride (**19**) with 4,4'-difluorobenzil in the presence of triethylamine afforded 2,3-bis(4-fluorophenyl)thieno[3,4-*b*]pyrazine (**20**), which was then brominated with NBS to give 5,7-dibromo-2,3-bis(4-fluorophenyl)thieno[3,4-*b*]pyrazine (**21**). Finally, compounds **21** and bis(4,4,5,5-tetramethyl-1,3,2-dioxaborolane)-9-(*N*-2-ethylhexyl)carbazole (**22**) were copolymerized through Suzuki coupling to afford **19** (PEC-FTP).

A solution of **23** in chloroform absorbed light in a spectral range from UV to near 740 nm, with absorption maxima at 339 and 564 nm. The solid film of **23** exhibited absorption maxima at 336 and 600 nm. The absorption maxima at 564 nm (solution) and 600 nm (solid film) originated from the conjugated π-system of **23**. The bathochromic shifts of the UV-visible absorption and

PL emission spectra of the polymer film, as compared to those of its solution sample, are due to closer intermolecular interactions in the solid state.[45]

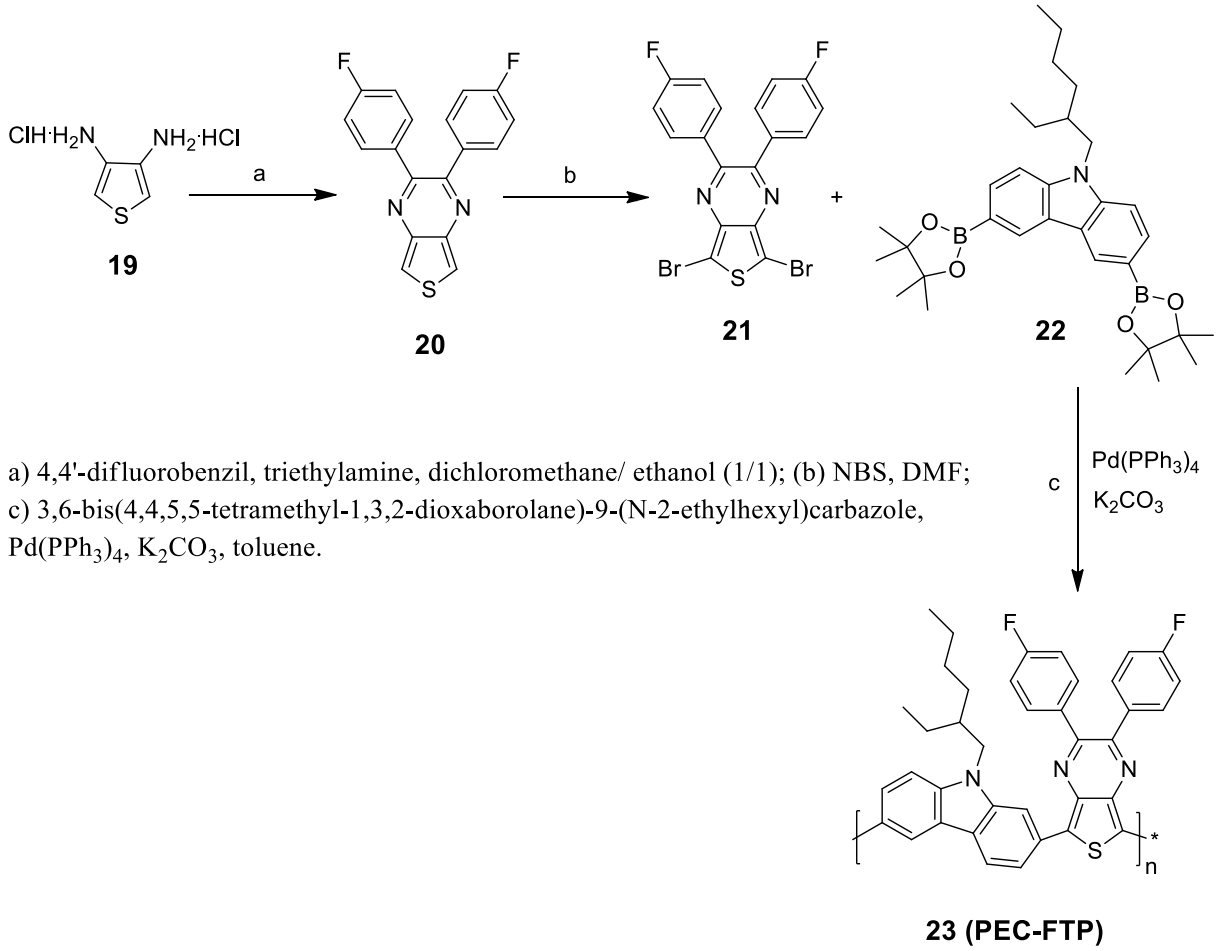


a) 4,4'-difluorobenzil, triethylamine, dichloromethane/ ethanol (1/1); (b) NBS, DMF;
c) 3,6-bis(4,4,5,5-tetramethyl-1,3,2-dioxaborolane)-9-(N-2-ethylhexyl)carbazole, $Pd(PPh_3)_4$, $K_2CO_3$, toluene.

Scheme 7 : Synthetic route to **23** (**PEC-FTP**).

### 2.4. Thieno[3,4-*b*]pyrazine containing polymer by using thiophene as a donor

2,3-Bis(4-fluorophenyl)thieno[3,4-*b*]pyrazine (20) and 3-hexylthiophene (24) units were used as electron-withdrawing and electron donating moieties, respectively, to further decrease the bandgap, as compared to the thienopyrazine-carbazole copolymer (**23**) (Scheme 7) because carbazole units may be more twisted from thieno[3,4-*b*]pyrazine units than from thiophene units, due to two hydrogen atoms of carbazole unit that are at *ortho* positions to the main chain.[46]

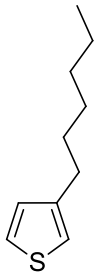

**24**

Scheme 8 shows the synthesis of poly(3-hexylthiophene-*alt*-2,3-bis(4-fluorophenyl)thieno-[3,4-*b*]-pyrazine) (**26**, PHT-FTP). Thus, 5,7-dibromo-2,3-bis(4-fluorophenyl)thieno[3,4-*b*]pyrazine (**21**) and 2,5-bis(4,4,5,5-tetramethyl-1,3,2-dioxaborolane)-3-hexylthiophene (**25**) were copolymerized through Suzuki coupling to afford **26**. The UV-visible absorption of **26** in chloroform showed an absorption range from UV to near 1200 nm with two absorption maxima at 356 and 729 nm. The absorption maxima of the solid film were red-shifted by 36-46 nm compared to the spectrum in solution, due to closer π-π interactions between the polymer chains in the solid state. The optical bandgap of the solid film was estimated to be 1.01 eV, which was much lower than the previously reported values for pyrazine-carbazole copolymer (**23**)[45] (~1.7-1.9 eV).

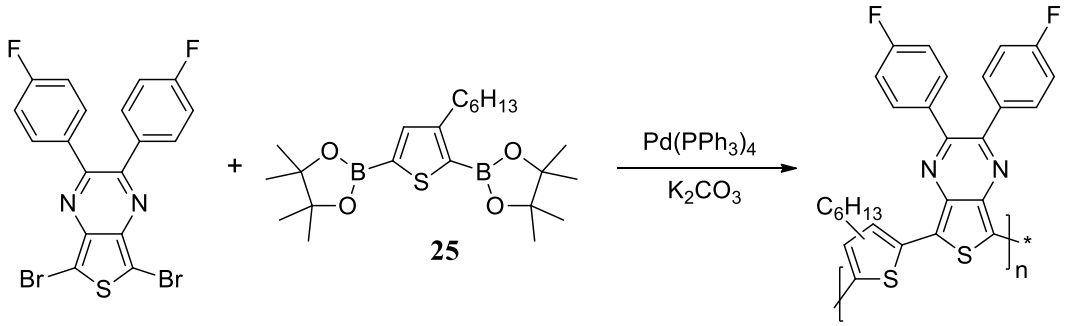


**21** **25** **26 (PHT-FTP)**

Scheme 8: Synthesis of poly(3-hexylthiophene-*alt*-2,3-bis(4-fluorophenyl)thieno-[3,4-*b*]-pyrazine) (**26**, **PHT-FTP**).

## 3. Objective of the work

The objectives of this thesis work is to synthesize seven donor-acceptor conjugated polymers based on substituted thieno[3,4-*b*]pyrazine derivatives using the Stille-cross-coupling polymerization reaction and the direct heteroarylation polymerization reaction. Thiophene will be the electron donating moiety in all polymers while substituted thieno[3,4-*b*]pyrazines will be the electron accepting moieties. All intermediate compounds will be characterized by using spectroscopic techniques such as $^{1}$H-NMR, $^{13}$C-NMR, DEPT-135, FT-IR and UV-Vis and the polymers will be characterized by using $^{1}$H-NMR, UV-Vis spectroscopy and square-wave voltammetry (SWV).

## 4. Results and Discussion

This paper describes the synthesis, optical and electrochemical properties of seven donor-acceptor copolymers based on thiophene and thieno[3,4-*b*]pyrazine. Two different methods, i.e., the direct heteroarylation polymerization and the Stille-cross-coupling polymerization methods were used to synthesize the polymers. In the following sections, the syntheses of these polymers starting from commercially available compounds will be described.

## 4.1. Syntheses of monomers

Scheme 9 shows the general strategy adopted to prepare 2,3-disubstituted thieno[3,4-*b*]pyrazines (**15** ) and 5,7-dibromothieno[3,4-*b*]pyrazines (**16**).

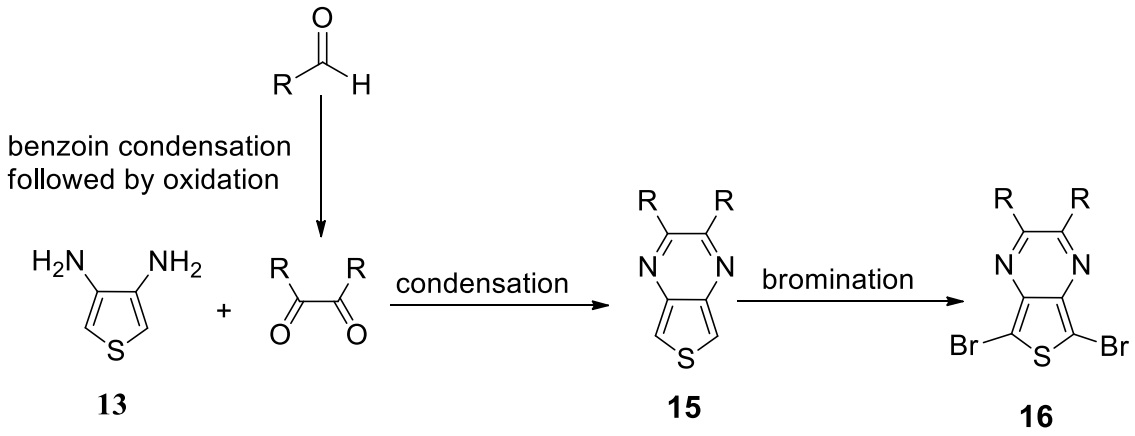


Scheme 9: General strategy towards the syntheses thieno[3,4-*b*]pyrazines and 5,7-dibromothieno[3,4-*b*]pyrazines.

The syntheses of intermediate compounds and monomers are described below.

### 4.1.1. 3,4-Diaminothiophene (13)

The synthesis of 3,4-diaminothiophene (**13**) began by treatment of 2,5-dibromothiophene (**11**) with a mixture of fuming $HNO_3$, fuming $H_2SO_4$ and conc.$H_2SO_4$ to give 2,5-dibromo-3,4-dinitrothiophene (**12**) [47,48] as shown in Scheme 10. Compound **12** was subsequently treated with Sn powder and HCl following a literature procedure[49] to afford 3,4-diaminothiophene (**13**). The reaction reduced the $NO_2$ functionalities and removed the Br groups.

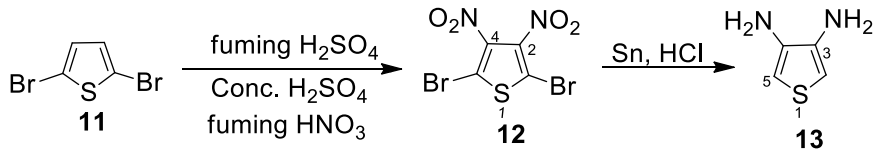


Scheme 10: Synthesis of 3,4-diaminothiophene (**13**)

Compound 12 was obtained as a yellowish solid with a melting point of 137–138.8$^{o}$C; Lit. mp: 135 –137$^{o}$C. The $^{1}$H-NMR spectrum of compound **12** in $CDCl_3$ showed no signals in both the aliphatic and aromatic regions. This indicated the absence of proton-bearing carbon atoms in the compound. The $^{13}$ C-NMR spectrum of **12** revealed the presence of only two carbon signals in the aromatic region. The quaternary carbon signal situated at δ 133.5 is ascribed to the carbons bearing bromine atoms (C-2 and C-5) while the signal at δ140.6 is due to C-3 and C-4 bearing nitro groups. Furthermore the absence of signals in the DEPT-135 spectrum of the compound also indicated that all the carbon atoms in this compound are quaternary. The UV-Vis spectrum of **12** was recorded in $CHCl_3$ and showed two absorption maxima at 244 and 313 nm. The FT-IR spectrum of **12** showed bands at 1546 and 1318 $cm^{-1}$ due to asymmetric stretching of N-O of nitro group in the compound. The band at 901$cm^{-1}$ is due to out-of-plane bending and ring bending and the band at 671$cm^{-1}$ is due to C-Br stretching. The IR data along with the $^{1}$H-NMR and $^{13}$C-NMR data agree very well with structure **12**.

The UV-Vis spectrum of **13** was recorded in $CHCl_3$ and showed two absorption maxima at 256 and 312 nm. The FT-IR spectrum of **13** showed a band at 3365 $cm^{-1}$ due to N-H stretching of amine. The band at 3093 $cm^{-1}$ is due to =C-H stretching of thiophene while the band at 1611 $cm^{-1}$ is due to C=C stretching. The $^{1}$HNMR spectrum of **13** showed a broad singlet at δ 3.40 which integrated for two protons due to the $NH_2$ groups at C-3 and C-4. The signal appearing at δ 6.17 (1H, s) is due to H-2 and H-5. The $^{13}$C-NMR spectrum of **13** showed only two carbon signals in the aromatic region. The signal at δ 101.5 is due to the two symmetrical methine carbons C-2 and C-5 of the thiophene ring. The quaternary carbon signal at δ 137.0 is due to C-3 and C-4. The IR data along with the $^{1}$H-NMR, $^{13}$C-NMR and DEPT spectral data agrees very well with the structure of compound **13**.

### 4.1.2. Synthesis of 1,2-bis(3-(dodecyloxy)phenyl)ethane-1,2-dione (40)

1,2-Bis(3-(dodecyloxy)phenyl)ethane-1,2-dione (**40**) was synthesized starting from 3-hydroxybenzaldehyde (**27**) as shown in Scheme 11. The reaction began by alkylation of **27** with 1-bromododecane (**28**) in the presence of $K_2CO_3$, in *N*,*N*-dimethylformamide (DMF) following a literature procedure[50] to afford 3-(dodecyloxy)benzaldehyde (**32**). Attempt to purify **32** by silica gel column chromatography using pentane as eluent could not remove unreacted 1-bromododecane (**28**) completely. Thus, the mixture was subjected to a benzoin condensation reaction using thiamine hydrochloride as a catalyst in distilled water and 95% ethanol to afford 1,2-bis(3-(dodecyloxy)phenyl)-2-hydroxyethanone (**36**) as a yellowish oily material after purification by silica gel column chromatography. The condensation product **36** was oxidized with DMSO/HBr to afford compound **40** (50.1%) as yellowish solid after recrystallization from ethanol. The above compounds **32**, **36**, and **40** were characterized based on their spectroscopic behaviors as discussed below.

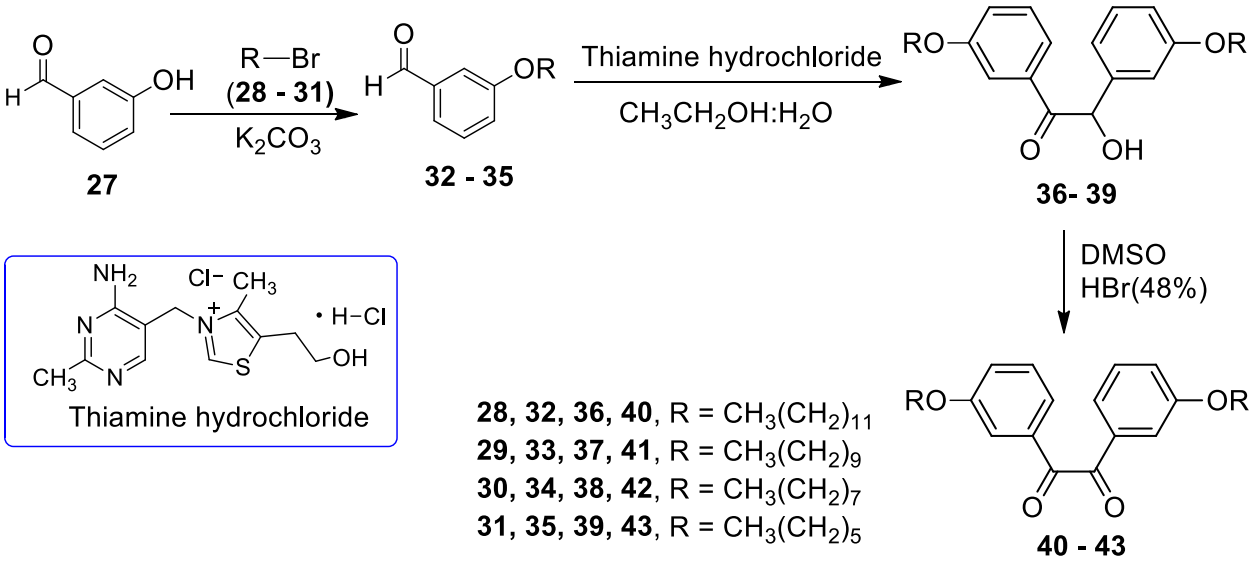


Scheme 11 : The synthesis of diketones **40**-**43**.

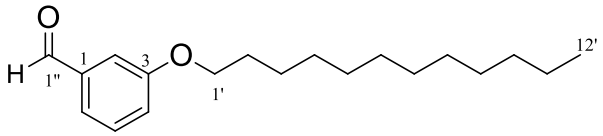


**32**

The UV-Vis spectrum of compound **32** was recorded in $CHCl_3$ and showed two absorption maxima at 254 and 311 nm due to π -π* and n- π* transitions, respectively. The FT-IR spectrum of **32** showed a band at 3018 $cm^{-1}$ due to C-H stretching of the benzene ring. The bands at 2926 and 2855 $cm^{-1}$ are due to stretching vibrations of the $CH_3$ and $CH_2$ groups, respectively. The carbonyl-stretching band appeared at 1699 $cm^{-1}$ and the bands at 1599 and 1455 $cm^{-1}$ are attributed to the C=C stretching vibration of the ring. The asymmetric and symmetric C-O-C stretching bands were observed at 1216 and 1034 $cm^{-1}$, respectively.

The $^{1}$H-NMR spectrum of **32** in $CDCl_3$ (Table 1) showed a one-proton singlet at δ 9.94 which is due to the aldehyde proton. The one-proton singlet at δ 7.37 is due to H-2. The unresolved signals at δ 7.43-7.40 are assigned to H-5 and H-6. The one-proton multiplet at δ 7.16 is ascribed to H-4. The multiplet signal at δ 3.99, which integrated for two protons, is ascribed to H-1'. The signals at δ 1.52 (2H, *m*) and δ 1.79 (2H, quintet) are assigned to H-11' and H-2', respectively. The sixteen-proton broad signal centered at δ 1.26 is due to eight methylene groups and is assigned to H-3' to H-10' and the three-proton triplet at δ 0.88 (H-12') is due to the terminal methyl group.

The $^{13}$C-NMR spectrum of compound **32** showed one carbon resonance in the aldehydic region, six resonances in the aromatic region, and twelve signals in the aliphatic region. The signal at δ 192.1 is assigned to the aldehyde carbonyl carbon (C-1''). The quaternary carbon signals at δ 159.7 and 137.7 are due to C-3 and C-1, respectively. The methine carbon signals at δ 129.9, 123.2, 121.9 and 112.7 are assigned to C-5, C-6, C-4 and C-2, respectively. The resonance of the oxygenated aliphatic carbon C-1' appeared at δ 68.2. The remaining ten methylene carbon resonances were detected in the region between δ 31.9 and 22.7. Furthermore the compound exhibited a carbon resonance at δ 14.1 due to the terminal methyl group (Table 2). The proton, $^{13}$C-NMR, DEPT-135, IR and UV spectra of the compound are in agreement with structure **32**.

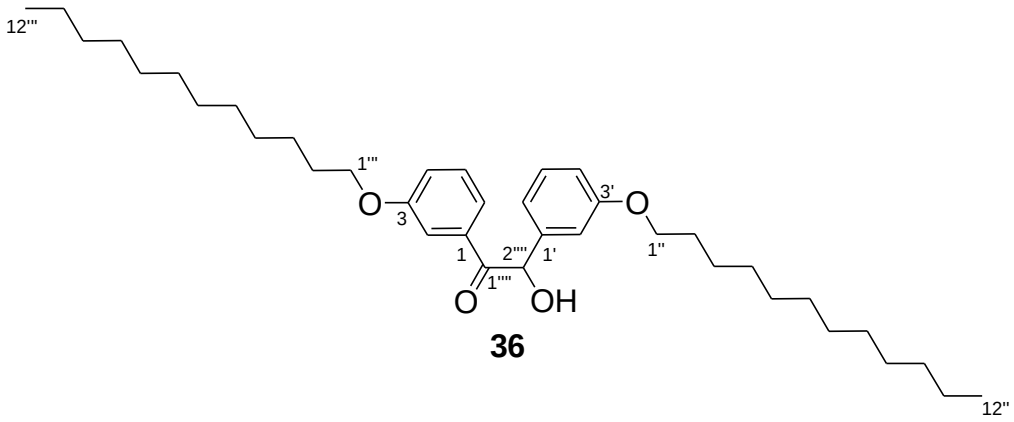


**36**

The benzoin condensation of **32** afforded compound **36** as a yellowish oily solid. The UV-Vis spectrum of compound **36** was recorded in $CHCl_3$ and showed two absorption maxima at 259 and 319 nm which are attributable to the π -π* and n- π* transitions, respectively. The FT-IR spectrum of **36** showed a broad band at 3392 $cm^{-1}$ due to O-H stretching. The band at 2926 $cm^{-1}$ is due to C-H stretching of alkane. The band at 1703 $cm^{-1}$ is due to C=O stretching of ketone functional group. The bands at 683 and 787 $cm^{-1}$are due to out-of-plane ring vibration and ring bending, respectively. The asymmetric and symmetric C-O-C stretching bands appeared at 1264 and 1035 $cm^{-1}$, respectively.

The $^{1}$H-NMR spectrum of compound **36** showed overlapping signals at δ 0.96 which integrated for six protons due to the two terminal methyl groups. The broad and unresolved signal centered at δ 1.35 which integrated for thirty-two protons is due to the sixteen methylene groups in the compound. The four-proton multiplet at δ 1.50 is due to H-3" and H-3"'. The two overlapping quintets at δ 1.82, which integrated for four hydrogens are due to H-2'' and H-2'''. The overlapping signals at δ 3.99 (4H) are due to H-1" and H-1"' and the singlet at δ 5.93 (1H) is due to the methine proton on the carbon atom (C-2"") next to the carbonyl carbon. The signals appearing in the region δ 6.85 to 7.53 are ascribed to the eight aromatic protons in the structure (Table 3).

The $^{13}$C-NMR spectrum of compound **36** revealed a signal at δ 198.7 attributable to the carbonyl carbon of a ketone. The presence of two oxygenated aromatic carbons was revealed by the signals at δ 159.6 and 159.3 which are assigned to C-3' and C-3, respectively. The signals due to the quaternary carbons C-1 and C-1' appeared at δ 140.3 and 134.6, respectively. The aromatic methine carbon signals appeared at δ 130.1, 129.6, 121.5, 121.0, 119.9, 114.7, 113.8 and 113.6

and are due to C-5', C-5, C-6', C-6, C-4, C-2', C-2 and C-4'. The aliphatic region of the spectrum revealed the presence of three oxygenated carbon atoms. The methine carbon signal at δ 76.7 is due to C-2"", while the signals at δ 68.2 and 68.0 are assigned to the methylene carbons C-1" and C-1"'. The signal at δ 14.1 is due to the terminal methyl groups. Furthermore the spectrum exhibited signals in the region between δ 31.9 and 22.6 which represent resonances of twenty carbons (Table 4). The FT-IR, UV, $^{1}H$, $^{13}C$-NMR data are in agreement with the structure **36**.

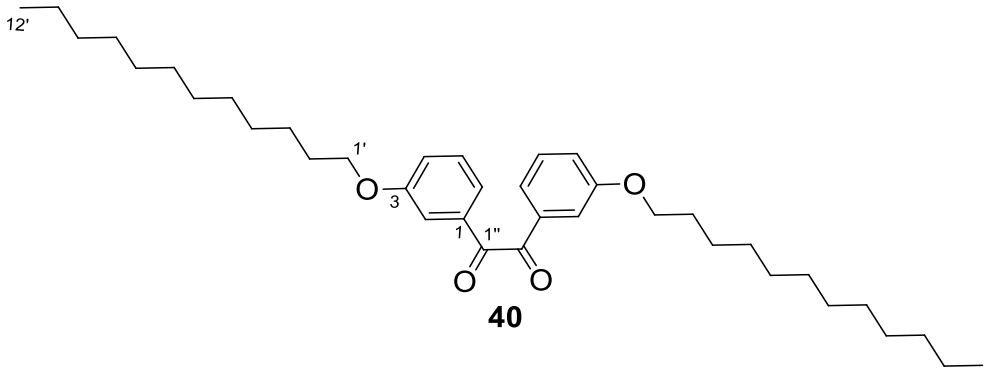


**40**

The oxidation of **36** with DMSO/HBr afforded diketone **40** as a yellow solid with a melting point of 61.3 – 62.0$^{o}$C. The UV-Vis spectrum of compound **40** was recorded in $CHCl_3$ and showed two absorption maxima at 265 and 325 nm due to the presence of conjugation in the compound. The FT-IR spectrum of compound **40** showed a band at 3076 $cm^{-1}$ due to aromatic C-H stretching. The bands at 2924 and 2853 $cm^{-1}$ are due to stretching vibrations of the $CH_3$ and $CH_2$ groups, respectively. The C═O stretching of ketone appeared at 1679 $cm^{-1}$. The bands at 1595 and 1438 $cm^{-1}$ are due to C=C stretching vibration of the aromatic rings. The asymmetric and symmetric C-O-C stretching bands appeared at 1264 and 1028 $cm^{-1}$, respectively.

The $^{1}H$-NMR spectrum of compound **40** (Appendix 13) in $CDCl_3$ showed a signal at δ 0.90 (3H, *t*) due to the terminal methyl groups. The broad singlet centered at δ 1.28 integrated for sixteen protons and is due to eight methylene groups. The signals at δ 1.47 (2H, *m*) and 1.81(2H, *q*) are assigned to H-3' and H-2', respectively. The signal at δ 4.02 (2H, *t*, $J$ = 6.6) is due H-1'. The aromatic proton signals appeared at δ 7.21 (1H, *dd*, $J$ = 8.0 Hz, 1.6Hz), 7.40 (1H, *t*, $J$ = 8.0 Hz), 7.48 (1H, *d*, $J$ = 8.0 Hz) and 7.53 (1H, *broad*) are assigned to H-4, H-5, H-6 and H-2, respectively (Table 5).

The $^{13}$C-NMR and DEPT-135 spectra of compound **40** (Appendix 14 and Appendix 15, respectively) in $CDCl_3$ displayed the presence of nineteen carbon signals, corresponding to three quaternary, four methine, one methyl and eleven methylene carbon atoms. The signal at δ 194.5 is due to the ketone carbonyl groups. The quaternary carbon signals that appeared at δ 159.6 and 134.2 are attributed to C-3 and C-1, respectively. The four methine carbon resonances situated at δ 113.5, 122.2, 122.9 and 130.0 are ascribed to C-2, C-4, C-6 and C-5, respectively. Among the eleven methylene carbon signals, the one appearing at δ 68.3 is due C-1'. The remaining ten methylene carbon signals appeared between δ 31.9 – 22.7. The signal due to the terminal methyl group appeared at δ 14.1 (Table 6). The IR, UV, $^1$H-NMR, $^{13}$C-NMR and DEPT-135 data agreed very well with the structure of compound **40**.

Table 1: $^1$H-NMR (400.13 MHz, $CDCl_3$) data ($\delta_{ppm}$) of compounds **32**, **33**, **34** and **35**

| **32** | **33** | **34** | **35** |
|---|---|---|---|
| 9.94 | 9.96 | 9.98 | 9.95 |
| (*s*, 1H, H-1'') | (*s*, 1H, H-1'') | (*s*, 1H, H-1'') | (*s*, 1H, H-1'') |
| 7.43-7.40 | 7.45-7.43 | 7.46-7.44 | 7.44-7.43 |
| (*unresolved***,** 2H, H-5, H-6) | (*unresolved*, 2H, H-5, H-6) | (*unresolved*, 2H, H-5, H-6) | (*unresolved*, 2H, H-5, H-6) |
| 7.37 | 7.39 | 7.40 | 7.38 |
| (*s*, 1H, H-2) | (*d*, 1H, *J* = 2Hz, H-2) | (*d*, 1H, *J* = 2Hz, H-2) | (*d*, 1H, *J* = 2Hz, H-2) |
| 7.16 | 7.17 | 7.18 | 7.16 |
| (*m*, 1H, H-4) | (1*m*, H, H-4) | (*m*, 1H, H-4) | (*m*, 1H, H-4) |
| 3.99 | 4.00 | 4.02 | 4.00 |
| (*m*, 2H, H-1') | ( *t*, *J* = 6.6 Hz, 2H, H-1') | ( *t*, *J* = 6.6 Hz, 2H, H-1') | (*t*, 2H, *J* = 6.6 Hz, H-1') |
| 1.79 | 1.81 | 1.82 | 1.80 |
| (*q*, 2H, H-2') | (*q*, 2H, 2') | (*q*, 2H, H-2') | (*q*, 2H, H-2') |
| 1.52 | 1.47 | 1.46 | 1.47 |
| (*m*, 2H, H-11') | (*m*, 2H, H-9') | (*m*, 2H, H-7') | (*m*, 2H, H-5') |
| 1.26 | 1.29 | 1.31 | 1.35 |
| (*br*, 16H, H-3' to H-10'') | (*br*, 12H, H-3' to H-8') | (*br*, 8H, H-3' to H-6') | (*m*, 4H, H-3', H-4') |
| 0.88 | 0.89 | 0.92 | 0.91 |
| (*t*, 3H, H-12') | (t , 3H, H-10') | (*t*, 3H, H-8') | (*t*, 3H, H-6') |

Table 2: $^{13}$C-NMR ($CDCl_3$, 100.6 MHz) data ($\delta_{ppm}$) for compounds **32**, **33**, **34** and **35**.

| Carbon | **32** | **33** | **34** | **35** |
|---|---|---|---|---|
| 1 | 137.7 | 137.7 | 137.7 | 137.7 |
| 2 | 112.7 | 112.7 | 112.7 | 112.7 |
| 3 | 159.7 | 159.7 | 159.7 | 159.7 |
| 4 | 121.9 | 121.9 | 121.9 | 121.9 |
| 5 | 129.9 | 129.9 | 129.9 | 129.9 |
| 6 | 123.2 | 123.2 | 123.2 | 123.2 |
| 1’ | 68.2 | 68.2 | 68.3 | 68.2 |
| 2’ | 29.7 | 29.6 | 29.4 | 29.1 |
| 3’ | 26.0 | 26.0 | 26.0 | 25.7 |
| 4’ | 29.5 | 29.6 | 29.3 | 31.6 |
| 5’ | 29.7 | 29.4 | 29.2 | 22.6 |
| 6’ | 29.7 | 29.4 | 31.9 | 14.0 |
| 7’ | 29.7 | 29.2 | 22.7 | - |
| 8’ | 29.4 | 31.9 | 14.1 | - |
| 9’ | 29.2 | 22.7 | - | - |
| 10’ | 31.9 | 14.1 | - | - |
| 11’ | 22.7 | - | - | - |
| 12’ | 14.1 | - | - | - |
| 1’’ | 192.1 | 192.1 | 192.1 | 192.2 |

### 4.1.3. Synthesis of 1,2-bis(3-(decyloxy)phenyl)ethane-1,2-dione (41)

1,2-Bis(3-(decyloxy)phenyl)ethane-1,2-dione was synthesized starting from 3-hydroxybenzaldehyde (**27**) as shown in Scheme 11. The reaction began by alkylation of **27** with 1-bromodecane (**29**) in the presence of $K_2CO_3$ in *N*,*N*-dimethylformamide to afford 3-(decyloxy)benzaldehyde (**33**). Attempt to purify **33** by silica gel column chromatography using petroleum ether as eluent could not remove unreacted 1-bromodecane completely. Hence, the mixture was subjected to benzoin condensation reaction using thiamine hydrochloride as a catalyst in distilled water and 95% ethanol following a literature procedure[51] to afford 1,2-bis(3-(decyloxy)phenyl)-2-hydroxyethanone (**37**) as a yellowish oily material after purification by silica gel column chromatography. The condensation product **37** was oxidized with DMSO/HBr to afford compound **41** (93.3%) as yellowish solid after washing with cold methanol.

Compounds **33**, **37** and **41** were characterized based on their spectroscopic behaviors as discussed below

The UV-Vis spectrum of compound **33** was recorded in $CHCl_3$ and showed two absorption maxima at 256 and 316 nm. The FT-IR spectrum of compound **33** showed a band at 3069 $cm^{-1}$ due to C-H stretching of aromatic ring. The bands at 2926 and 2855 $cm^{-1}$ are due to stretching vibrations of the $CH_3$ and $CH_2$ groups, respectively. The aldehyde carbonyl stretching band appeared at 1702 $cm^{-1}$. The bands at 1599 and 1453 $cm^{-1}$ are attributed to the C=C stretching vibration of the aromatic ring. Furthermore, the asymmetric and symmetric C-O-C stretching bands appeared at 1263 and 1041$cm^{-1}$, respectively.

The $^{1}$H-NMR spectrum of **33** showed a signal at δ 9.96 (1H, *s*) due to the aldehydic proton. The aromatic proton resonances at δ 7.45-7.43 (2H, *unresolved*), 7.39 (1H, *d*) and 7.17 (1H, *m*) are assigned to H-5, H-6, H- 2 and H-4, respectively. The triplet signal at δ 4.00 (2H, *t*, *J* = 6.6 Hz) is assigned to H-1' while the quintet at δ 1.81 is due to H-2'. The multiplet at 1.47 which integrated for two protons is attributable to H-9'. The broad signal at δ 1.29 integrated for 12 protons and is due to six methylene groups. The signal due to the terminal methyl protons appeared at δ 0.89 as a triplet (Table 1).

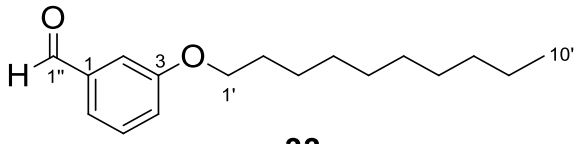


**33**

The $^{13}$C-NMR spectrum of compound **33** with the aid of DEPT-135 revealed the presence of three quaternary, four methine, nine methylene and one methyl carbon atoms. The signal at δ 192.1 is due to the aldehyde carbonyl carbon while the quaternary carbon signals at δ 159.7 and 137.7 are attributed to C-3 and C-1, respectively. The methine carbon resonances at δ 129.9, 123.2, 121.9 and 112.7 are due to C-5, C-6, C-4 and C-2, respectively. The signal at δ 68.2 is due to C-1' and the remaining methylene carbon resonances appeared between δ 31.9 and 22.7. The signal due to the terminal methyl carbon appeared at δ 14.1 (Table 2). The IR, UV, $^{1}$H-NMR, $^{13}$C-NMR and DEPT-135 data agree very well with structure **33**.

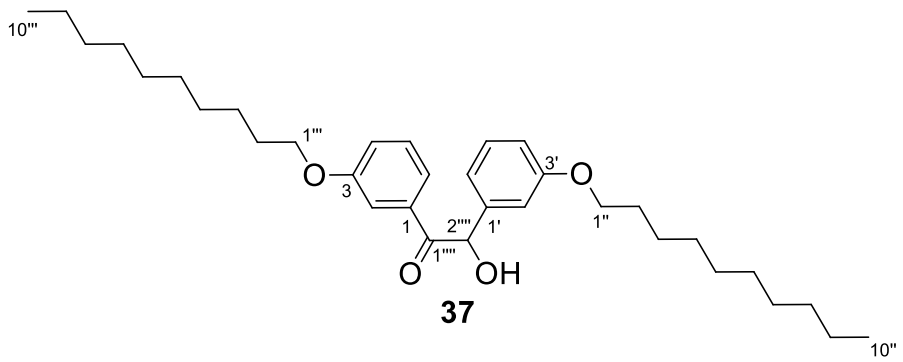


**37**

The benzoin condensation of **33** afforded compound **37** as a yellowish solid with a melting point of 42.2– 43.5$^{o}$C. The UV-Vis spectrum of **37** was recorded in $CHCl_3$ and showed two absorption maxima at 259 and 316 nm which correspond to π -π* and n- π* transitions, respectively. The FT-IR spectrum of **37** showed a band at 3446 cm$^{-1}$ due to O–H stretching of alcohol functional group. The bands at 2922 and 2856 cm$^{-1}$ are due to C-H stretching of $CH_3$ and $CH_2$ groups, respectively. The band at 1676 cm$^{-1}$ is due to C=O stretching of ketone functional group. The bands at 1585 and 1473 cm$^{-1}$ due to C=C ring stretching of the benzene rings. The asymmetric and symmetric C-O-C stretching bands appeared at 1269 and 1030 cm$^{-1}$, respectively. Out-of-plane ring vibration and out-of-plane bending bands appeared at 605 and 782 cm$^{-1}$, respectively.

The $^{1}$H-NMR spectrum of **37** depicted two overlapping signals at δ 0.91 which integrated for six protons indicating the presence of two terminal methyl groups in the structure of the compound. This also confirmed the unsymmetrical nature of the compound. The unresolved broad signal centered at δ 1.29, which integrated for twenty four protons, is due to twelve methylene groups. Another unresolved multiplet centered at δ 1.42 integrated for four protons and is due to H-9'' and H-9'''. The two overlapping quintets at δ 1.76 integrating for four protons are due to H-2" and H-2"'. The four-proton signal at δ 3.94 is attributed to H-1'' and H-1'''. The signal at δ 5.90 (1H, *s*) is due to the methine proton on the carbon atom (C-2'''') adjacent to the ketone carbonyl. The aromatic proton resonances appeared in the region between δ 6.80 and 7.49 (Table 3).

The $^{13}$C-NMR spectrum of compound **37** revealed a signal at δ 198.7 due to the ketone carbonyl group. The signals at δ 159.6 and 159.3 are due to two oxygenated positions in the aromatic rings and are assigned to C-3' and C-3, respectively. The quaternary carbon signals at δ 140.4 and 134.6 are attributed to C-1 and C-1', respectively. Besides, the spectrum revealed the presence of eight aromatic methine carbons. In the aliphatic region, the methine carbon signals at δ 76.2 is

assigned to C-2”” and the oxygenated methylene carbon resonances at δ 68.2 and 68.0 are due to C-1” and C-1”’. The spectrum also revealed the presence of sixteen methylene carbon resonances in the region between δ 31.9 to 22.7 and a signal due to the terminal methyl groups at δ 14.1 (Table 4). Hence, the IR, UV $^{1}$H-NMR, $^{13}$C-NMR and DEPT-135 data support the assignment of structure **37** to this compound.

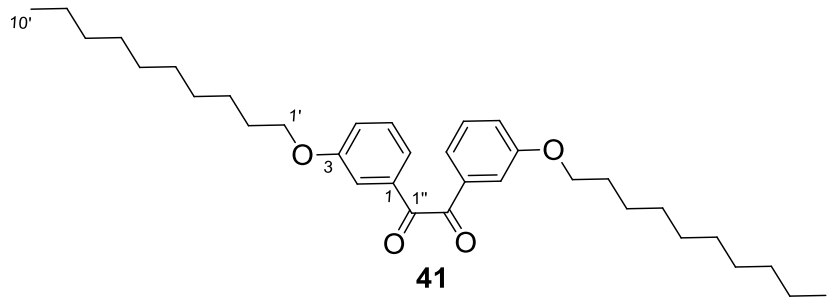


**41**

The oxidation of **37** with DMSO/HBr afforded diketone **41** as a yellow solid with a melting point of 57.6 –58.4$^{o}$C. The UV-Vis spectrum of **41** was recorded in $CHCl_3$ and showed two absorption maxima at 265 and 325 nm showing the presence of conjugation in the compound. The FT-IR spectrum of **41** showed a band at 3076 cm$^{-1}$ due to C-H stretching of the aromatic rings. The bands at 2925 and 2853 cm$^{-1}$ are due to stretching vibrations of the $CH_3$ and $CH_2$ groups, respectively. The carbonyl stretching of ketones appeared at 1678 cm$^{-1}$. The bands at 1594 and 1471 cm$^{-1}$ are ascribed to the C=C stretching vibration of the aromatic rings. Moreover, the asymmetric and symmetric C-O-C stretching bands appeared at 1262 and 1031 cm$^{-1}$, respectively.

The $^{1}$H-NMR spectrum of **41** (Appendix 10) in $CDCl_3$ revealed a signal at δ 0.90 (3H, *t*) due to the terminal methyl groups. The broad signal centered at δ 1.30 is due to six methylene groups. The signals at δ 1.48 (2H, *m*) and 1.81(2H, quintet) are assigned to H-9’ and H-2’, respectively. The signal at δ 4.03 (2H, *t*, *J* = 6.4 Hz) is assigned to H-1’. The presence of signals at δ 7.22 (1H, *m*), 7.40 (1H, *t*, *J* = 7.8 Hz), 7.48 (1H, *d*, *J* = 7.8 Hz), 7.53 (1H, *d*, *J* = 2.4) are assigned to H-4, H-5 and H-6 and H-2 of the aromatic rings, respectively (Table 5).

The $^{13}$C-NMR and DEPT-135 spectra of compound **41** (Appendix 11 and Appendix 12, respectively) in $CDCl_3$ displayed the presence of seventeen carbon signals due to one methyl, nine methylene, four methine and three quaternary carbon atoms. The signal at δ 194.5 is due to

the ketone carbonyl groups. The quaternary carbon signals at δ 159.6 and 134.2 are attributed to C-3 and C-1, respectively. The four methine carbon signals at δ 129.9, 122.9, 122.2 and 113.6 are ascribed to C-5, C-6, C-4 and C-2, respectively. Among the nine methylene carbon signals the one appearing at δ 68.3 is due to C-1', the carbons bearing oxygen atoms on the side chain. The remaining eight methylene carbon signals are observed between δ 31.9–22.6. The presence of terminal methyl group was also confirmed by the presence of a carbon signal at δ 14.1(Table 6). The IR, UV, $^{1}$H-NMR, $^{13}$C-NMR and DEPT-135 agree with the assignment of structure **41** for the compound.

Table 3: $^{1}$H-NMR (400.13MHz, $CDCl_3$) data ($\delta_{ppm}$) of compound **36**, **37**, **38** and **39**.

| **36** | **37** | **38** | **39** |
|---|---|---|---|
| 7.53 -6.85 (*m*, 8H, H-2', H-4', H-5', H-6', H-2, H-4, H-5, H-6) | 7.49 -6.80 (*m*, H-2',H-4',H-5',H-6', H-2, H-4, H-5, H-6.) | 7.53- 6.83 (*m*, H-2',H-4',H-5',H-6' ,H-2 , H-4, H-5 ,H-6) | 7.49 -6.80 (*m*, 8H, H-2', H-4', H-5', H-6', H-2, H-4, H-5, H-6) |
| 5.93 (*s*, 1H, H-2'''') | 5.90 (*s*, 1H, H-2'''') | 5.94 (*s*, 1H, H-2'''') | 5.80 (*s*, 1H, H-2'''') |
| 3.99 (*m*, 4H, H-1'', H-1''') | 3.94 (*m*, 4H, H-1'', H-1''') | 3.96 ( *t*, 4H, H-1'',H-1''') | 3.95 (*t*, 4H, H-1'', H-1''') |
| 1.82 (*q*, 4H, H-2'', H-2''') | 1.76 (*q*, 4H, H-2'', H-2''') | 1.79 (*q*, 4H, H-2'', H-2''') | 1.77 (*q*, 4H, H-2'', H-2''') |
| 1.50 (*m*, 4H, H-11') | 1.42 (*m*, 4H, H-9'', H-9''') | 1.48 (*m*, 4H, H-7'', H-7''') | 1.45 (*m*, 4H, H-5', H-5'') |
| 1.35 (*br.m*, 32 H, H-3'' to H-10'', H-3'''to H-10''') | 1.29 (*br.m*, 24H, H-3'' to H-8'', H-3'''to H-8''') | 1.36 (*br. m*, 16H, H-3'' to H-6'', H-3''' to H-6''') | 1.35 (*br.m*, 8H, H-3'' to H-4'', H-3''' to H-4''') |
| 0.96 (*t*, 6H, H-12'', H-12''') | 0.91 (*t*, 6H, H-10'', H-10''') | 0.95 (*t*, 6H, H-8'', H-8''') | 0.98 (*t*, 6H, H-6'', H-6''') |

Table 4: $^{13}$C-NMR ($CDCl_3$, 100.6 MHz) data ($\delta_{ppm}$) for compound **36**, **37**, **38** and **39**.

| Carbon | **36** | **37** | **38** | **39** |
|---|---|---|---|---|
| 1 | 140.3 | 140.4 | 140.4 | 140.4 |
| 2 | 113.8 | 113.8 | 113.8 | 113.8 |
| 3 | 159.3 | 159.3 | 159.3 | 159.3 |
| 4 | 119.9 | 119.9 | 119.9 | 119.9 |
| 5 | 129.6 | 129.6 | 129.6 | 129.6 |
| 6 | 121.0 | 121.0 | 121.6 | 121.4 |
| 1’ | 134.6 | 134.6 | 134.7 | 134.6 |
| 2’ | 114.7 | 114.7 | 114.7 | 114.7 |
| 3’ | 159.6 | 159.6 | 159.7 | 159.6 |
| 4’ | 113.6 | 113.6 | 113.7 | 113.6 |
| 5’ | 130.1 | 130.1 | 130.1 | 130.1 |
| 6’ | 121.5 | 121.5 | 121.6 | 121.5 |
| 1’’ | 68.2 | 68.2 | 68.2 | 68.2 |
| 2” | 29.7 | 29.4 | 29.6 | 29.2 |
| 3” | 26.0 | 26.0 | 26.0 | 25.7 |
| 4” | 29.6 | 29.4 | 29.4 | 31.6 |
| 5” | 29.7 | 29.3 | 29.2 | 22.6 |
| 6” | 29.7 | 29.3 | 31.8 | 14.1 |
| 7” | 29.5 | 29.2 | 22.3 | - |
| 8” | 29.3 | 31.9 | 14.1 | - |
| 9” | 29.1 | 22.7 | - | - |
| 10” | 31.9 | 14.1 | - | - |
| 11” | 22.6 | - | - | - |
| 12” | 14.1 | - | - | - |
| 1’’’ | 68.0 | 68.0 | 68.0 | 68.0 |
| 2’’’ | 29.7 | 29.4 | 29.6 | 29.1 |
| 3’’’ | 26.0 | 26.0 | 26.0 | 25.7 |
| 4’’’ | 29.6 | 29.4 | 29.4 | 31.6 |
| 5’’’ | 29.7 | 29.3 | 29.1 | 22.6 |
| 6’’’ | 29.7 | 29.3 | 31.8 | 14.1 |
| 7’’’ | 29.5 | 29.2 | 22.3 | - |
| 8’’’ | 29.3 | 31.9 | 14.1 | - |
| 9’’’ | 29.1 | 22.7 | - | - |
| 10’’’ | 31.9 | 14.1 | - | - |
| 11’’’ | 22.6 | - | - | - |
| 12’’’ | 14.1 | - | - | - |
| 1’’’’ | 198.7 | 198.7 | 198.7 | 198.7 |
| 2’’’’ | 76.7 | 76.2 | 76.2 | 76.2 |

### 4.1.4. Synthesis of 1,2-bis(3-(octyloxy)phenyl)ethane-1,2-dione (42)

1,2-Bis(3-(octyloxy)phenyl)ethane-1,2-dione (**42**) was synthesized starting from 3-hydroxybenzaldehyde (**27**) as shown in Scheme 11. The reaction began by alkylation of **27** with 1-bromooctane (**30**) in the presence of $K_2CO_3$ in DMF to afford 3-(octyloxy)benzaldehyde (**34**). The crude product (**34**) was subjected to benzoin condensation reaction without purification using thiamine hydrochloride as a catalyst in distilled water and 95% ethanol to afford 2-hydroxy-1,2-bis(3-(octyloxy)phenyl)ethanone (**38**) as a yellow oil after purification by silica gel column chromatography. The condensation product **38** was oxidized with DMSO/HBr following a literature procedure[52] to afford compound **42** (82.7%) as yellowish solid after washing with cold methanol. The above compounds **34**, **38**, and **42** were characterized based on their spectroscopic behaviors as discussed below.

The UV-Vis spectrum of compound **34** was recorded in $CHCl_3$ and showed two absorption maxima at 256 and 316 nm which are attributable to the π -π* and n- π* transitions, respectively. The FT-IR spectrum of compound **34** showed a band at 3069 $cm^{-1}$ due to C-H stretching of the benzene ring. The bands at 2925 and 2855 $cm^{-1}$ are due to stretching vibrations of the $CH_3$ and $CH_2$ groups, respectively. The band due to stretching of the aldehyde carbonyl group appeared at 1703 $cm^{-1}$. In addition, the bands at 1598 and 1452 $cm^{-1}$ are attributed to the C=C stretching vibration of the aromatic ring. The asymmetric and symmetric C-O-C stretching bands appeared at 1263 and 1048 $cm^{-1}$, respectively.

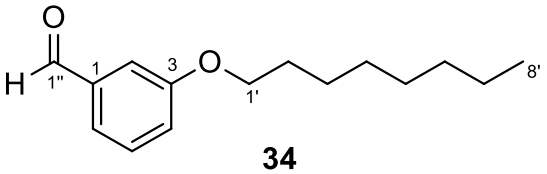


**34**

The $^1$H-NMR spectrum of **34** in $CDCl_3$ showed a signal at δ 9.98 indicating the presence of an aldehyde. The aromatic proton signals appeared at δ 7.44–7.46 (2H, *unresolved*), 7.40 (1H, *d*) and 7.18 (1H, *m*) and are assigned to H-5, H-6, H-2 and H-4, respectively. The triplet at δ 4.02 (2H, *t*, *J* = 6.6 Hz) is due to H-1'. The quintet at δ 1.82 (2H) is assigned to H-2'. The multiplet at δ 1.46 which integrated for two protons is assigned to H-7' while the broad signal at δ 1.31

integrating for eight protons is due to H-3' to H-6'. The triplet at δ 0.92 which integrated for three protons is due to the terminal methyl group (H-8') (Table 1).

The $^{13}$C-NMR and DEPT-135 spectra of compound **34** in $CDCl_3$ displayed the presence of fifteen carbon signals, of which one is a methyl, seven are methylene, four are methine and three are quaternary carbon resonances. The quaternary carbon signals at δ 192.1, 159.7 and 137.7 are attributable to the aldehydic carbon, C-3 and C-1, respectively. The four methine carbon resonances at δ 129.9, 123.2, 121.9 and 112.7 are ascribed to C-5, C-6, C-4 and C-2, respectively. Among the five methylene carbon signals, the one appearing at δ 68.3 is accounted for the oxygen-bearing carbon C-1' of the *n*-octyl group. The remaining six methylene signals appeared between δ 31.9 and 22.7 and are due to C-2' – C-7'. The signal at δ 14.1 is due to the terminal methyl group (Table 2).

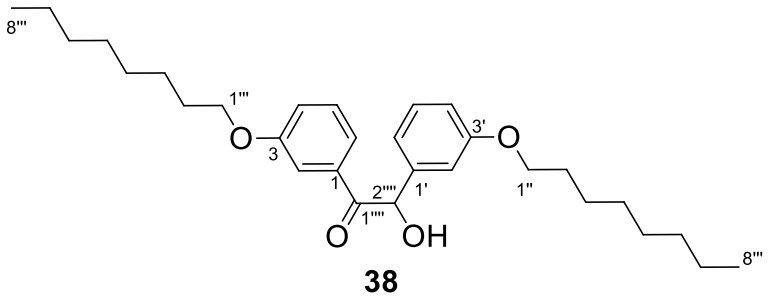


**38**

Compound **38** was obtained by the benzoin condensation of **34** using thiamine hydrochloride as catalyst. The UV-Vis spectrum of **38** was recorded in $CHCl_3$ and showed two absorption maxima at 259 and 316 nm suggesting the presence of conjugation in the compound. The FT-IR spectrum of **38** indicated a band at 3461 $cm^{-1}$ due to O-H stretching of alcohol. The bands at 2941 and 2856 $cm^{-1}$ are due to C-H stretching of $CH_3$ and $CH_2$ groups, respectively. The band at 1681 $cm^{-1}$ is due to C=O stretching of ketone functional group. The bands at 674 and 780 $cm^{-1}$ are due to out-of-plane ring vibration and out-of-plane C-H bending, respectively. The bands due to stretching of C=C bonds of the rings appeared at 1596 and 1443 $cm^{-1}$. The asymmetric and symmetric C-O-C stretching bands appeared at 1266 and 1034 $cm^{-1}$, respectively.

The $^{1}$H-NMR spectrum of compound **38** revealed the presence of two terminal methyl groups due to the overlapping signals at δ 0.95(6H). The broad signal centered at δ 1.36, which

integrated for sixteen protons, is due to the presence eight methylene groups. The broad overlapping multiplets at δ 1.48 (4H) are due to H-7'' and H-7''' while the quintet at δ 1.79 (4H) is due to H-2'' and H-2'''. The spectrum exhibited a singlet, which integrated for one proton at δ 5.94 due to H-2''''. Eight proton signals were observed in the aromatic region between δ 6.83 and 7.53 indicating the presence of two aromatic rings in the structure of the compound (Table-3).

The $^{13}$C-NMR spectrum of **38** showed a signal at δ 198.7 indicating the presence of a ketone moiety in the structure of the compound. The signals at δ 159.7 and 159.3 revealed the presence of two oxygenated carbon atoms and are assigned to C-3 and, C-3' respectively. The other aromatic carbon signals appeared at δ 140.5, 134.7, 130.1, 129.6, 121.6, 121.0, 119.9, 114.7, 113.8 and 113.7 and are due to C-1, C-1', C-5', C-5, C-6', C-6, C-4, C-2', C2 and C-4', respectively. The spectrum showed the presence of three oxygenated aliphatic carbon atoms. Thus, the methine carbon signal at δ 76.2 is due to C-2'''' while the methylene carbon resonances at δ 68.2 and 68.0 are due to C-1'' and C-1''', respectively. The aliphatic methylene carbon resonances appeared between δ 31.8 and 21.3. The spectrum also showed a signal at δ 14.1 due to the terminal methyl groups (Table 4).

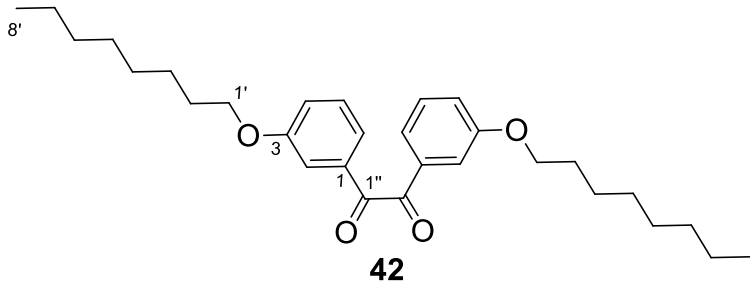


**42**

The oxidation of **38** with DMSO/HBr afforded diketone **42** as a yellow solid with a melting point of 50.7– 51.6$^{o}$C. The UV-Vis spectrum of **42** was recorded in $CHCl_3$ and showed two absorption maxima at 265 and 325 nm due to π -π* and n- π* transitions, respectively. The FT-IR spectrum of **42** showed a band at 3074 cm$^{-1}$ due to C-H stretching of the aromatic rings. The bands at 2927 and 2856 cm$^{-1}$ are due to stretching vibrations of the $CH_3$ and $CH_2$ groups, respectively. The stretching vibration of the ketone carbonyl appeared at 1679 cm$^{-1}$. Similarly, the bands at 1597 and 1438 cm$^{-1}$ are attributed to the C=C stretching vibrations of the aromatic rings. The asymmetric and symmetric C-O-C stretching bands appeared at 1265 and 1032 cm$^{-1}$, respectively.

The $^{1}$H-NMR spectrum of **42** (Appendix 7) in $CDCl_3$ showed the presence of a signal at δ 0.91 indicating the presence of terminal methyl groups. The broad signal centered at δ 1.31 integrated for eight protons and is due to the presence four methylene groups. The signals at δ 1.48 (2H, *m*) and 1.81(2H, quintet) are assigned to H-7' and H-2', respectively. The triplet at δ 4.02 (2H, *t*, 6.4 Hz) is due to C-1' and is characteristic of protons on oxygenated carbon atoms. The aromatic proton signals at δ 7.21 (1H, *d*, *J* = 8.0 Hz), 7.39 (1H, *t*, *J* = 8.0 Hz), 7.48 (1H, *d*, *J* = 8.0 Hz) and 7.53 (1H, *unresolved*) are assigned to H-4, H-5, H-6 and H- 2 respectively (Table 5).

The $^{13}$C-NMR and DEPT-135 spectra of **42** (Appendix 8 and Appendix 9, respectively) in $CDCl_3$ displayed the presence of fifteen carbon signals, of which, three are quaternary, four are methine, seven are methylene and one is methyl carbon signals. The signal at δ 194.5 is due to the ketone carbonyl groups. The quaternary carbon signals at δ 159.6 and 134.1 are attributed to C-3 and C-1, respectively. The four methine carbon resonances at δ 130.0, 122.9, 122.2 and 113.5 are ascribed to C-5, C-6, C-4 and C-2, respectively. The signal at δ 68.3 is due to C-1'. The remaining six methylene carbon signals appeared between δ 31.8 and 22.6. The signal at δ 14.1 is due to the terminal methyl groups (Table 6). The UV, IR, $^{1}$H-NMR, $^{13}$C-NMR and DEPT-135 data are in good agreement with structure **42**.

### 4.1.5. Synthesis of 1,2-bis(3-(hexyloxy)phenyl)ethane-1,2-dione (43)

1,2-Bis(3-(hexyloxy)phenyl)ethane-1,2-dione (**43**) was synthesized starting from 3-hydroxybenzaldehyde (**27**) as shown in Scheme 11. The reaction began by alkylation of **27** with 1-bromohexane (**31**) in the presence of $K_2CO_3$, in DMF to afford 3-(hexyloxy)benzaldehyde (**35**). The crude product was subjected to benzoin condensation reaction without purification using thiamine hydrochloride as a catalyst in distilled water and 95% ethanol to afford 1,2-bis(3-(hexyloxy)phenyl)-2-hydroxyethanone (**39**) as a yellow solid material after purification by silica gel column chromatography. The condensation product **39** was oxidized with DMSO/HBr to afford compound **43** (96.4%) as yellowish solid in pure form after washing with cold methanol. Compounds **35**, **39** and **43** were characterized based on their spectroscopic behaviors as discussed below.

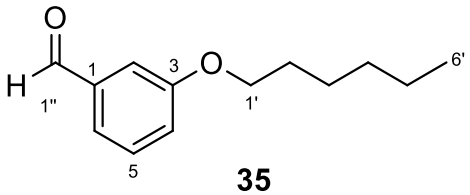


**35**

The UV-Vis spectrum of compound **35** was recorded in $CHCl_3$ and showed two absorption maxima at 255 and 312 nm indicating the presence of conjugation in the compound. The FT-IR spectrum of **35** showed bands at 2932 and 2859 $cm^{-1}$ due to stretching vibrations of $CH_2$ and $CH_3$ groups, respectively. The band at 3018 $cm^{-1}$ is due to C-H stretching of benzene ring. The carbonyl stretching band appeared at 1699 $cm^{-1}$. The bands at 1586 and 1452 $cm^{-1}$ are attributed to the C=C stretching vibration of the aromatic ring. Moreover, the asymmetric and symmetric C-O-C stretching bands appeared at 1263 and 1030 $cm^{-1}$, respectively.

The $^1$H-NMR spectrum of **35** was recorded in $CDCl_3$. The most deshielded proton signal at δ 9.95 indicated the presence of an aldehyde in the structure. The unresolved signals at δ 7.44-7.43 (2H) and multiplet at 7.16 (1H) are assignable to H-5, H-6 and H-4, respectively. The one-proton doublet at δ 7.38 is ascribed to H-2. The two-proton triplet at δ 4.00 is due to H-1'. The multiplet at δ 1.47 (2H) and the quintet at δ 1.80 (2H) are assigned to H-5' and H-2', respectively. The signal at δ 1.35 is due to two methylene groups. Furthermore the triplet at δ 0.91 is due to the terminal methyl group (Table 1).

The $^{13}$C-NMR and DEPT-135 spectra of compound **35** displayed thirteen carbon signals, of which, two are quaternary, four are methine, one is methyl and five are methylene carbon signals. The aldehyde carbonyl carbon signal appeared at δ 192.2. The quaternary carbon signals at δ 159.7 and 137.7 are attributed to C-3 and C-1, respectively. The four methine carbon resonances at δ 129.9, 123.2, 121.9 and 112.7 are ascribed to C-5, C-6, C-4 and C-2, respectively. Among the five methylene carbon signals in the aliphatic region, the one appearing at δ 68.2 is accounted for C-1'. The remaining four methylene carbon signals were observed between δ 31.6–22.6. The signal at δ 14.0 is due to the terminal methyl group (Table 2). The IR, UV, $^1$H-NMR, $^{13}$C-NMR and DEPT-135 spectral data agree with the structure of compound **35**.

The benzoin condensation of **35** catalyzed by thiamine hydrochloride afforded compound **39** with a melting point 54.8 –55.3$^o$C. The UV-Vis spectrum of **39** was recorded in $CHCl_3$ and

showed two absorption maxima at 259 and 317 nm. The FT-IR spectrum of **39** showed a band at 3447 $cm^{-1}$ due to O-H stretching. The band at 2941 $cm^{-1}$ is due to C-H stretching of $CH_3$. The C=O stretching band of the ketone functional group appeared at 1679 $cm^{-1}$. The spectrum also revealed bands at 1600 and 1444 $cm^{-1}$ due to C=C stretching of the rings. Bands due to out-of-plane ring vibration and out-of-plane bending appeared at 586 and 783 $cm^{-1}$, respectively. The asymmetric and symmetric C-O-C stretching bands appeared at 1269 and 1033 $cm^{-1}$, respectively.

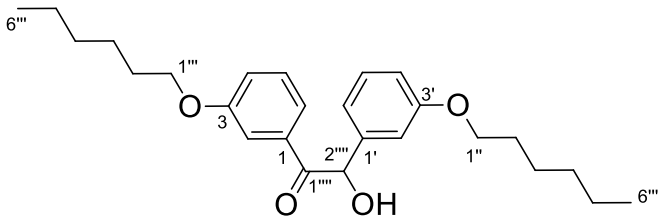


**39**

The $^{1}$H-NMR spectrum of compound **39** showed overlapping signals at δ 0.98, which integrated for six protons, due to the two terminal methyl groups. The broad signal centered at δ 1.35 integrated for eight protons and the multiplet at δ 1.45 integrated for four protons and account for a total of six methylene groups. The spectrum also exhibited a quintet at δ 1.77 (4H) due to H-2'' and H-2'''. The spectrum showed overlapping triplets at δ 3.95 (4H) due to H-1" and H-1"'. The singlet at δ 5.8 (1H) is due to H-2''''. The eight aromatic proton signals appeared between δ 6.80 and 7.49 (Table 3).

The $^{13}$C-NMR spectrum of compound **39** revealed the presence of twenty-four carbon signals. The quaternary carbon signals at δ 198.7, 159.6, 159.3, 140.4 and 134.6 are ascribed to the ketone carbonyl, C-3', C-3, C-1 and C-1', respectively. The other aromatic methine carbon signals appeared at δ 130.1, 129.6, 121.5, 121.0, 119.9, 114.7, 113.8 and 113.6 and are due to C-5', C-5, C-6', C-6, C-4, C-2', C-2 and C-4', respectively. The methine carbon signal at δ 76.2 is attributed to C-2''''. The signals at δ 68.2 and 68.0 are due to methylene carbons C-1" and C-1"'. The signals due to the remaining six methylene carbons appeared between δ 31.6 and 25.7 (Table 4). The above spectroscopic data agreed with the structure of compound **39**.

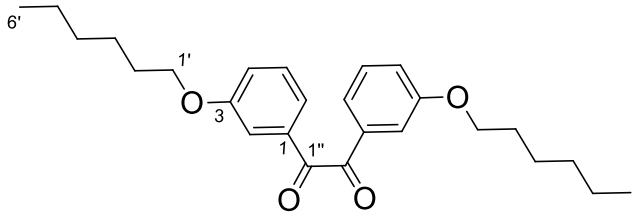


**43**

The oxidation of **39** with DMSO/HBr gave compound **43** as a yellowish solid with a melting point of 50.5–51.8$^{o}$C. The UV-Vis spectrum of **43** was recorded in $CHCl_3$ and showed two absorption maxima at 265 and 325 nm which correspond to π -π* and n- π* transitions, respectively. The FT-IR spectrum of **38** showed a band at 3082 $cm^{-1}$ due to C-H stretching of benzene rings. The bands at 2933 and 2871 $cm^{-1}$ are due to stretching vibrations of the $CH_3$ and $CH_2$ groups, respectively. The carbonyl-stretching band appeared at 1672 $cm^{-1}$. The bands at 1599 and 1444 $cm^{-1}$ are attributed to the C=C stretching vibrations of the rings. In addition, the asymmetric and symmetric C-O-C stretching bands appeared at 1266 and 1030 $cm^{-1}$, respectively.

Table 5: $^{1}$H-NMR (400.13 MHz, $CDCl_3$) data ($\delta_{ppm}$) of compounds **40**, **41**, **42** and **43**.

| **40** | **41** | **42** | **43** |
|---|---|---|---|
| 7.53 | 7.53 | 7.53 | 7.53 |
| (*br*, 1H, H-2) | (*d*, *J* = 2.4, 1H, H-2) | (*br*, 1H, H-2) | (*d*, *J* = 1.6Hz, 1H, H-2) |
| 7.48 | 7.48 | 7.48 | 7.48 |
| (*d*, *J* = 8.0 Hz, 1H, H-6) | (*d*, *J* = 7.8 Hz, 1H, H-6) | (*d*, *J* = 8.0 Hz, 1H, H-6) | (*d*, *J* = 8.0 Hz, 1H, H-6) |
| 7.40 | 7.40 | 7.39 | 7.39 |
| (*t*, *J* = 8.0 Hz, 1H, H-5) | (*t*, *J* = 7.8 Hz, 1H, H-5), , | (*t*, *J* = 8.0 Hz, 1H, H-5), , | (*t*, *J* = 8.0 Hz, 1H, H-5) |
| 7.21 | 7.22 | 7.21 | 7.21 |
| (*dd*, *J* = 8.0, 1.6 Hz, 1H, H-4) | (*m*, 1H, H-4), | ( *d*, *J* = 8.0 Hz, 1H, H-4), | (*dd*, *J* = 8.0, 1.6 Hz, 1H, H-4) |
| 4.02 | 4,03 | 4,02 | 4.02 |
| (*t*, *J* = 6.6 Hz, 2H, H-1') | (*t*, *J* = 6.4 Hz, 2H, H-1') | (*t*, *J* = 6.4 Hz, 2H, H-1') | (*t*, *J* = 6.6 Hz, 2H, H-1') |
| 1.81 | 1.81 | 1.81 | 1.81 |
| (*q*, 2H, H-2') | (*q*, 2H, H-2') | (*q*, 2H, H-2') | (*q*, 2H, H-2') |
| 1.47 | 1.48 | 1.48 | 1.45 |
| (*m*, 2H, H-11') | (*m*, 2H, H-9') | ( *m*, 2H, H-7') | (*m*, 2H, H-5') |
| 1.28 | 1.30 | 1.31 | 1.35 |
| (*br.s*, 16H, H-3' to H-10') | (br.*s*, 12H, H-3' to H-8') | (*br.s*, 6H, H-3' to H-6') | (*br.s*, 4H, H-3'to H-4') |
| 0.98 | 0.91 | 0.91 | 0.93 |
| (*t*, 3H, H-12') | (*t*, 3H, H-10') | (*t*, 3H, H-8') | (*t*, 3H, H-6') |

The $^{1}$H-NMR spectrum of **43** (Appendix 4) in $CDCl_3$ showed a triplet at δ 0.93 (3H) indicating the presence of terminal methyl groups. An unresolved signal centered at δ 1.35 integrated for four protons and is due to two methylene groups. The signals at δ 1.45 (2H, *m*) and 1.81 (2H, quintet) are assigned to H-5' and H-2', respectively. The signal at δ 4.02 (2H, *t*, *J* = 6.6 Hz) is

due to H-1'. The aromatic proton resonances at δ 7.21 (1H, *dd*, *J* = 8.0, 1.6 Hz), 7.39 (1H, *t*, *J* = 8.0 Hz), 7.48 (1H, *d*, *J* = 8.0 Hz) and 7.53 (1H, *d*, *J* = 1.6Hz) are assigned to H- 4, H- 5, H-6 and H-2, respectively (Table 5).

Table 6: $^{13}$C-NMR ($CDCl_3$, 100.6 MHz) data ($\delta_{ppm}$) of compounds **40**, **41**, **42** and **43**.

| Carbon | **40** | **41** | **42** | **43** |
|---|---|---|---|---|
| 1 | 134.2 | 134.2 | 134.1 | 134.2 |
| 2 | 113.5 | 113.6 | 113.5 | 113.6 |
| 3 | 159.6 | 159.6 | 159.6 | 159.6 |
| 4 | 122.2 | 122.2 | 122.2 | 122.2 |
| 5 | 130.0 | 129.9 | 130.0 | 130.0 |
| 6 | 122.9 | 122.9 | 122.9 | 122.9 |
| 1' | 68.3 | 68.3 | 68.3 | 68.3 |
| 2' | 29.6 | 29.3 | 29.3 | 29.1 |
| 3' | 26.0 | 26.0 | 26.0 | 25.6 |
| 4' | 29.6 | 29.3 | 29.2 | 31.5 |
| 5' | 29.3 | 29.5 | 29.1 | 22.6 |
| 6' | 29.3 | 29.5 | 31.8 | 14.0 |
| 7' | 29.3 | 29.1 | 22.7 | - |
| 8' | 29.6 | 31.9 | 14.1 | - |
| 9' | 31.5 | 22.6 | - | - |
| 10' | 29.1 | 14.1 | - | - |
| 11' | 22.7 | - | - | - |
| 12' | 14.1 | - | - | - |
| 1'' | 194.5 | 194.5 | 194.5 | 194.5 |

The $^{13}$C-NMR and DEPT-135 spectra of compound **43** (Appendix 5 and Appendix 6, respectively) in $CDCl_3$ displayed thirteen carbon signals corresponding to three quaternary, four methine, one methyl and five methylene carbon resonances. The signal at δ 194.5 is due to the ketone carbonyl group. The quaternary carbon signals at δ 159.6 and 134.2 are ascribed to C-3 and C-1, respectively. The four methine carbon signals at δ 113.6, 122.2, 122.9 and 130.0 are due to C-2, C-4, C-6 and C-5, respectively. Among the five methylene carbon signals, the one at δ 68.3 is due to the oxygenated carbon C-1' of the *n*-hexyl group. The remaining four methylene carbon signals appeared between δ 31.5 and 22.6. The signal due to the terminal methyl groups

appeared at δ 14.0 (Table 6). The above spectroscopic data agreed very well with the structure of compound **43**.

## 4.2. Syntheses of thieno[3,4-*b*]pyrazines

Thieno[3,4-*b*]pyrazines **44**, **45**, **46**, and **47** and the corresponding 5,7-dibromo derivatives **48**, **49**, **50** and **51** were synthesized starting from diketones **40-43** and 3,4-diaminothiophene (**13)** as described below.

### 4.2.1. Syntheses of thieno[3,4-*b*]pyrazine derivatives 44, 45, 46, and 47

Thieno[3,4-*b*]pyrazines **44**, **45**, **46**, and **47** were synthesized by modifications of published procedures.[44] Thus, condensation reactions between 3,4-diaminothiophene (**13**) with diketones **40**-**43** (Scheme 12) in absolute ethanol afforded **44** (86.5%), **45** (74.9%), **46** (70.8%) and **47** (78%). Compounds **45** and **47** were purified by silica gel column chromatography while **44** and **46** were obtained in pure form after washing the crude products with cold methanol. The identities of the thieno[3,4-*b*]pyrazines were confirmed based on their spectroscopic data as discussed below.

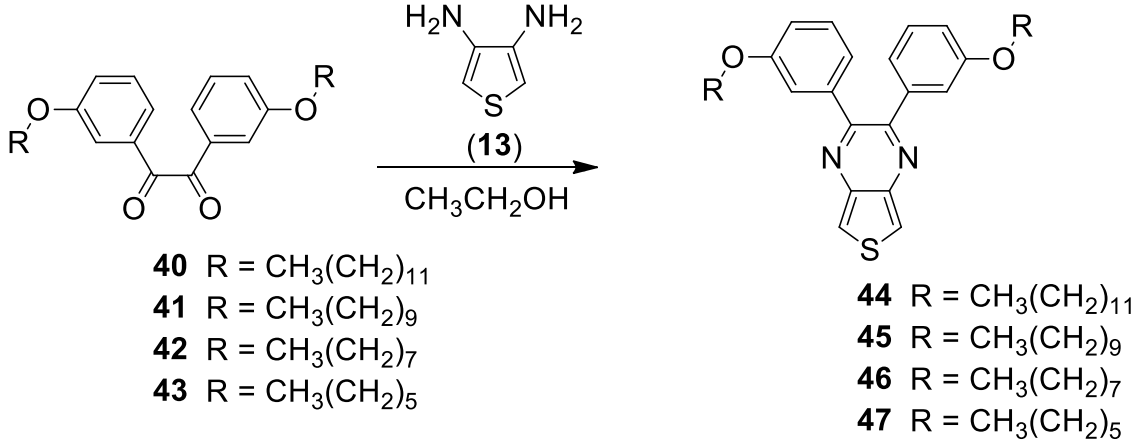


**40** R = $CH_3(CH_2)_{11}$
**41** R = $CH_3(CH_2)_9$
**42** R = $CH_3(CH_2)_7$
**43** R = $CH_3(CH_2)_5$

**44** R = $CH_3(CH_2)_{11}$
**45** R = $CH_3(CH_2)_9$
**46** R = $CH_3(CH_2)_7$
**47** R = $CH_3(CH_2)_5$

Scheme 12: The syntheses of compounds **44-47.**

The UV-Vis spectrum of **44** was recorded in $CHCl_3$ and showed two absorption maxima at 256 and 355 nm (Figure 5) which correspond to π -π* and n- π* transitions, respectively. The FT-IR spectrum of **44** (Appendix 44 ) displayed bands at 3070 and 2920 $cm^{-1}$ due to C-H stretching of

aromatic ring and C-H stretching of the $CH_3$, respectively. The imine C=N band appeared at 1601 $cm^{-1}$ while the band due to the C=C stretching of ring appeared at 1441 $cm^{-1}$. Furthermore, the asymmetric and symmetric C-O-C stretching bands appeared at 1222 and 1032 $cm^{-1}$, respectively.

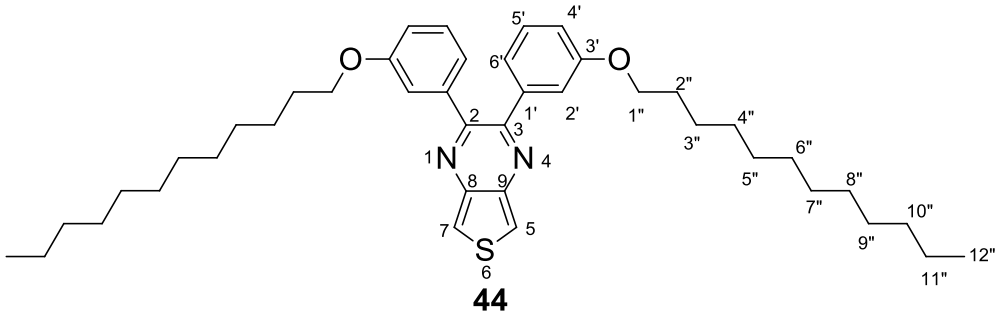


**44**

The $^1$H-NMR spectrum of compound **44** (Appendix 25) showed a signal at δ 0.93 (3H, *t*, *J* = 6.6 Hz) indicating the presence of terminal methyl groups. The broad signal centered at δ 1.29 which integrated for sixteen protons is due to eight methylene groups. The signals at δ 1.40 (2H, *m*) and 1.71 (2H, quintet) are assigned to H-11'' and H-2'', respectively. The signal at δ 3.83 (2H, *t*, *J* = 6.4 Hz) is due to H-1''. The aromatic proton signals appeared at δ 6.91, 7.00-7.02 and 7.21 and are assigned to H- 4', H-2', H-6' and H-5', respectively. The signal at δ 8.09 (1H, *s*) is attributed to H-5 and H-7 (Table 7).

The $^{13}$C-NMR and DEPT-135 spectra of compound **44** (Appendix 26 and Appendix 27, respectively) in $CDCl_3$ showed twenty one carbon signals corresponding to four quaternary, five methine, one methyl and eleven methylene carbon signals. The quaternary carbon signals at δ 158.9, 153.1, 141.3 and 129.1 are attributed to C-3', C-3, C-1' and C-9, respectively. The five methine carbon signals at δ 115.1, 116.0, 117.6, 121.9 and 140.1 are ascribed to C-2', C-4', C-6', C-5 and C-5', respectively. The signal at δ 68.0 is due to C-1''. The remaining eleven methylene signals appeared between δ 31.9 and 22.7. The presence of terminal methyl group was also confirmed by the presence of a carbon signal at δ 14.1 (Table 8). The IR, UV, $^1$H-NMR, $^{13}$C-NMR and DEPT-135 agree with the assignment of structure **44** for the compound.

Table 7: $^{1}$H-NMR (400.13MHz, $CDCl_3$) data ($\delta_{ppm}$) of Compound **44**, **45**, **46** and **47**.

| **44** | **45** | **46** | **47** |
|---|---|---|---|
| 8.09 (*s*, 1H, H-5, H-7) | 8.07 (*s*,1H, H-5, H-7) | 8.09 (*s*, 1H, H-5, H-7) | 8.12 (*s*, 1H, H-5, H-7) |
| 7.21 (*t*, *J* = 8.8 Hz, 1H, H-5') | 7.21 (*t*, *J* = 7.8 Hz, 1H ,H-5') | 7.21 (*t*, *J* = 7.8, 1H, H-5') | 7.22 (*t*, *J* = 7.8 Hz, 1H, H-5') |
| 7.0 – 7.02 (*unresolved*, 2H, H-2', H-6') | 7.0 – 7.02 (*unresolved*, 2H, H-2', H-6') | 7.0 – 7.02 (*unresolved*, 2H, H-2', H-6') | 7.0 – 7.02 (*unresolved*, 2H, H-2', H-6') |
| 6.91 (*d*, *J* = 8.8, 1H, H-4') | 6.91 (*d*, *J* = 7.8 Hz,1H, H-4') | 6.91 (*d*, *J* = 7.8, 1H, H-4') | 6.92 (*dt*, 1H, H-4') |
| 3.83 (*t*, *J* = 6.4Hz, 1H, H-1'') | 3.83 (*t*, *J* = 6.4Hz, 1H, H-1'') | 3.83 (*t*, *J* = 6.4Hz, 1H, H-1'') | 3.83 (*t*, *J* = 6.6Hz, 2H, H-1'') |
| 1.71 (*q*, 2H, H-2'') | 1.71 (*q*, 2H, H-2'') | 1.71 (*q*, 2H, H-2'') | 1.71 (*q*, 2H, H-2'') |
| 1.41 (*m*, 2H ,H-11'') | 1.41 (*m*, 2H ,H-9'') | 1.41 (*br*, 2H, H-7'') | 1.42 (*m*, 2H, H-5'') |
| 1.29 (*br*, 16H, H-3''to H-10'') | 1.32 (*br*, 12H, H-3''to H-8'') | 1.32 (*br*, 8H, H-3''to H-6'') | 1.31 (*br*, 4H, H-3'', H-4'') |
| 0.90 (*t*, 3H, H-12'') | 0.91 (*t*, 3H, H-10'') | 0.91 (*t*, 3H, H-8'') | 0.93 (*t*, 3H, H-6'') |

Table 8: $^{13}$C-NMR ($CDCl_3$, 100.6 MHz) data ($\delta_{ppm}$) for compound **44**, **45**, **46** and **47**.

| Carbon | **44** | **45** | **46** | **47** |
|---|---|---|---|---|
| 2,3 | 153.1 | 153.2 | 153.0 | 153.0 |
| 5,7 | 121.9 | 121.9 | 121.9 | 122.0 |
| 8.9 | 129.1 | 129.1 | 129.2 | 129.2 |
| 1’ | 141.3 | 141.5 | 141.1 | 141.1 |
| 2’ | 115.1 | 115.1 | 115.0 | 115.1 |
| 3’ | 158.9 | 158.8 | 158.9 | 158.9 |
| 4’ | 116.0 | 115.9 | 116.1 | 116.1 |
| 5’ | 140.1 | 140.3 | 140.2 | 139.8 |
| 6' | 117.6 | 117.5 | 117.5 | 117.7 |
| 1’’ | 68.0 | 68.0 | 68.0 | 68.0 |
| 2’’ | 29.6 | 29.6 | 29.3 | 29.0 |
| 3’’ | 26.0 | 26.0 | 26.0 | 25.6 |
| 4’’ | 29.1 | 29.4 | 29.3 | 31.5 |
| 5’’ | 29.6 | 29.4 | 29.1 | 22.6 |
| 6’’ | 29.6 | 29.4 | 31.8 | 14.1 |
| 7’’ | 29.6 | 29.1 | 22.7 | - |
| 8’’ | 29.6 | 31.9 | 14.1 | - |
| 9’’ | 29.4 | 22.7 | - | - |
| 10’’ | 31.9 | 14.1 | - | - |
| 11’’ | 22.7 | - | - | - |
| 12’’ | 14.1 | - | - | - |

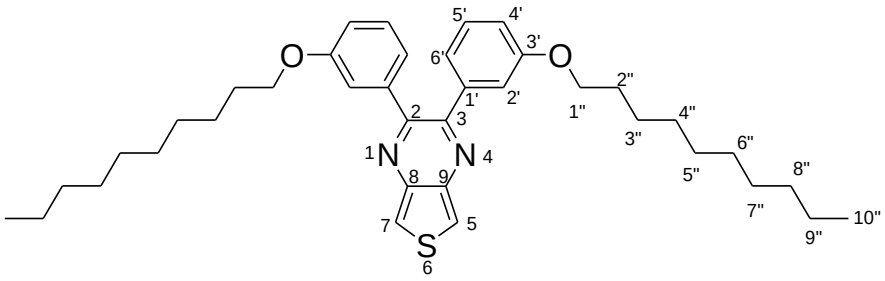


**45**

The UV-Vis spectrum of **45** was recorded in $CHCl_3$ and showed two absorption maxima at 255 and 336 nm (Figure 5) which are attributable to the π -π* and n- π* transitions, respectively . The FT-IR spectrum of **45** (Appendix 45) showed bands at 3069 and 2920 $cm^{-1}$ due to C-H stretching of benzene ring and stretching vibrations of the $CH_3$, respectively. The C=N and C=C ring stretching bands were observed at 1577 and 1441 $cm^{-1}$, respectively. The asymmetric and symmetric C-O-C stretching bands appeared at 1222 and 1022 $cm^{-1}$, respectively.

The $^1$H-NMR spectrum of **45** (Appendix 22) showed a triplet at δ 0.91 (3H) due to the terminal methyl groups. The broad signal at δ 1.32 integrated for twelve protons corresponding to six methylene groups. The two-proton multiplet at δ 1.49 was assigned to H-9'' and the quintet at δ 1.71 is due to H-2". The signal at δ 3.83 (2H, *t, J* = 6.4 Hz) is assigned to H-1''. The aromatic proton signals appeared at δ 6.91 (1H, *d, J* = 7.8 Hz), 7.00-7.02 (2H, *unresolved*) and, 7.21 (1H, *t, J* = 7.8 Hz) are assigned to H-4', H-2', H-6' and H-5', respectively. The signal at δ 8.07 (1H, *s*) is due to the thiophene ring protons H-5 and H-7 (Table-7).

The $^{13}$C-NMR and DEPT-135 spectra of **45** (Appendix 23 and Appendix 24, respectively) in $CDCl_3$ displayed nineteen carbon signals corresponding to four quaternary, five methine, one methyl and nine methylene carbon signals. The quaternary carbon signals appeared at δ 158.8, 153.2, 141.5 and 129.1 and are attributed to C-3', C-3, C-1' and C-9, respectively. The five methine carbon signals at δ 115.1, 115.9, 117.5, 121.9 and 140.3 are ascribed to C-2', C-4', C-6', C-5 and C-5', respectively. The signal at δ 68.0 is due to the oxygen-bearing carbon of the *n*-decyl group. The remaining nine methylene signals appeared between δ 31.9 and 22.7. The signal at δ 14.1 is due to terminal methyl groups (Table 8). The IR, UV, $^1$H-NMR, $^{13}$C-NMR and DEPT-135 data agree very well with the structure of compound **45**.

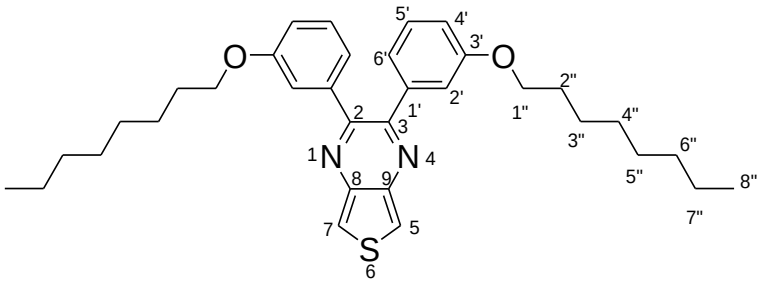

**46**

The UV-Vis spectrum of **46** was recorded in $CHCl_3$ and showed two absorption maxima at 257 and 354 nm (Figure 5) which correspond to π -π* and n- π* transitions, respectively. The FT-IR spectrum of **46** (Appendix 46) showed a band at 3067 $cm^{-1}$ due to C-H stretching of the aromatic rings. The band at 2923 $cm^{-1}$ is due to C-H stretching vibration of the $CH_3$. The imine C=N band and C=C stretching band of the rings appeared at 1600 and 1440 $cm^{-1}$, respectively. The asymmetric and symmetric C-O-C stretching bands appeared at 1222 and 1045 $cm^{-1}$, respectively.

The $^{1}$H-NMR spectrum of **46** (Appendix 19) showed a triplet at δ 0.91 due to the terminal methyl groups. The broad signal centered at δ 1.32 which integrated for eight protons is due to four methylene groups. The signals at δ 1.41 (2H, *br*) and 1.71 (2H, quintet) are assigned to H-7'' and H-2'', respectively. The signal at δ 3.83 (2H, *t*, *J* = 6.4 Hz) is assigned to H-1''. The aromatic proton signals appeared at δ 6.91 (1H, *d*, *J* = 7.8 Hz, H-4'), 7.00 – 7.13 (2H, *unresolved*, H-2' and H-6'), 7.21 (1H, *t*, *J* = 7.8 Hz, H-5'). The signal at δ 8.09 (1H, *s*) is assigned to H-5 and H-7 (Table 7).

The $^{13}$C-NMR and DEPT-135 spectra of **46** (Appendix 20 and Appendix 21, respectively**)** in $CDCl_3$ displayed seventeen carbon signals corresponding to four quaternary, five methine, one methyl and seven methylene carbon signals. The quaternary carbon signals at δ 158.9, 153.0, 141.1 and 129.2 are assigned to C-3', C-3, C-1' and C-9, respectively. The five methine carbon signals at δ 115.1, 116.0, 117.5, 121.9 and 140.2 are ascribed to C-2', C-4', C-6', C-5 and C-5', respectively. The signal at δ 68.05 is due to the oxygen-bearing carbon of the *n*-octyl group. The remaining seven methylene signals appeared between δ 31.8 and 22.7. The signal at δ 14.1 is attributed to the terminal methyl groups (Table 8). The above spectroscopic data agree very well with the structure of compound **46**.

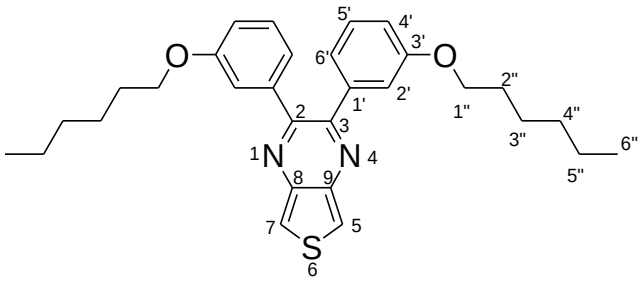

**47**

The UV-Vis spectrum of **47** was recorded in $CHCl_3$ and showed two absorption maxima at 256 and 352 nm (Figure 5) indicating the presence of conjugation in the structure of the compound. The FT-IR spectrum of **47** (Appendix 47) showed bands at 3108 and 2930 $cm^{-1}$ due to C-H stretching of the aromatic rings and stretching vibrations of the $CH_3$, respectively. The band at 1599 $cm^{-1}$ is typical of C=N stretching of imine and the band at 1436 $cm^{-1}$ is due to C=C stretching of the rings. In addition, the asymmetric and symmetric C-O-C stretching bands appeared at 1289 and 1033 $cm^{-1}$, respectively.

The $^1$H-NMR spectrum of compound **47** (Appendix 16) in $CDCl_3$ showed a signal at δ 0.93 (3H, *t, J* = 6.8 Hz) indicating the presence of terminal methyl groups in the compound. A broad signal centered at δ 1.31 integrating for four protons is due to the two methylene groups H-3'' and H-4''. The signals at δ 1.42 (2H, *m*) and 1.71 (2H, quintet) are assigned to H-5'' and H-2'', respectively. The signal at δ 3.83 (2H, *t, J* = 6.6 Hz) is assigned to H-1''. The aromatic proton signals appeared at δ 6.92 (1H, *dt,*), 7.00 – 7.02 (2H, *unresolved*) and, 7.22 (1H, *t, J* = 7.8 Hz) and are assigned to H- 4', H- 6', H-2' and H-5, respectively. The signal at δ 8.12 (1H, *s*) is assigned to H-5 (and H-7) the thiophene protons α to the sulfur (Table 7).

The $^{13}$C-NMR and DEPT-135 spectra of **47** (Appendix 17 and Appendix 18, respectively) in $CDCl_3$ displayed fifteen carbon signals due to four quaternary, five methine, one methyl and five methylene carbon signals. The quaternary carbon signals at δ 158.9, 153.0, 141.1 and 129.2 are attributed to C-3', C-3, C-1' and C-9, respectively. The five methine carbon signals at δ 115.1, 116.1, 117.7, 122.0 and 139.8 are ascribed to C-2', C-4', C-6', C-5 and C-5', respectively. The signal at δ 68.0 is due to C-1''. The remaining four methylene carbon signals appeared between δ 31.5 and 22.6. The signal at δ 14.0 is attributed to the terminal methyl groups (Table 8). The IR,

UV, $^{1}$H-NMR, $^{13}$C-NMR and DEPT-135 agree with the assignment of structure **47** for the compound.

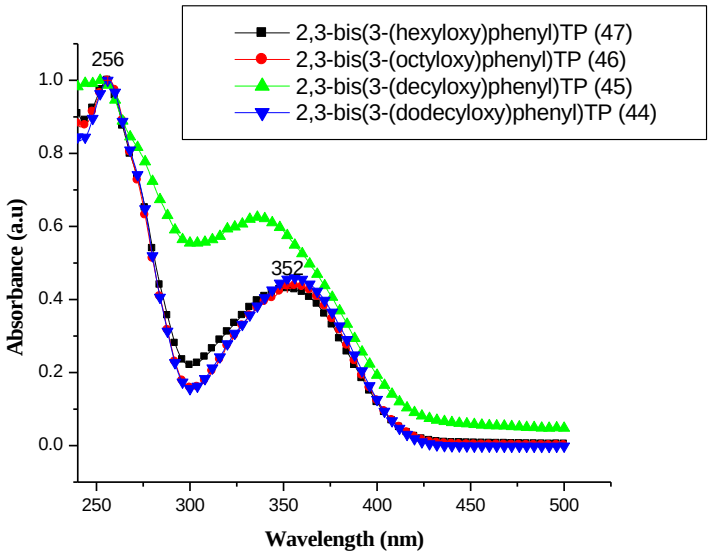


Figure 5: UV-Vis spectra of monomers **44** (blue), **45** (green), **46** (red) and **47** (black).

### 4.2.2. Bromination of the thieno[3,4-*b*]pyrazines 44-47

Thieno[3,4-*b*]pyrazines **44**-**47** were subjected to bromination reactions using NBS in DMF or NBS in $CHCl_3$:acetic acid (1:1) to afford the corresponding dibromides **48**-**51** (Scheme 13).

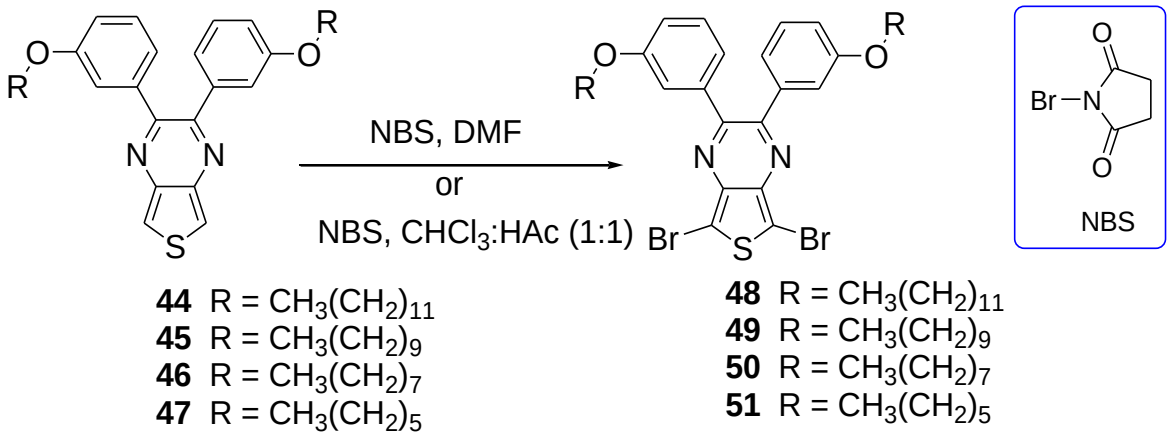


Scheme 13: Conversion of thieno[3,4-*b*]pyrazines **44**-**47** to the corresponding dibromides.

The syntheses and characterization of the dibromides are described below.

**4.2.2.1. Synthesis of monomers 48 and 50**

5,7-Dibromo-2,3-bis(3-(dodecyloxy)phenyl)thieno[3,4-*b*]pyrazine (**48**) and 5,7-dibromo-2,3-bis(3-(octyloxy)phenyl)thieno[3,4-*b*]pyrazine (**50**) were synthesized by bromination of 2,3-bis(3-(dodecyloxy)phenyl)thieno[3,4-*b*]pyrazine (**44**) and 2,3-bis(3-(octyloxy)phenyl)thieno[3,4-*b*]pyrazine (**46**), respectively, using *N*-bromosuccinimide in DMF in dark (Scheme 14). These compounds were obtained in pure form after silica gel column chromatography and were characterized using different spectroscopic techniques as described below. Bromination with NBS in DMF as compared to $CHCl_3$/HAC gives better result. Bromination with NBS in $CHCl_3$/HAC was obtained mixture of products because of their poor solubility.

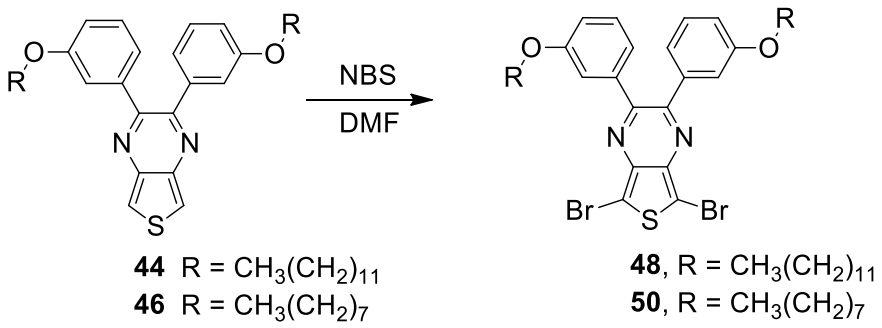


Scheme 14: Synthesis of dibromides **48** and **50**.

The UV-Vis spectrum of **48** was recorded in $CHCl_3$ and showed two absorption maxima at 267 and 371 nm (Figure 6) which correspond to π -π* and n- π* transitions, respectively. The FT-IR spectrum of **48** (Appendix 48) showed band at 2919 $cm^{-1}$ due to stretching of alkane. The band at 1604 $cm^{-1}$ is attributed to the imine C=N vibration. The asymmetric and symmetric stretching bands of the C-O-C groups appeared at 1222 and 1035 $cm^{-1}$, respectively. The band at 1464 $cm^{-1}$ is due to the stretching vibration of the ring C=C bonds. The bands due to out-of-plane C-H and C=C bending vibrations of the aromatic and rings appeared at 983 and 795 $cm^{-1}$, respectively. The C—Br stretching band appeared at 523 $cm^{-1}$.

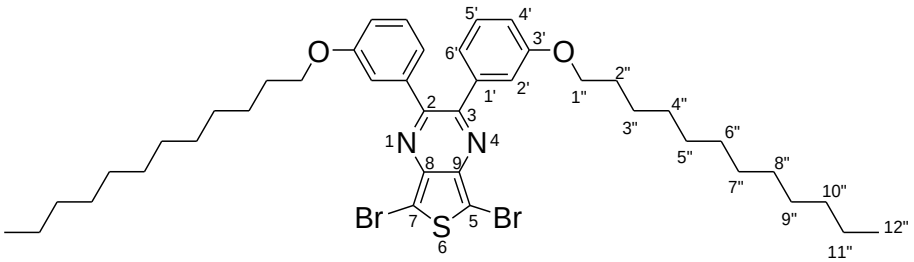

**48**

The $^{1}$H-NMR spectrum of **48** (Appendix 34) in $CDCl_3$ revealed the presence of a triplet at δ 0.90 indicating the presence of terminal methyl groups. A broad signal centered at δ 1.29 integrating for sixteen protons is due to eight methylene groups. The signals at δ 1.42 (2H, *m*) and 1.72 (2H, quintet) are assigned to H-11'' and H-2'', respectively. The signal at δ 3.83 (2H, *t, J* = 6.6 Hz) is assigned to H-1''. The aromatic proton signals at δ 6.92 (1H, *dd, J* = 8.0 Hz, 2.4 Hz), 7.03 (*d, J* = 8.0 Hz, 1H), 7.05 (1H, *d, J* = 2.4 Hz) and 7.20 (1H, *t, J* = 8.0 Hz) are assigned to H-4', H-6', H-2' and H-5', respectively (Table 9).

The $^{13}$C-NMR and DEPT-135 spectra of **48** (Appendix 35 and Appendix 36, respectively) in $CDCl_3$ showed twenty-one carbon signals corresponding to five quaternary, four methine, one methyl and eleven methylene carbons. The quaternary carbon signals at δ 158.8, 154.5, 139.4, 139.2 and 104.9 are attributed to C-3', C-3, C-1', C-9 and C-5, respectively. The four methine carbon signals at δ 115.4, 116.3, 129.1 and 122.2 are ascribed to C-2', C-4', C-5' and C-6', respectively. The signal at δ 68.1 is due to C-1''. The remaining ten methylene carbon signals appeared between δ 31.9 and 22.7. The signal at δ 14.1 is due to terminal methyl group (Table 10). The UV, IR, $^{1}$H-NMR, $^{13}$C-NMR and DEPT-135 data agree very well with structure **48**.

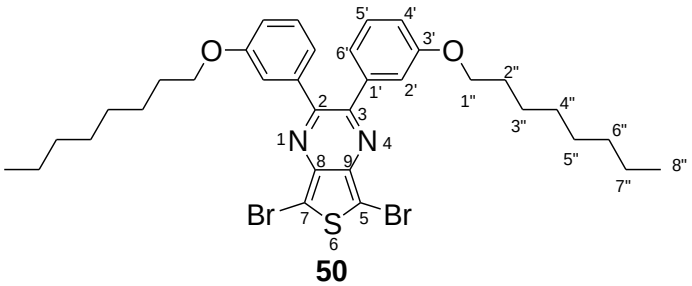

**50**

The UV-Vis spectrum of **50** was recorded in $CHCl_3$ and showed two absorption maxima at 267 and 367 nm (Figure 6) due to π -π* and n- π* transitions, respectively. The FT-IR spectrum of **50** (Appendix 49) showed a band at 2920 $cm^{-1}$ due to C-H stretching of $CH_3$ group. The bands at

1603 and 1466 $cm^{-1}$ are attributed to the C=N of imine and the ring C=C stretching vibrations, respectively. The asymmetric and symmetric C-O-C stretching bands appeared at 1221 and 1032 $cm^{-1}$, respectively. Out-of -plane C-H bending vibration of the aromatic rings appeared at 981 $cm^{-1}$ and the ring C=C bending vibration at 796 $cm^{-1}$. The band at 524 $cm^{-1}$ is due to C—Br stretching.

Table 9: $^{1}$H-NMR (400.13MHz, $CDCl_3$) data ($\delta_{ppm}$) of compound **48**, **50** and **51**.

| **48** | **50** | **51** |
|---|---|---|
| 7.20 | 7.20 | 7.21 |
| ( *t*, *J* = 8.0 Hz, 1H, H-5' ) | ( *t*, *J* = 8.0 Hz, 1H, H-5' ) | ( *t*, *J* = 8.2 Hz, 1H, H-5') |
| 7.05 | 7.05 | 7.05 |
| (*d*, *J* = 2.4 Hz, 1H, H-2') | (t, *J* = 1.6 Hz, 1H, H-2') | (*d*, *J* = 1.6 Hz, 1H, H-2') |
| 7.03 | 7.03 | 7.03 |
| ( *d*, *J* = 8.0 Hz,1H, H-6') | ( *d*, *J* = 8.0 Hz, 1H, H-6') | (*d*, *J* = 8.2 Hz, 1H, H-6') |
| 6.92 | 6.92 | 6.92 |
| (*dd*, *J* = 8.0 Hz, 2.4 Hz, 1H, H-4' ) | (*dd*, *J* = 8.0 Hz, 1.6.Hz, 1H, H-4') | (*dd*, *J* = 8.2 Hz, 1.6 Hz, 1H, H-4' ) |
| 3.83 | 3.83 | 3.83 |
| ( *t*, *J* = 6.6 Hz, 2H, H-1'') | ( *t*, *J* = 6.6 Hz, 2H, H-1'') | ( *t*, *J* = 6.6 Hz, 2H, H-1'') |
| 1.72 | 1.72 | 1.72 |
| ( *q*, 2H, H-2'' ) | ( *q*, 2H, H-2'' ) | ( *q*, 2H, H-2'' ) |
| 1.42 | 1.42 | 1.42 |
| ( *m*, 2H, H-11'' ) | ( *m*, 2H, H-7'' ) | ( *m*, 2H, H-5'' ) |
| 1.29 | 1.32 | 1.34 |
| ( *s*, 16H, H-3'' to H-10'') | ( *s*, 8H, H-3'' to H-6'') | ( *s*, 4H, H-3'' to H-4'') |
| 0.90 | 0.90 | 0.93 |
| ( *t*, *J* = 6.8 Hz, 3H, H-12'' ) | ( *t*, 3H, H-8'' ) | ( *t*, *J* = 6.8 Hz, 3H, H-6'' ) |

The $^{1}$H-NMR spectrum of **50** (Appendix 31) in $CDCl_3$ displayed a triplet at δ 0.90 due to the terminal methyl groups. The broad signal centered at δ 1.32, which integrated for eight protons,

is due to four methylene groups. The signals at δ 1.42 (2H, *m*) and 1.72 (2H, quintet) are assigned to H-7'' and H-2'', respectively. The signal at δ 3.83 (2H, *t*, *J* = 6.6 Hz) is due to H-1''. The aromatic proton signals at δ 6.92 (1H, *dd*, *J* = 8.0 Hz, 1.6 Hz), 7.03 (1H, *d*, *J* = 8.0 Hz), 7.05 (1H, *t*, *J* = 1.6 Hz) and 7.20 (1H, *t*, *J* = 8.0 Hz) are assigned to H-4', H-6', H-2' and H-5', respectively (Table 9).

Table 10: $^{13}$C-NMR ($CDCl_3$, 100.6 MHz) data ($\delta_{ppm}$) for compound **48**, **50** and **51**.

| Carbon | **48** | **50** | **51** |
|---|---|---|---|
| 2,3 | 154.5 | 154.5 | 154.5 |
| 5,7 | 104.9 | 104.9 | 104.9 |
| 8,9 | 139.2 | 139.2 | 139.2 |
| 1' | 139.4 | 139.4 | 139.4 |
| 2' | 115.4 | 115.4 | 115.4 |
| 3' | 158.8 | 158.8 | 158.8 |
| 4' | 116.3 | 116.3 | 116.3 |
| 5' | 129.1 | 129.1 | 129.1 |
| 6' | 122.2 | 122.2 | 122.2 |
| 1'' | 68.1 | 68.1 | 68.0 |
| 2'' | 29.7 | 29.3 | 29.0 |
| 3'' | 26.0 | 26.0 | 25.7 |
| 4'' | 29.6 | 29.2 | 31.5 |
| 5'' | 29.4 | 29.1 | 22.6 |
| 6'' | 29.4 | 31.8 | 14.1 |
| 7'' | 29.4 | 22.7 | - |
| 8'' | 29.6 | 14.1 | - |
| 9'' | 29.1 | - | - |
| 10'' | 31.7 | - | - |
| 11'' | 22.7 | - | - |
| 12'' | 14.1 | - | - |

The $^{13}$C-NMR and DEPT-135 spectra of **50** (Appendix 32 and Appendix 33, respectively) displayed seventeen carbon signals corresponding to five quaternary, four methine, one methyl and seven methylene carbon. The quaternary carbon signals at δ 158.8, 154.5, 139.4, 139.2 and 104.9 are attributed to C-3', C-3, C-1', C-9 and C-5, respectively. The four methine carbon signals at δ 115.4, 116.3, 129.1 and 122.2 are ascribed to C-2', C-4', C-5' and C-6', respectively.

The signal at δ 68.0 is due to the oxygen-bearing carbon (C-1") of the *n*-octyl group. The remaining six methylene carbon signals appeared between at δ 31.8 and 22.7. The presence of terminal methyl groups was evident from the carbon signal at δ 14.1 (Table 10). The UV, IR, $^{1}$H-NMR, $^{13}$C-NMR and DEPT-135 data agree very well with structure **50**.

### 4.2.2.2. Synthesis of monomers 49 and 51

5,7-Dibromo-2,3-bis(3-(decyloxy)phenyl)thieno[3,4-*b*]pyrazine (**49**) and 5,7-dibromo-2,3-bis(3-(hexyloxy)phenyl)thieno[3,4-*b*]pyrazine (**51**) were synthesized by bromination of thienopyrazines **45** and **47**, respectively, using *N*-bromosuccinimide in $CHCl_3/CH_3COOH$ (1:1) in the dark as shown in Scheme 15. Compound **51** was obtained in a pure form after purification by silica gel column chromatography. However, compound **49** could not be obtained in a pure form even after column chromatography on silica gel. The difficulty with this route is due to formation of mixture of mono- and dibrominated products, which was difficult to separate because of their poor solubility and similar Rf values.

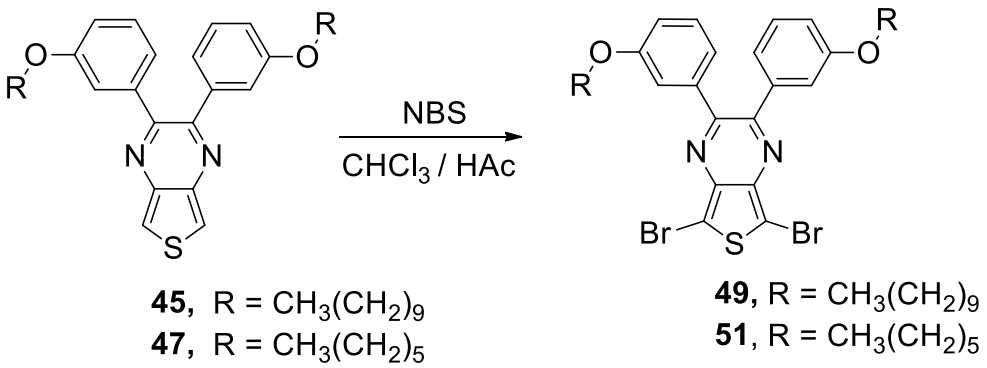


Scheme 15: Synthesis of compounds **49** and **51**.

The UV-Vis spectrum of **51** (Figure 6) was recorded in $CHCl_3$ and showed two absorption maxima at 266 and 366 nm due to π -π* and n- π* electronic transitions, respectively. The FT-IR spectrum of **51** (Appendix 50) showed a band at 3061cm$^{-1}$ due to C-H stretching of the aromatic rings. The band at 2934 cm$^{-1}$ is ascribed to C-H stretching of alkane. The band at 1602 cm$^{-1}$ is attributed to the C=N stretching of imine. The aryl ether displayed an asymmetric and symmetric stretching band of C-O-C appeared at 1221 and 1032 cm$^{-1}$, respectively. The C=C ring stretching and bending vibrations occurred at 1442 cm$^{-1}$ and 796 cm$^{-1}$, respectively. Bands due to out-of-

plane C-H bending vibration of aromatic compound and C−Br stretching were observed at 983 $cm^{-1}$ and 523 $cm^{-1}$, respectively.

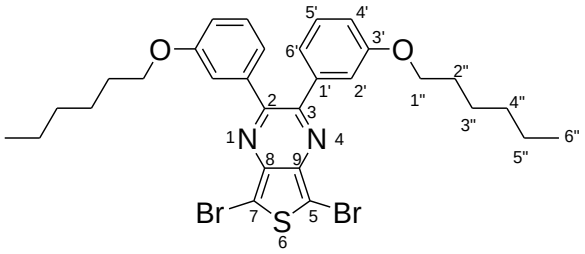


**51**

The $^{1}$H-NMR spectrum of **51 (**Appendix 28) in $CDCl_3$ showed a triplet at δ 0.93 due to the terminal methyl groups. A broad signal centered at δ 1.34, which integrated for four protons, is due to two methylene groups. The signal at δ 1.43 (2H, *m*) and 1.72 (2H, quintet) are assigned to H-5'' and H-2'', respectively. The signal at δ 3.83 (2H, *t*, *J* = 6.6 Hz) is assigned to H-1''. The aromatic proton signals at δ 6.92 (1H, *dd*, *J* = 8.2 Hz, 1.6 Hz), 7.03 (1H, *d*, *J* = 8.2 Hz), 7.05 (*d*, 1H, *J* = 1.6 Hz) and 7.21 (1H, *t*, *J* = 8.2 Hz) are due to H-4', H-6', H-2' and H-5', respectively (Table 9).

The $^{13}$C-NMR and DEPT-135 spectra of **51** (Appendix 29 and Appendix 30, respectively) in $CDCl_3$ displayed fifteen carbon signals corresponding to five quaternary, four methine, one methyl and five methylene carbons. The quaternary carbon signals at δ 158.8, 154.5, 139.4, 139.2 and 104.9 are attributed to C-3', C-3, C-1', C-9 and C-5, respectively. The four methine carbon signals at δ 115.4, 116.3, 129.1 and 122.2 are ascribed to C-2', C-4', C-5' and C-6', respectively. The signal at δ 68.0 is due to the oxygenated carbon C-1'' of the *n*-hexyl group. The remaining four methylene signals were observed between δ 31.5 and 22.6. The presence of a signal at δ 14.0 confirmed the presence of terminal methyl groups (Table 10). The IR, UV, $^{1}$H-NMR, $^{13}$C-NMR and DEPT-135 data are in agreement with structure **51**.

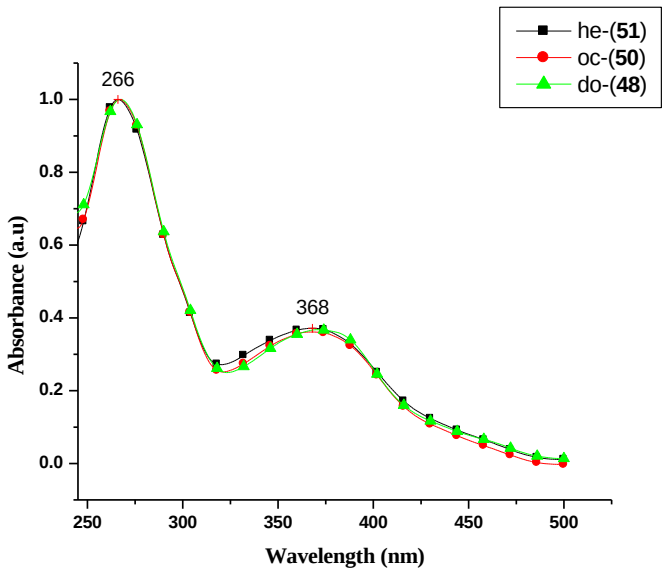


Figure 6: UV-Vis spectra of monomers **48**, **50** and **51**.

### 4.3. Syntheses of polymers

Seven thieno[3,4-*b*]pyrazine-based donor-acceptor polymers, namely, poly[2,3-bis(3-(dodecyloxy)phenyl)thieno[3,4-*b*]pyrazine-5,7-diyl-*alt*-thiophene-2,5-diyl] (**52**, **52'**), poly[2,3-bis(3-(decyloxy)phenyl)thieno[3,4-*b*]pyrazine-5,7-diyl-*alt*-thiophene-2,5-diyl] (**53**), poly[2,3-bis-(2,3-bis(3-(octyloxy)phenyl)thieno[3,4-*b*]pyrazine-5,7-diyl-*alt*-thiophene-2,5-diyl] (**54**, **54'**) and poly[2,3-bis(3-(hexyloxy)phenyl)thieno[3,4-*b*]pyrazine-5,7-diyl-*alt*-thiophene-2,5-diyl] (**55**, **55'**) were synthesized and characterized. The polymers were synthesized by using the Stille cross coupling polymerization and the direct heteroarylation polymerization techniques. For the Stille cross coupling polymerization reactions, the monomers used were the dibromides **48**, **50**, and **51** and 2,5-bis(tributylstannyl)thiophene (**56**). On the other hand, the monomers used for the direct heteroarylation polymerization reactions were thieno[3,4-*b*]pyrazines **44**, **45**, **46** and **47** and 2,5-dibromothiophene (**11**) as described below.

#### 4.3.1. Syntheses of polymers by direct heteroarylation polymerization.

The four thieno[3,4-*b*]pyrazine-based polymers (**52-55**) were synthesized as shown in Scheme 16 by using a modified literature procedure.[53] Thus, equimolar quantities of thieno[3,4-*b*]pyrazines

**44**, **45**, **46** and **47** with 2,5-dibromothiophene (**11**) were reacted using $Pd(OAc)_2$ as a catalyst in the presence of pivalic acid in DMAc. All polymers were purified by successive Soxhlet extractions with methanol and acetone to remove catalyst residue and oligomers and then with $CHCl_3$. Polymers **52** (36.4%), **53** (39.0%), **54** (69.9%) and **55** (45.3%) were obtained as deep green solids. The polymers were characterized by $^1$HNMR and UV-Vis spectroscopy.

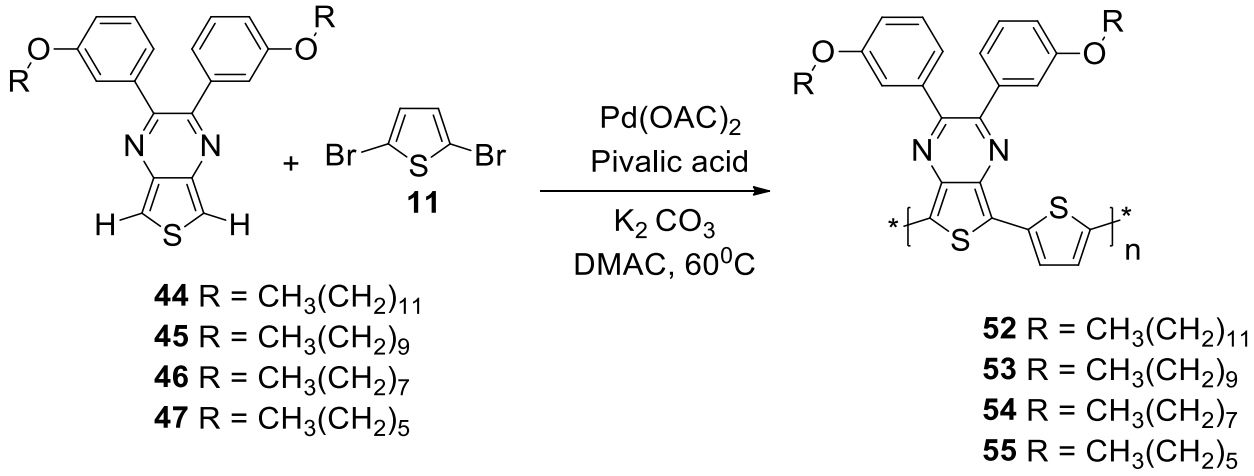


Scheme 16: Synthesis of polymers **52-55**.

### 4.3.2. Syntheses of polymers by Stille-cross-coupling reaction

The three thieno[3,4-*b*]pyrazine-based donor-acceptor polymers **52'**, **54'** and **55'** were synthesized using modified literature procedure.[54] Thus, equimolar quantities of 2,5-dibromothieno[3,4-*b*]pyrazines **48**, **50**, and **51** with 2,5-bis(tributylstannyl)thiophene (**56**) were reacted in the presence of $Pd(PPh_3)_4$ in anhydrous DMF and anhydrous toluene (Scheme 17). The polymers were purified by Soxhlet extraction with acetone and methanol to remove oligomers and then with $CHCl_3$. Polymers **52'** (69.2%), **54'** (74.9%) and **55'** (10%) were obtained as deep-green solids. The polymers were characterized by $^1$H-NMR, UV-Vis and square-wave voltammetry (SWV).

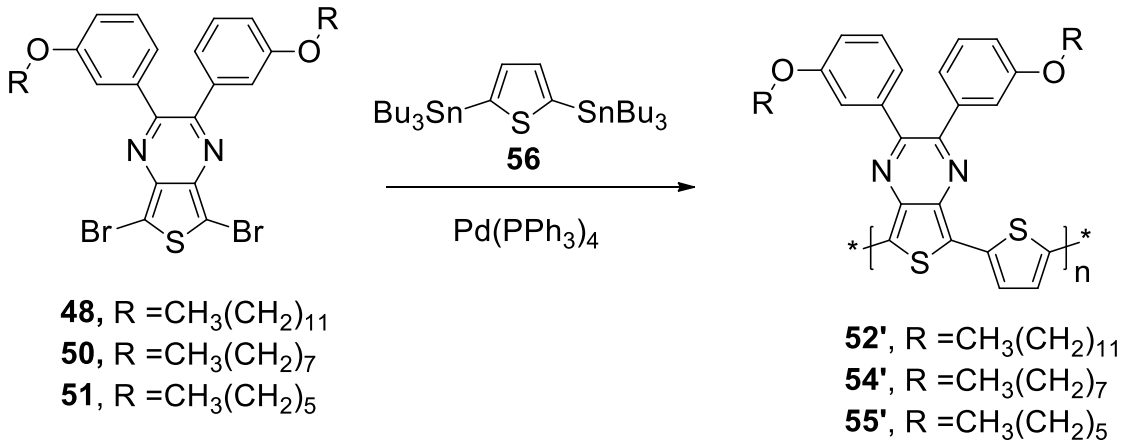


**48,** R =$CH_3(CH_2)_{11}$
**50,** R =$CH_3(CH_2)_7$
**51**, R =$CH_3(CH_2)_5$

**52'**, R =$CH_3(CH_2)_{11}$
**54'**, R =$CH_3(CH_2)_7$
**55'**, R =$CH_3(CH_2)_5$

Scheme 17: Synthesis of polymer **52'**, **54'** and **55'**.

### 4.3.3. Optical properties of the polymers

Optical spectra of conjugated polymers provide information about the electronic structure and the bandgap. The energy gap for π-π* transition is directly affected by the degree of conjugation. The higher the conjugation length the smaller the energy gap for the transition between the two orbitals. The UV-Vis absorption spectra of polymers **52**, **52'**, **53**, **54**, **54'**, **55** and **55'** were measured in chloroform solutions and as thin films on glass slides. The solution and thin film spectra of the polymers exhibited broad absorption ranging from 300 – *ca* 1150 nm with two absorption maxima as shown in Table 11 and Figures 7 to 10.

Table 11: Optical properties of polymers **52**, **53**, **54**, **55**, **52'**, **54'** and **55**

| | **Solution** | | | **Film** | | |
|---|---|---|---|---|---|---|
| | $\lambda_{max}$ (nm) | λonset | $E_g^{op}$ (eV) | $\lambda_{max}$ (nm) | λonset | $E_g^{op}$ (eV) |
| **52** | 387, 806 | 1056 | 1.17 | 403, 819 | 1160 | 1.07 |
| **53** | 362, 727 | 1114 | 1.22 | 371, 756 | 1140 | 1.09 |
| **54** | 386, 829 | 1130 | 1.10 | 404, 861 | 1159 | 1.06 |
| **55** | 330, 749 | 1076 | 1.15 | 363, 757 | 1135 | 1.09 |
| **52'** | 393, 950 | 1228 | 1.01 | 413, 967 | 1293 | 0.96 |
| **54'** | 407, 996 | 1290 | 0.96 | 424, 1000 | 1324 | 0.94 |
| **55'** | 330, 1024 | 1290 | 0.96 | 384, 1111 | 1338 | 0.93 |

The UV-Vis spectra of polymers **52**, **53**, **54** and **55** in $CHCl_3$ solution showed two absorption maxima in the range between 330 and 829 nm (Figure 7, Table 11). The optical absorption spectra (Figure 8) of **52**, **53**, **54** and **55** were recorded as thin films on glass slides. The onsets of absorption of **52**, **53**, **54** and **55** extended up to 1160 nm. The long wavelength absorption maxima appeared at 819, 756, 861 and 757 nm for **52**, **53**, **54** and **55**, respectively. The optical bandgaps ($E_g^{opt}$) were estimated to be 1.07, 1.09, 1.06 and 1.09 eV for polymer **52**, **53**, **54** and **55**, respectively, from the onsets of absorption in the thin film spectra while band-gaps of 1.17, 1.22, 1.10, 1.15, respectively, were estimated from the onsets of absorption in the solution spectra (Table 11). Polymers **52-55** exhibit bathochromic shifts of their absorptions in the film state compared with the solution state, presumably as a result of donor–acceptor structures leading to strong π–π stacking interactions.

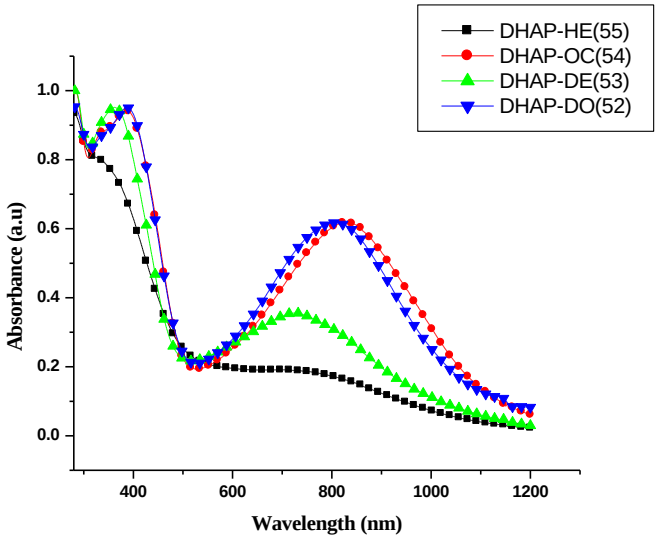


Figure 7: Uv-Vis absorption spectra of **52** (blue), **53** (green), **54** (red) and **55** (black) in $CHCl_3$ solution.

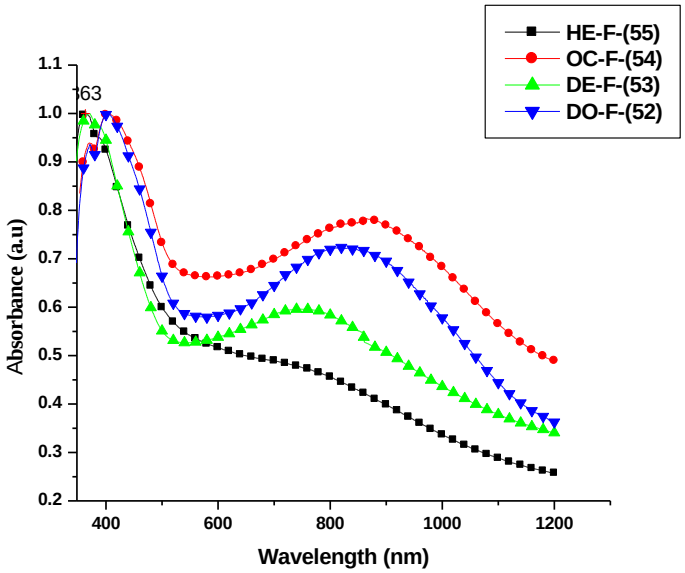


Figure 8: Uv-Vis absorption spectra of **52** (blue), **53** (green), **54** (red) and **55** (black) as thin films.

The chloroform solutions of polymers **52'**, **54'** and **55'** exhibited broad absorptions extending into the near-infrared region with two absorption maxima in the range between 330 and 1024 nm (Figure 9, Table 11). The long wavelength absorption maxima appeared at 950, 996 and 1024 nm for **52'**, **54'** and **55'**, respectively. The optical absorption spectra of **52'**, **54'** and **55'** (Figure 10, Table 11) showed broad absorption in the range between 384 and 1111 nm. The long wavelength absorption maxima appeared at 967, 1000 and 1111 nm, respectively. Red shifts were observed in the thin-film spectra compared to the solution spectra presumably because of π–π interaction between the closely packed polymer backbones in the solid state and ICT transitions in the thin film.[33] The onsets of absorption in thin film spectra of **52'**, **54'** and **55'** appeared at 1293, 1324 and 1338 nm, respectively, which correspond to optical bandgaps of 0.96, 0.94 and 0.93 eV, respectively (Table 11).

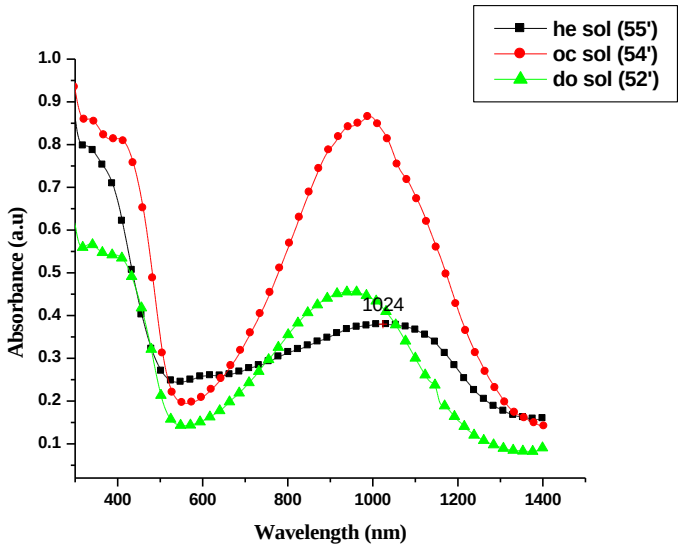


Figure 9: Uv-Vis absorption spectra of **52'** (green), **54'** (red) and **55'** (black) in $CHCl_3$ solution.

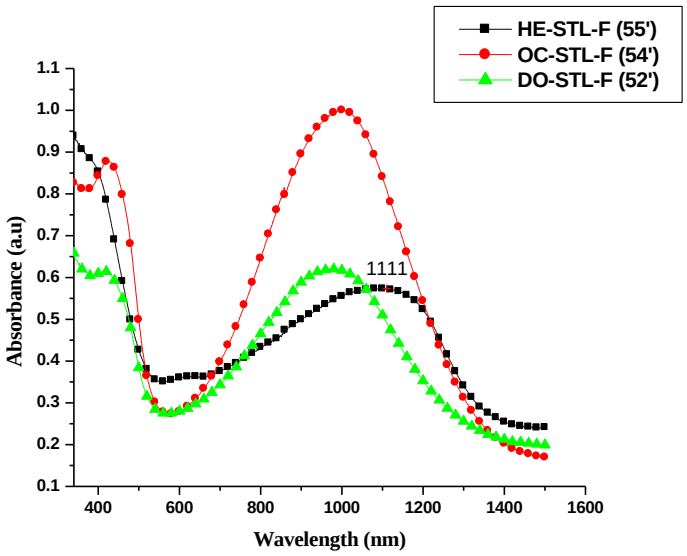


Figure 10: Uv-Vis absorption spectra of **52'** (green), **54'** (red) and **55'** (black) as thin films.

All of the polymers showed two distinct absorption bands around 300–410 nm which can be assigned to the π–π* transition while the long-wavelength absorption peaks can be attributed to intramolecular charge transfer between the thiophene donor and the thienopyrazine acceptor moieties. The bandgaps of polymers **52**, **52'**, **53**, **54**, **54'**, **55** and **55'** calculated from the onsets

of absorptions of thin films of the polymers were lower than the bandgaps calculated from the onsets of absorptions of the solution spectra. This difference may be due to solid state ordering compared to the disorder in solution.[16] Polymers synthesized by direct heteroarylation (**52-55)** exhibited different absorption maxima in comparison to those polymers synthesized by Stille-coupling reaction (**52'**, **54'** and **55'**) (Figure 7-10, Table 11). The thin films of the polymers obtained by Stille coupling showed red shift in their absorption spectra relative to those polymers( **52-55**) obtained by direct heteroarylation. The optical bandgaps ($E_g^{opt}$) of polymers **52-55** are very close to each other and lie between 1.06 and 1.09 eV, which are slightly higher than for polymers **52'**, **54'** and **55'** (~0.96-0.93 eV) (Table 11).

### 4.3.4. Electrochemical properties

Cyclic voltammetry (CV) was used to determine the HOMO and LUMO energy levels ($E_{HOMO}$ and $E_{LUMO}$, respectively) of polymers. Square-wave voltammetry (SWV) was used for similar materials to determine the HOMO and LUMO energy levels of polymers **52'** and **54'**. Square-wave voltammetry was found to be more sensitive than CV resulting in much clearer peaks in the voltammograms.[50] The onsets of oxidation potentials correspond to the HOMO levels, and the onsets of reduction potential correspond to the LUMO levels. From the values of $E_{ox,onset}$ and $E_{red,onset}$, HOMO and LUMO[55,56,57] as well as the electrochemical bandgaps ($E_g^{ec}$) of the polymers could be calculated using Equations 1-3.

$$E_{HOMO} = - (E_{ox,\ onset} + 4.4)\ (eV) \qquad (1)$$

$$E_{LUMO} = - (E_{red,\ onset} + 4.4)\ (eV) \qquad (2)$$

$$E_g^{ec} = E_{LUMO} - E_{HOMO} \qquad (3)$$

The estimated $E_g^{ec}$ values are somewhat higher than the $E_g^{op}$ values estimated from the onsets of absorption in the thin film spectra of the polymers, probably due to the barriers for charge transfer between the electrodes, the polymer films and the supporting electrolyte, resulting in lags between voltage input and current measurement.[33,58]

The square-wave voltammetry was conducted with a three-electrode setup consisting of platinum wires, both as working electrode and counter electrode and Ag/AgCl as reference electrode. A 0.10 M tetrabutylammoniumperchlorate ($Bu_4NClO_4$) in anhydrous acetonitrile was used as

supporting electrolyte at a scanning rate of 100 mV/s. The polymer films for electrochemical measurements were coated from chloroform solutions of the polymers.

The electrochemical properties of polymers **52'** and **54'** were studied using square-wave voltammetry (Figure 11). The oxidation-onset potentials of polymers **52'** and **54'** were 0.49 and 0.51 V, respectively. On the basis of these potentials, HOMO energy levels of polymers **52'** and **54'** were estimated to be -4.89 and -4.91eV, respectively. Similarly from reduction onset potentials, the LUMO energy levels were estimated to be -3.67 and -3.96 eV, respectively. The electrochemical bandgaps of polymers **52'** and **54'** were 1.22 and 0.95eV, respectively. The electrochemical bandgap of polymer **52'** was slightly larger than the electrochemical bandgap of **54'**. The bandgap values obtained from electrochemical and optical measurements agree well for polymer **54'**.

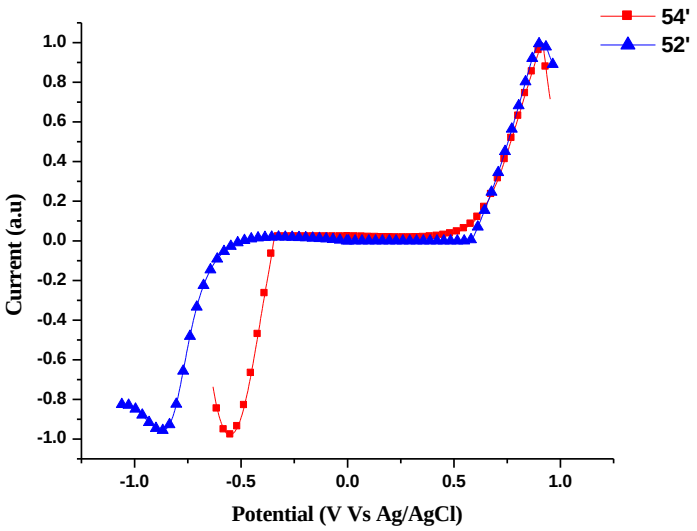


Figure 11: Square-wave voltammograms of polymers **52'** and **54'**.

## 5. Conclusion

Seven thieno[3,4-*b*]pyrazine-based donor-acceptor polymers, namely, poly[2,3-bis(3-(dodecyloxy)phenyl)thieno[3,4-*b*]pyrazine-5,7-diyl-*alt*-thiophene-2,5-diyl] (**52**, **52'**), poly[2,3-bis(3-(decyloxy)phenyl)thieno[3,4-*b*]pyrazine-5,7-diyl-*alt*-thiophene-2,5-diyl] (**53**), poly[2,3-bis-(2,3-bis(3-(octyloxy)phenyl)thieno[3,4-*b*]pyrazine-5,7-diyl-*alt*-thiophene-2,5-diyl] (**54**, **54'**) and poly[2,3-bis(3-(hexyloxy)phenyl)thieno[3,4-*b*]pyrazine-5,7-diyl-*alt*-thiophene-2,5-diyl] (**55**, **55'**) were synthesized and characterized. The polymers were prepared by employing the Stille cross coupling polymerization and the direct heteroarylation polymerization techniques. The polymers were deep green solids and soluble in common organic solvents like $CHCl_3$ and chlorobenzene. The polymers showed optical absorptions that extended up to *ca* 1150 nm. The optical bandgaps of the polymers synthesized by direct heteroarylation polymerization (**52**-**55**) and Stille-coupling polymerization (**52'**, **54'** and **55'**) had no significant differences. The electrochemical bandgap of polymer **52'** was slightly larger than the electrochemical bandgap of **54'**. Further studies of the physical properties such as molecular weight determination, charge carrier mobility, solar cell device fabrication and characterization, photoluminescence and electroluminescence properties, etc., are necessary to fully characterize the polymers.

# 6. Experimental

## 6.1. Materials and Methods

All of the compounds prepared in the course of the synthetic work were purified and characterized by UV-Vis, FT-IR and NMR techniques. $^{1}$H-NMR and $^{13}$C-NMR spectra were recorded on a Bruker Avance 400 spectrometer in $CDCl_3$ as a solvent and are reported in δ units. The UV-Vis spectra of the monomers and polymers were recorded on PERKIN-ELMER LAMBDA 950 UV/Vis/NIR spectrophotometer at room temperature. Infrared spectra were obtained using a PERKIN ELMER Spectrum 65 infrared spectrophotometer. Melting points were measured using Mettler-Toledo FP82HT hot stage with FP90 central processor and LEICA GALEN$^{TM}$ III microscope apparatus and are uncorrected. Cyclic voltammograms (CVs) were recorded on a BASi Epsilon-EC potentiostat using platinum electrodes at a scan rate of 100 $mV.s^{-1}$ and a Ag/Ag+ (0.10 M of $AgNO_3$ in acetonitrile) reference electrode in solution of 0.1 M of tetrabutylammonium perchlorate in acetonitrile.

## 6.2. Reagents

All reagents were purchased from commercial suppliers. The chemicals used were 2,5-dibromothiophene (Aldrich), potassium carbonate (Aldrich), anhydrous sodium sulfate (Aldrich), $Pd(OAc)_2$ (Fluka), *N*-bromosuccinimide (NBS) (Aldrich), 1-bromooctane, 1-bromohexane, 1-bromodecane and 1-bromododecane (Aldrich), DMF (Aldrich), $CHCl_3$ (Carlo-Erba), methanol (Carlo-Erba), diethyl ether (BDH), petroleum ether (Aldrich), acetone (Aldrich), ethyl acetate (Carlo-Erba), n-pentane (Aldrich), NaOH (Scharlau), toluene (Riedel-De Haën), propan-2-ol (BDH), ethanol (Carlo-Erba), acetic acid (Aldrich), iron metal (Fluka), tin powder (Fluka), tetrahydrofuran (Riedel-De Haën), KOH, acetonitrile (Aldrich), Conc.$H_2SO_4$ (Aldrich), fuming $H_2SO_4$ (Aldrich), fuming $HNO_3$ (Aldrich), conc.$HNO_3$ (Aldrich), 37% HCl (Aldrich), 3-hydroxybenzaldehyde (Aldrich), triethylamine (Riedel-De Haën), $CH_2Cl_2$ (Carlo-Erba), $NaHCO_3$, NaCN (Analar), thiamine hydrochloride (BDH), 3-methoxybenzaldehyde (Aldrich), n-hexane, DMSO (Aldrich), 48% HBr (Aldrich), pivalic acid, DMAc (Aldrich), EDTA (Aldrich). All reactions were carried out under nitrogen atmosphere. The progresses of reactions were monitored by analytical thin-layer chromatography using 0.25 mm pre-coated silica gel plates. Column chromatography was conducted on silica gel (70-230mesh) . 0.45 μm PTFE filters were

used to filter polymeric materials under reduced pressure. THF was freshly dried over sodium and benzophenone, prior to use.

## 6.3. Procedures

### 6.3.1. Syntheses of monomers.

#### 6.3.1.1. Synthesis of 2, 5-dibromo-3,4-dinitrothiophene ( 12)

A dried three-necked flask containing a mixture of conc. $H_2SO_4$ (11.27 mL), fuming $H_2SO_4$ (17.36 mL), and fuming $HNO_3$ (9.54 mL) was cooled in an ice bath and 2,5-dibromothiophene (3.00 mL, 6.4 g, 26.60 mmol) was added dropwise maintaining the temperature at 15 °C. After the addition was complete, the reaction mixture was stirred for an additional 4 hr at room temperature and then poured into ice (91 g). The solid product was collected by vacuum filtration, washed with cold water, dried and recrystallized from isopropanol to give **12** (6.0 g, 67.9 %) as a shiny yellow solid.

Mp: 137–138.8$^{o}$C; Lit. mp: 135 –137$^{o}$C; $^{13}$C- NMR (100 MHz, $CDCl_3$): δ 133.5, 140.6

#### 6.3.1.2. Synthesis of 3,4-diaminothiophene (13)

2,5-Dibromo-3,4-dinitrothiophene (**12**) (6.0 g, 18.07 mmol) and 37% conc. HCl (74.5 mL) were combined. Tin powder (13.27 g, 92.66 mmol) was added in small portion in about 1 hr and 20 min maintaining the temperature at 15$^{o}$C. After the addition was complete, the mixture was stirred at 0$^{o}$C overnight. The solid residue was filtered by vacuum filtration and washed with diethyl ether and acetonitrile until the wash was colorless, giving the diammonium salt (2.14 g). The salt was dissolved in distilled water and basified with 0.89 M KOH solution until pH reached to 7-8. The aqueous solution was extracted with ethyl acetate. The organic layer was separated, dried over anhydrous $Na_2SO_4$ and the solvent was removed by rotary evaporation at room temperature to afford **13** (1.0 g, 48.5%) as shiny solid.

$^{1}$H- NMR (400 MHz, $CDCl_3$): δ 3.40 (*br.s*, 2H, H-3), 6.17 (*s*, 1H, H-2). $^{13}$C- NMR (100 MHz, $CDCl_3$): δ 101.4, 137.0.

**6.3.1.3. Synthesis of 3-dodecyloxybenzaldehyde (32).**

In to a 250 mL, three-necked round bottom flask, $K_2CO_3$ (56.7 g, 410 mmol) was suspended in a solution of 3-hydroxybenzaldehyde (10 g, 81.88 mmol) in DMF (100 mL) and heated to 100$^oC$ under nitrogen atmosphere. To the heated mixture, 1-bromododecane (41.2 g, 39.7 mL, 165 mmol) was added dropwise from a pressure-equalizing dropping funnel over 1 hr and 40 min and the reaction mixture was stirred at 100$^oC$ under nitrogen for 26 hr. After cooling to room temperature, the solid material was filtered off and water was added to the filtrate, which was extracted three times with diethyl ether. The ether extract was combined and washed with 2M HCl followed by 1M NaOH and water. The organic layer was separated, dried over anhydrous $Na_2SO_4$ and the solvent was removed by rotary evaporation. The crude product was purified by silica gel column chromatography using pentane as eluent to afford **32** (22.2 g) as a yellow oil.

$^1$H- NMR (400 MHz, $CDCl_3$): Table 1. $^{13}$C- NMR (100 MHz, $CDCl_3$): Table 2.

**6.3.1.4. Synthesis of 3-decyloxybenzaldehyde (33**).

3-Decyloxybenzaldehyde (**33**) was prepared following the procedure described above for the preparation of compound **32** by reacting 3-hydroxybenzaldehyde (10 g, 81.88 mmol) with 1-bromodecane (36.8 g, 166.6 mmol) to afford crude **33** (24.75 g) as yellow oil after purification by silica gel column chromatography using petroleum ether as eluent.

$^1$H- NMR (400 MHz, $CDCl_3$): Table 1. $^{13}$C- NMR (100 MHz, $CDCl_3$): Table 2.

**6.3.1.5. Synthesis of 3-octyloxybenzaldehyde (34).**

3-Octyloxybenzaldehyde (**34**) was prepared following the procedure described above for the preparation of compound **32** by reacting 3-hydroxybenzaldehyde (10 g, 81.88 mmol) with 1-bromooctane (31.7 g, 164.4 mmol) to afford **34** (22.5 g) as yellow oil which was used in the next reaction without further purification.

$^1$H-NMR (400 MHz, $CDCl_3$): Table 1. $^{13}$C- NMR (100 MHz, $CDCl_3$): Table 2.

### 6.3.1.6. Synthesis of 3-hexyloxybenzaldehyde (35).

3-Hexyloxybenzaldehyde (**35**) was synthesized following the procedure described above for the preparation of compound **32** by reacting 3-hydroxybenzaldehyde (10 g, 81.88 mmol) with 1-bromohexane (27.2 g, 23.2 mL, 165 mmol) to afford **35** (18.4 g) as yellow oil which was used in the next reaction without further purification.

$^{1}$H- NMR (400 MHz, $CDCl_3$): Table 1. $^{13}$C- NMR (100 MHz, $CDCl_3$): Table 2.

### 6.3.1.7. Synthesis of 1,2-bis(3-(dodecyloxy)phenyl)-2-hydroxyethanone (36).

Thiamine hydrochloride (1.92 g, 5.69 mmol) and distilled water (3.90 mL) were added in to two-necked flask (250 mL). The mixture was stirred until the white powder was completely dissolved. To the colorless solution, 95% ethanol (15.30 mL) was added and the solution was cooled in ice bath to less than 20$^{o}$C. Sodium hydroxide (2M, 5.72 mL) was added slowly to the flask. Up on addition of base, a yellow color was formed and faded. 3-Dodecyloxybenzaldehyde (**32**) (21.73 g, 74.80 mmol) was added and the mixture was stirred and heated to 60$^{0}$C for 4 hr and 50 min. The progress of the reaction was monitored by TLC using hexane:ethyl acetate (12:1) as eluent. The mixture was the cooled to room temperature and extracted with chloroform twice. The chloroform extract was washed twice with distilled water, dried over anhydrous $Na_2SO_4$ and the solvent was removed by rotary evaporation. The residue was purified by silica gel column chromatography using hexane:ethyl acetate (12:1) as eluent to afford **36** (5.61 g) as yellowish oily solid.

$^{1}$H- NMR (400 MHz, $CDCl_3$): Table 2. $^{13}$C- NMR (100 MHz, $CDCl_3$): Table 3.

### 6.3.1.8. Synthesis of 1,2-bis(3-(decyloxy)phenyl)-2-hydroxyethanone (37)

1,2-Bis(3-(decyloxy)phenyl)-2-hydroxyethanone (**37**) was synthesized following the procedure described above for the preparation of compound **36** by reacting crude 3-(decyloxy)benzaldehyde (**33**) (23.3 g) with thiamine hydrochloride (1.95 g, 5.79 mmol) to afford **37** (6.2 g) as yellow solid**.**

Mp: 42.2– 43.5$^{o}$C; $^{1}$H- NMR (400 MHz, $CDCl_3$): Table 3. $^{13}$C- NMR (100 MHz, $CDCl_3$): Table 4.

### 6.3.1.9. Synthesis of 1,2-bis(3-(octyloxy)phenyl)-2-hydroxyethanone (38)

1,2-Bis(3-(octyloxy)phenyl)-2-hydroxyethanone (**38**) was synthesized following the procedure described above for the preparation of compound **36** by reacting crude 3-(octyloxy)benzaldehyde **(34)** (22.89 g) with thiamine hydrochloride (3.49 g, 10.34 mmol) to afford compound **38** (3.5 g) as yellow oil.

$^{1}$H- NMR (400 MHz, $CDCl_3$): Table 3. $^{13}$C- NMR (100 MHz, $CDCl_3$): Table 4.

### 6.3.1.10. Synthesis of 1,2-bis(3-(hexyloxy)phenyl)-2-hydroxyethanone (39)

1,2-Bis(3-(hexyloxy)phenyl)-2-hydroxyethanone (**39)** was prepared following the procedure described above for the preparation of compound **36** by reacting crude 3-hexyloxybenzaldehyde (18.3 g) with thiamine hydrochloride (2.26 g, 6.70 mmol) to provide **39** (5.5 g) as yellow solid.

Mp: 54.8–55.3, $^{1}$H- NMR (400 MHz, $CDCl_3$): Table 3. $^{13}$C- NMR (100 MHz, $CDCl_3$): Table 4.

### 6.3.1.11. Synthesis of (1,2-bis(3-dodecyloxy)phenyl)ethane-1,2-dione (40)

In a 250 mL three-necked round bottom flask equipped with a reflux condenser and a dropping funnel, 1,2-bis(3-(dodecyloxy)phenyl)-2-hydroxyethanone (**36**) (3.81g, 6.56 mmol) in DMSO (12.3 mL). Then 48% HBr (8 mL) was added dropwise from the dropping funnel over 1 hr and 50 min. The reaction mixture was heated to 50$^{o}$C for 5 hr. The temperature was further raised to 90$^{o}$C and was maintained at that temperature overnight. The reaction mixture was then cooled and poured on to ice-water where up on a solid precipitate was formed which was collected by vacuum filtration and washed with cold methanol, dried and recrystallized from ethanol to afford **40** (1.9 g, 50.1%) as yellow solid.

Mp: 61.3 –62.0$^{o}$C; $^{1}$H- NMR (400 MHz, $CDCl_3$): Table 5. $^{13}$C- NMR (100 MHz, $CDCl_3$): Table 6.

### 6.3.1.12. Synthesis of 1,2-bis(3-(decyloxy)phenyl)ethane-1,2-dione (41).

1,2-Bis(3-(decyloxy)phenyl)ethane-1,2-dione (**41**) was synthesized following the procedure described above for the preparation of compound **40** by reacting 1,2-bis(3-(decyloxy)phenyl)-2-hydroxyethanone (**37**) (4.2 g, 8.02 mmol) in DMSO (9.3 mL) with 48% HBr (4.49 mL). Compound **41** (3.9 g, 93.3%) was obtained as a yellow solid after washing with cold methanol.

Mp: 57.6 – 58.4$^{o}$C; $^{1}$H-NMR (400 MHz, $CDCl_3$): Table 5. $^{13}$C- NMR (100 MHz, $CDCl_3$): Table 6.

**6.3.1.13. Synthesis of 1,2-bis(3-(octyloxy)phenyl)ethane-1,2-dione (42)**

Compound **42** was synthesized following the procedure described above for the preparation of compound **40** by reacting 2-hydroxy-1,2-bis(3-(octyloxy)phenyl)ethanone (**38**) (3.4 g, 7.27 mmol) in DMSO (8.43 mL) with 48% HBr, (4.1 mL) to afford. Compound **42** was obtained as the yellow solid (2.8 g, 82.7 %) after washing with cold methanol.

Mp: 50.7–51.6$^{o}$C; $^{1}$H- NMR (400 MHz, $CDCl_3$): Table 5. $^{13}$C- NMR (100 MHz, $CDCl_3$): Table 6.

**6.3.1.14. Synthesis of (1,2-bis(3-hexyloxy)phenyl)ethane-1,2-dione (43).**

In a 250 mL three-necked round bottom flask equipped with a reflux condenser and a dropping funnel, 1,2-bis(3-(hexyloxy)phenyl)-2-hydroxyethanone (**39**) ( 3.91 g, 9.49 mmol) was dissolved in DMSO (17.8 mL). Then 48% HBr (11.3 mL) was added dropwise from the dropping funnel over 1 hr and 50 min. The reaction mixture was heated to 50$^{o}$C for 5 hr. The temperature was further raised to 90$^{o}$C and was maintained at that temperature overnight. The mixture was then cooled and poured on to ice-water where up on a solid precipitate was formed which was collected by vacuum filtration and washed with cold methanol to afford **43** (3.76 g, 96.4%) as yellow solid.

Mp: 50.5–51.8$^{o}$C; $^{1}$H-NMR (400 MHz, $CDCl_3$): Table 5. $^{13}$C- NMR (100 MHz, $CDCl_3$): Table 6.

**6.3.1.15 Synthesis of 2,3-bis(3-(dodecyloxy)phenyl)thieno[3,4-*b*]pyrazine (44)**

1,2-Bis(3-(dodecyloxy)phenyl)ethane-1,2-dione (**40**) (1.05 g, 1.82 mmol) and 3,4-diaminothiophene (0.27 g, 2.32 mmol) were dissolved in ethanol (110 mL) to yield a red brown solution which was stirred for 48 hr at room temperature in the dark. The solvent was then removed by rotary evaporation without heating to yield a deep brown oil which was purified by silica gel column chromatography using dichloromethane as eluent to give **44** (1.03 g, 86.5%) as greenish yellow solid after washing with cold methanol.

Mp: 69.5–71.0$^{o}$C; $^{1}$H- NMR (400 MHz, $CDCl_3$): Table 7. $^{13}$C-NMR (100 MHz, $CDCl_3$): Table 8.

### 6.3.1.16. Synthesis of 2,3-bis(3-(decyloxy)phenyl)thieno[3,4-*b*]pyrazine (45)

2,3-Bis(3-(decyloxy)phenyl)thieno[3,4-b]pyrazine (**45**) was synthesized following the procedure described above for the preparation of **45** by reacting 1,2-bis(3-(decyloxy)phenyl)ethane-1,2-dione (**41**) (1.5 g, 2.87 mmol) with 3,4-diaminothiophene (330 mg, 2.87 mmol). Compound **45** (1.3 g, 74.9%) was obtained as a brown solid after purification by silica gel column chromatography using dichloromethane:hexane (3:1) as eluent.

$^{1}$H- NMR (400 MHz, $CDCl_3$): Table 7. $^{13}$C- NMR (100 MHz, $CDCl_3$): Table 8.

### 6.3.1.17. Synthesis of 2,3-bis(3-(octyloxy)phenyl)thieno[3,4-*b*]pyrazine (46)

2,3-Bis(3-(octyloxy)phenyl)thieno[3,4-*b*]pyrazine (**46**) was synthesized following the procedure described above for the preparation of **45** by reacting 1,2-bis(3-(octyloxy)phenyl)ethane-1,2-dione (**42**) (810 mg, 1.74 mmol) with 3,4-diaminothiophene (221 mg, 1.94 mmol) . Compound **46** (760.5 mg, 70.8%) was obtained in pure form after washing with cold methanol.

Mp: 47.3–49.0$^{o}$C; $^{1}$H- NMR (400 MHz, $CDCl_3$): Table 7. $^{13}$C- NMR (100 MHz, $CDCl_3$): Table 8.

### 6.3.1.18. Synthesis of 2,3-bis(3-(hexyloxy)phenyl)thieno[3,4-*b*]pyrazine (47)

1,2-Bis(3-(hexyloxy)phenyl)ethane-1,2-dione (**43**) (1.20 g, 2.92 mmol) and 3,4-diaminothiophene (323 mg, 2.83 mmol) were dissolved in ethanol (134 mL) to yield a red brown solution. The mixture was stirred at room temperature in the dark for 48 hr and then the solvent was removed by rotary evaporation without heating to yield a deep brown oil which was purified by silica gel column chromatography using dichloromethane as eluent to afford **47** (1.08 g, 78 %) as a brown oil.

$^{1}$H- NMR (400 MHz, $CDCl_3$): Table 7. $^{13}$C-NMR (100 MHz, $CDCl_3$): Table 8.

### 6.3.1.19. Synthesis of 5,7-dibromo-2,3-bis(3-(dodecyloxy)phenyl)thieno[3,4-*b*]pyrazine (48)

A solution of NBS (523 mg, 2.94 mmol) in anhydrous DMF (8.5 mL) was added dropwise from a syringe to a solution of 2,3-bis(3-(dodecyloxy)phenyl)thieno[3,4-*b*]pyrazine (**44**) (552 mg, 0.84

mmol) in anhydrous DMF (28 mL) in the dark at -56°C. The mixture was allowed to warm slowly to room temperature and stirred at this temperature for 48 hr in the dark. The crude solid product was collected by vacuum filtration and washed with cold methanol and water. The resulting yellow solid was subjected to silica gel column chromatography by using pentane: $CH_2Cl_2$ (2:1) as eluent to afford **48** (250 mg, 36.5%).

Mp: 89.8– 91.0$^oC$; $^1H$- NMR (400 MHz, $CDCl_3$): Table 9. $^{13}C$- NMR (100 MHz, $CDCl_3$): Table 10.

### 6.3.1.20. Attempted Synthesis of 5,7-dibromo-2,3-bis(3-(decyloxy)phenyl)thieno[3,4-*b*]pyrazine (49)

2,3-Bis(3-(decyloxy)phenyl)thieno[3,4-*b*]pyrazine (**45**) (802 mg, 1.33 mmol) in chloroform: acetic acid (1:1, 16 mL) was cooled in ice bath. NBS (523 mg, 2.94 mmol) was added in three portions in the dark and the mixture was stirred overnight under nitrogen atmosphere. Then, water was added and the chloroform layer was separated and washed thoroughly with water, dried over anhydrous $Na_2SO_4$ and the solvent was removed by rotary evaporation. The residue was purified by silica gel column chromatography (dichloromethane:hexane, 2:1) to give a greenish yellow solid (650 mg). NMR showed that this material contained impurities. Further attempt to purify compound **49** by silica gel column chromatography using pentane: dichloromethane (2:1) as eluent did not give a pure compound.

### 6.3.1.21. Synthesis of 5,7-dibromo-2,3-bis(3-(octyloxy)phenyl)thieno[3,4-*b*]pyrazine (50)

A solution of NBS (380.4 mg, 2.14 mmol) in anhydrous DMF (3.5 mL) was added dropwise from a syringe to a solution of 2,3-bis(3-(octyloxy)phenyl)thieno[3,4-*b*]pyrazine (**46**) (447 mg, 0.82 mmol) in anhydrous DMF (12.7 mL) in the dark at -56°C. The mixture was allowed to warm slowly to room temperature and stirred at this temperature for 24 hr in the dark. The reaction mixture was poured into cold water and extracted with chloroform. The organic layer was separated and washed with water, dried over anhydrous $Na_2SO_4$ and the solvent was removed under reduced pressure. The crude product was purified by silica gel column chromatography using hexane:$CH_2Cl_2$ (1:1) as eluent to afford **50** (310 mg, 53.8%) as yellow solid.

Mp: 89.3–90.9$^{o}$C; $^{1}$H- NMR (400 MHz, $CDCl_3$): Table 9. $^{13}$C- NMR (100 MHz, $CDCl_3$): Table 10

**6.3.1.22. Synthesis of 5,7-dibromo-2,3-bis(3-(hexyloxy)phenyl)thieno[3,4-*b*]pyrazine (51)**

A solution of 2,3-bis(3-(hexyloxy)phenyl)thieno[3,4-*b*]pyrazine (**47**) (753 mg, 1.54 mmol) in chloroform:acetic acid (1:1, 18 mL) was cooled to 0°C and NBS (0.60 g, 3.39 mmol) was added in three portions in the dark. The reaction mixture was stirred overnight at room temperature under nitrogen atmosphere. Water was then added to the mixture and the chloroform layer was separated and washed with 2M KOH solution and distilled water. The organic layer was dried over anhydrous $Na_2SO_4$ and the solvent was removed under reduced pressure to give a greenish yellow solid which was purified by silica gel column chromatography (hexane:$CH_2Cl_2$, 1:2) to afford **51** (450 mg, 45.2%) as a yellowish green solid.

Mp: 88–89$^{o}$C; $^{1}$H- NMR (400 MHz, $CDCl_3$): Table 9 $^{13}$C- NMR (100 MHz, $CDCl_3$): Table 10.

**6.3.2. Syntheses of polymers**

**6.3.3. Syntheses of polymers by direct heteroarylation polymerization.**

**6.3.3.1 Poly[2,3-bis(3-(dodecyloxy)phenyl)thieno[3,4-*b*]pyrazine-5,7-diyl-*alt*-thiophene-2,5-diyl] (52)**

2,3-Bis(3-(dodecyloxy)phenyl)thieno[3,4-*b*]pyrazine (**44**) (124.83 mg, 0.19 mmol), 2,5-dibromothiophene (**11**) (46 mg, 0.19 mmol), $Pd(OAc)_2$ (2 mg, 0.089 mmol), $K_2CO_3$ (66 mg, 0.478 mmol), pivalic acid (5.85 mg, 0.055mmol), DMAc (0.65 mL), toluene (0.5 mL) and chloroform (0.5 mL) were placed in a round-bottomed flask and kept under nitrogen atmosphere. Then the reaction mixture was heated at 60$^{o}$C for 11 hr under nitrogen, cooled down to room temperature and precipitated from MeOH and filtered. The precipitate was dissolved in $CHCl_3$ and washed successively with aqueous solution of EDTA, 0.1 N HCl and distilled water. The organic layer was separated, concentrated to a small volume and reprecipitated from MeOH. The polymer was collected by filtration and then purified by Soxhlet extraction with acetone, methanol, and $CHCl_3$. The $CHCl_3$ extract was concentrated, precipitated from MeOH, filtered and dried in vacuum oven to give **52** (51 mg, 36.4%) as a deep green solid.

$^1$H- NMR (400 MHz, $CDCl_3$): δ 6.93-7.54 (*br. m*, 4H, Ar-H), 3.87(*br. m*, 2 H, ArOC$H_2$), 1.59(*br. m*, 2H, $ArOCH_2CH_2$-), 1.29 (*br. m*, 16H), $ArOCH_2CH_2(CH_2)_9$- ), 0.87(*br. m*, 3H, $CH_3$).

### 6.3.3.2. Poly[2,3-bis(3-(decyloxy)phenyl)thieno[3,4-*b*]pyrazine-5,7-diyl-*alt*-thiophene-2,5-diyl] (53)

2,3-Bis(3-(decyloxy)phenyl)thieno[3,4-*b*]pyrazine (**45**) (228.3 mg, 0.38 mmol), 2,5-dibromothiophene (**11**) (91.9 mg, 0.38 mmol), $Pd(OAc)_2$ (6.0 mg, 0.0267 mmol), $K_2CO_3$ (132 mg, 0.95 mmol), pivalic acid (11.7 mg, 0.11 mmol), DMAc (1.8 mL) and chloroform (0.3 mL) were placed in a round-bottomed flask and kept under nitrogen atmosphere. Then the reaction mixture was heated at $60^0$C for 23 hr under nitrogen, cooled down to room temperature and precipitated from MeOH and filtered. The residue was dissolved in $CHCl_3$ and was washed successively with aqueous solution of EDTA, 0.1 N HCl and distilled water. The organic layer was separated, concentrated to a small volume and reprecipitated from MeOH. The polymer was collected by filtration and then purified by Soxhlet extraction with acetone, methanol and $CHCl_3$. The $CHCl_3$ extract was concentrated, precipitated from MeOH, filtered and dried in vacuum oven to give **53** (101 mg, 39.0%) as a dark green solid.

$^1$H- NMR (400 MHz, $CDCl_3$): δ 6.94-7.28 (*br. m*, 4H, Ar-H), 3.86(*br. m*, 2 H, ArOC$H_2$), 1.69(*br. m*, 2H, $ArOCH_2CH_2$-), 1.29 ((*br. m*, 16H, $ArOCH_2CH_2(CH_2)_7$- ), 0.94(*br. m*, 3H, $CH_3$).

### 6.3.3.3. Poly[2,3-bis(3-(octyloxy)phenyl)thieno[3,4-*b*]pyrazine-5,7-diyl-*alt*-thiophene-2,5-diyl] (54)

Polymer **54** was synthesized following the procedure described above for the synthesis of **53**. Thus, 2,3-bis(3-(octyloxy)phenyl)thieno[3,4-*b*]pyrazine (**46**) (207 mg, 0.38 mmol) and 2,5-dibromothiophene (**11**) (91.9 mg, 0.38 mmol), $Pd(OAc)_2$ (6.0 mg, 0.0267 mmol), $K_2CO_3$ (132 mg, 0.95 mmol) and pivalic acid (11.7 mg, 0.11 mmol), were reacted to afford polymer **54** (166 mg, 69.9%) as a dark green solid.

$^1$H- NMR (400 MHz, $CDCl_3$): δ 6.92-7.21 (*br. m*, 4H, Ar-H), 3.86(*br. m*, 2 H, ArOC$H_2$), 1.27 (*br. m*, 12H, $ArOCH_2(CH_2)_6$- ), 0.94(*br. m*, 3H, $CH_3$).

### 6.3.3.4. Poly[2,3-bis(3-(hexyloxy)phenyl)thieno[3,4-*b*]pyrazine-5,7-diyl-*alt*-thiophene-2,5-diyl] (55)

2,3-Bis(3-(hexyloxy)phenyl)thieno[3,4-*b*]pyrazine (**47**) (278.7 mg, 0.57 mmol), 2,5-dibromothiophene (**11**) (137.9 mg, 0.57 mmol), $Pd(OAc)_2$ (10 mg, 0.04 mmol), $K_2CO_3$ (198 mg, 1.44 mmol), pivalic acid (17.55 mg, 0.17 mmol), DMAc (2.2 mL), toluene (0.6 mL) and chloroform (1.2 mL) were placed in a round-bottomed flask and kept under nitrogen atmosphere. Then the reaction mixture was heated at $60^0$C for 37 hr under nitrogen, cooled down to room temperature and precipitated from MeOH and filtered. The precipitate was dissolved in $CHCl_3$ and was washed successively with aqueous solution of EDTA, 0.1N HCl and distilled water. The organic layer was separated, concentrated to a small volume and reprecipitated from MeOH. The polymer was collected by filtration and then purified by Soxhlet extraction with acetone, methanol, and $CHCl_3$. The $CHCl_3$ extract was concentrated, precipitated from MeOH, filtered and dried in vacuum oven to give **55** (146.8 mg, 45.3%) as a dark green solid.

$^1$H- NMR (400 MHz, $CDCl_3$): δ 6.94-7.54 (*br. m*, 4H, Ar-H), 1.27 (*br. m*, 8H, $ArCH_2(CH_2)_4$- ), 3.92(*br. m*, 2 H, $ArOCH_2$), 0.91(*br. m*, 3H, $CH_3$).

### 6.3.4. Syntheses of polymers by Stille-cross coupling reaction

### 6.3.4.1. Poly[2,3-bis(3-(dodecyloxy)phenyl)thieno[3,4-*b*]pyrazine-5,7-diyl-*alt*-thiophene-2,5-diyl] (52')

5,7-Dibromo-2,3-bis(3-(dodecyloxy)phenyl)thieno[3,4-*b*]pyrazine (**48**) (97.5 mg, 0.12 mmol) and 2,5-bis(tributylstannyl)thiophene (**56**) (79.2 mg, 0.12 mmol), $Pd(PPh_3)_4$ (18 mg), anhydrous DMF (0.45 mL) and anhydrous toluene (1.75 mL) were mixed in a round-bottomed flask equipped with a reflux condenser. The solution was flushed with nitrogen for 20 min and heated to $100^o$C under nitrogen. After 11 hr, the reaction mixture was cooled down to room temperature and precipitated from MeOH and filtered. The residue was dissolved in $CHCl_3$ and washed successively with aqueous solution of EDTA and distilled water. The organic layer was separated, concentrated to a small volume and reprecipitated from MeOH. The polymer was collected by filtration and then purified by Soxhlet extraction with acetone, methanol, and $CHCl_3$. The $CHCl_3$ extract was concentrated, precipitated from MeOH, filtered and dried in vacuum oven to give **52'** (61 mg, 69.2%) as a deep green solid.

$^1$H- NMR (400 MHz, $CDCl_3$): δ 6.94-7.98 (*br. m*, 4H, Ar-H), 3.87(*br. m*, 2 H, $ArOCH_2$), 1.59(*br. m*, 2H, $ArOCH_2CH_2$-), 1.27((*br. m*, 18H, $ArOCH_2CH_2(CH_2)_9$- ), 0.87(*br. m*, 3H, $CH_3$).

### 6.3.4.2. Poly[2,3-bis(3-(octyloxy)phenyl)thieno[3,4-*b*]pyrazine-5,7-diyl-*alt*-thiophene-2,5-diyl] (54')

5,7-Dibromo-2,3-bis(3-(octylloxy)phenyl)thieno[3,4-*b*]pyrazine (**50**) (182.4 mg, 0.26 mmol) and 2,5-bis(tributylstannyl)thiophene (**56**) (171 mg, 0.26 mmol), $Pd(PPh_3)_4$ (30 mg), anhydrous DMF (0.86 mL) and anhydrous toluene (3.75 mL) were mixed in a round-bottomed flask equipped with a reflux condenser. The solution was flushed with nitrogen for 20 min and heated to 100$^o$C under nitrogen. After 12 hr, the reaction mixture was cooled down to room temperature and precipitated from MeOH and filtered. The precipitate was dissolved in $CHCl_3$ and was washed successively with aqueous solution of EDTA and distilled water. The organic layer was separated, concentrated to a small volume and reprecipitated from MeOH. The polymer was collected by filtration and then purified by Soxhlet extraction with acetone, methanol, and $CHCl_3$. The $CHCl_3$ extract was concentrated, precipitated from MeOH, filtered and dried in vacuum oven to give **54'** (121.38 mg, 74.9%) as a deep green solid.

$^1$H- NMR (400 MHz, $CDCl_3$): δ 6.94 -7.74 (*br. m*, 4H, Ar-H), 3.98(br. m, 2 H, $ArOCH_2$), 1.27 (*br.m*, 10H, $ArOCH_2CH_2(CH_2)_5$- ), 1.61(*br. s*, 2H, $ArOCH_2CH_2$-), 0.94(*br. m*, 3H, $CH_3$).

### 6.3.4.3. Poly[2,3-bis(3-(hexyloxy)phenyl)thieno[3,4-*b*]pyrazine-5,7-diyl-*alt*-thiophene-2,5-diyl] (55')

5,7-Dibromo-2,3-bis(3-(hexyloxy)phenyl)thieno[3,4-*b*]pyrazine (**51**) (196.7 mg, 0.30 mmol) , 2,5-bis(tributylstannyl)thiophene (**56**) (201.6 mg, 0.30 mmol), $Pd(PPh_3)_4$ (60 mg) and toluene (10 mL) were mixed in a round-bottomed flask equipped with nitrogen. The mixture was flushed with nitrogen and heated at 75$^o$C for 100 hr followed by stirring at 90$^0$C for 11 hr. The reaction mixture was cooled down to room temperature and precipitated from MeOH and filtered. The precipitate was dissolved in $CHCl_3$ and was washed with aqueous solution of EDTA and distilled water. The organic layer was separated, concentrated to a small volume and reprecipitated from MeOH. The polymer was collected by filtration and then purified by Soxhlet extraction with acetone, methanol, and $CHCl_3$. The $CHCl_3$ extract was concentrated, precipitated from MeOH, filtered and dried in vacuum oven to afford **55'** (17.3 mg, 10%) as a deep green solid.

$^{1}$H- NMR (400 MHz, $CDCl_3$): δ 6.89-7.74 (*br*. *m*, 4H, Ar-H), 1.27 (*br*. *m*, 8H, $ArCH_2(CH_2)_4$- ), 3.97(*br*. *m*, 2 H, $ArOCH_2$), 0.91(*br*. *m*, 3H, $CH_3$).

## 7. References


1. Afshin, H.; de Boer, B.; Wildeman, J.; Kooistra, F. B.; Hummelen, J. C.; Turbiez, M. G. R.; Wienk, M. M.; Janssen, R. A. J.; Blom, P. W. M. Solution-Processed Organic Tandem Solar Cells. *Adv. Funct. Mater.* **2006**, *16*, 1897.
2. Son, H. J.; Carsten, B.; Jung, I. H.; Yu, L. Overcoming Efficiency Challenges in Organic Solar Cells: Rational Development of Conjugated Polymers. *Energy Environ. Sci.* **2012**, *5*, 8158.
3. Mühlbacher, D.; Scharber, M.; Morana, M.; Zhengguo, Z.; Waller, D.; Gaudiana, R.; Brabec, C. High Photovoltaic Performance of a Low-Bandgap Polymer. *Adv. Mater.* **2006**, *18*, 2884.
4. Wang, E.; Hou, L.; Wang, Z.; Hellström, S.; Zhang, F.; Inganäs, O.; Andersson, M. R. An Easily Synthesized Blue Polymer for High-Performance Polymer Solar Cells. *Adv. Mater* **2010**, *22*, 5240.
5. Cai, T.; Zhou, Y.; Wang, E.; Hellström, S.; Zhang, F.; Shiai, X.; Inganäs, O.; Andersson, M. R. Low Bandgap Polymers Synthesized by $FeCl_3$ Oxidative Polymerization. *Solar Energy Materials & Solar Cells* **2010**, *94*, 1275.
6. Wu, P.; Bull, T.; Kim, F.S .; Luscombe, C. K.; Jenkhe, S.A. Organometallic Donor–accepter Conjugated Polymer Semiconductors: Tunable Optical, Electrochemical, Charge Transport and Photovoltaic Properties. *Macromolecules* **2009**, *42*, 671.
7. Beaujuge, P.M .; Ellingerand, S.; Reynolds, J. R. The Donor–accepter Approach Allows a Black-to-Transmissive Switching Polymeric Electrochrome. *Nat. Mater.* **2008**, 795.
8. Oosterhout, S.D.; Wienk, M.M.; Van Bavel, S.S.; Thiedimann, R.; Koster, L. J.A.; Gilot, J.; Loos, J.; Schmidit, V.; Janssen, R. A. J. The Effect of Three Dimensional Morphology on the Efficiency of Hybrid Polymer Solar Cells. *Nat. Mater* **2009**, *8*, 818.
9. Zhu, Z.; Waller, D.; Gaudiana, R. New Polymer for Optimizing Organic Photovoltaic Cell Performances. *J. Macromol. Sci. Part A: Pure Appl.Chem.* **2007**, *44*, 1249.
10. Yue, W.; Zhao, Y.; Tian, H.; Song, D.; Xie, Z.; Yan, D.; Geng, Y.; Wang, F. Poly(oligothiophene-*alt*-benzothiadazole)s: Tuning the Structures of Oligothiophene Units toward High Mobility "black" Conjugated Polymers. *Macromolecules* **2009**, *42*, 6510.

11. Fukuda, M.; Sawada, K.; Yoshino, K. J. Fusible Conducting Poly(9-alkylfluorene) and Poly(9,9-dialkylfluorene) and Their Characteristics *J. Appl. Phys. Part 2 -Lett* **1989**, *28*, L1433.
12. Hou, J.; Park, M.-H.; Zhang, S.; Yao, Y.; Chen, L.-M.; Li, J.-H.; Yang, Y. Bandgap and Molecular Energy Level Control of Conjugated Polymer Photovoltaic Materials Based on Benzo[1,2-*b*:4,5-*b′*]dithiophene. *Macromolecules* **2008**, *41*, 6012.
13. Roncali, J. Synthetic Principles for Bandgap Control in Linear π-Conjugated Systems. *Chem. Rev.* **1997**, *97*, 173.
14. Grimsdale, A. C.; Chan, K. L.; Martin, R. E.; Jokisz, P. G.; Holmes, A. B. Synthesis of Light-Emitting Conjugated Polymers for Applications in Electroluminescent Devices. *Chem. Rev* **2009**, *109*, 897.
15. Shirakawa, H. The Discovery of Polyacetylene Film: The Dawning of an Era of Conducting Polymers (Nobel Lecture). *Angew. Chem. Int. Ed* **2001**, *40*, 2574.
16. Bundgaard, E.; Krebs, F. C. Low Bandgap Polymers for Organic Photovoltaics. *Solar Energy Materials & Solar Cells* **2007**, *91*, 954.
17. Dhanabalan, A.; van Duren, J. K. J.; van Hal, P. J.; van Dogen, J. L. J.; Janssen, R. A. J. Synthesis and Characterization of a Low Bandgap Conjugated Polymer for Bulk Heterojunction Photovoltaic Cells. *Adv. Funct. Mater* **2001**, *11*, 255.
18. Van Duren, J. K. J.; Dhanabalan, A.; van Hal, P. A.; Janssen, R. A. J. Low Bandgap Polymer Photovoltaic Cells. *Synth. Met* **2001**, *121*, 1587.
19. Cheng, Y.-J.; Yang, S.-H.; Hsu, C.-S. Synthesis of Conjugated Polymers for Organic Solar Cell Applications. *Chem. Rev.* **2009**, *109*, 5868.
20. Ajayaghosh, A. Donor–Acceptor Type Low Bandgap Polymers: Polysquaraines and Related Systems. *Chem. Soc. Rev.* **2003**, *32*, 181.
21. Huang, Y.; Zhang, M.; Ye, L.; Guo, X.; Han, C. C.; Li, Y.; Hou, J. Molecular Energy Level Modulation by Changing the Position of Electron-Donating Side Groups. *J. Mater. Chem* **2012**, *22*, 5700.
22. Becerril, H. A.; Miyaki, N.; Tang, M. L.; Mondal, R.; Sun, Y.-S.; Mayer, A. C.; Parmer, J. E.; McGehee, M. D.; Bao, Z. Transistor and Solar Cell Performance of Donor–acceptor Low Bandgap Copolymers Bearing an Acenaphtho[1,2-*b*]thieno[3,4-*e*]pyrazine (ACTP) Motif. *J. Mater. Chem* **2009**, *19*, 591.

23. Svensson, M.; Zhang, F. L.; Veenstra, S. C.; Verhees, W. J. H.; Hummelen, J. C.; Kroon, J. M.; Inganäs, O.; Andersson, M. R. High-Performance Polymer Solar Cells of an Alternating Polyfluorene Copolymer and a Fullerene Derivative. *Adv. Mater* **2003**, *15*, 988.
24. Wang, E. G.; Wang, M.; Wang, L.; Duan, C. H.; Zhang, J.; Ca, W. Z.; He, C.; Wu Y. Cao, H. Bc. Donor Polymers Containing Benzothiadiazole and Four Thiophene Rings in Their Repeating Units with Improved Photovoltaic Performance. *Macromolecules* **2009**, *42*, 4410.
25. Zoombelt, A. P.; Gilot, J.; Wienk, M. M.; Janssen, R. A. J. Effect of Extended Thiophene Segments in Small Bandgap Polymers with Thienopyrazine. *Chem.Mater.* **2009**, *21*, 1663.
26. Soci, C.; Hwang, I. W.; Moses, D.; Zhu, Z.; Waller, D.; Gaudiana, R.; Brabec, C. J.; Heeger, A. J. Photo Conductivity of a Low-Band Gap Conjugated Polymer. *Adv. Funct. Mater.* **2007**, *17*, 632.
27. Carsten, B.; He, F.; Son, H. J.; Xu, T.; Yu, L. Stille Polycondensation for Synthesis of Functional Materials. *Chem. Rev.* **2011**, *111*, 1493.
28. Andersson, M. R.; Selse, D.; Berggren, M.; J ¨arvinen, H.; Hjertberg, T.; Inganäs, O.; Wennerstr¨om, O.; O¨sterholm, J. E. Regioselective Polymerization of 3-(4-Octyl-Phenyl)thiophene with $FeCl_3$. *Macromolecules* **1994**, *27*, 6503.
29. Berrouard, P.; Najari, A.; Pron, A.; Gendron, D.; Morin, P.-O.; Pouliot, J.-R.; Veilleux, J.; Leclerc, M. Synthesis of 5-Alkyl[3,4-*c*]thienopyrrole-4,6-Dione-Based Polymers by Direct Heteroarylation. *Angew. Chem.* **2012**, *124*, 2110.
30. Nicolaou, K. C.; Bulger, P. G.; Sarlah, D. Palladium-Catalyzed Cross-Coupling Reactions in Total Synthesis. *Angew. Chem. Int. Ed,* **2005**, *44*, 4442.
31. Fujinami, Y.; Kuwabara, J.; Lu, W.; Hayashi, H.; Kanbara, T. Synthesis of Thiophene- and Bithiophene-Based Alternating Copolymers via Pd-Catalyzed Direct C−H Arylation. *ACS Macro Lett* **2012**, *1*, 67.
32. Kuwabara, J.; Nohara, Y.; Choi, S. J.; Fujinami, Y.; Lu, W.; Yoshimura, K.; Oguma, J.; Suenobu, K.; Kanbara, T. Direct Arylation Polycondensation for the Synthesis of Bithiophene-Based Alternating Copolymers. *Polym. Chem* **2013**, *4*, 947.
33. Abdo, N. I.; El-Shehawy, A. A.; El-Barbary, A. A.; Lee, J.-S. Palladium-Catalyzed Direct C–H Arylation of Thieno[3,4-*b*]pyrazines: Synthesis of Advanced Oligomeric and Polymeric Materials. *Eur. J. Org. Chem.* **2012**, 5540.

34. Chen, J.; Cao, Y. Development of Novel Conjugated Donor Polymers for High-Efficiency Bulk-Heterojunction Photovoltaic Devices. *Acc. Chem. Res.* **2009**, *42*, 1709.
35. Ashraf, R. S.; Shahid, M.; Klemm, E.; Al-Ibrahim, M.; Sensfuss, S. Thienopyrazine-Based Low-Bandgap Poly(heteroaryleneethynylene)s for Photovoltaic Devices. *Macromol. Rapid Commun.* **2006**, *27*, 1454.
36. Wang, X.-Z.; Wong, W.-Y.; Cheung,, K.-Y.; Fung,, M.-K.; Djuriˇsi´c, A. B.; Chan, W.-K. Polymer Solar Cells Based on Very Narrow-Bandgap Polyplatinynes with Photocurrents Extended into the near-Infrared Region. *Dalton Trans.* **2008**, 5484.
37. Motoyama, R.; Sato, D.; Imoto, E. *Nippon Kagaku Zasshi* **1957**, *78*, 793; *Chem. Abstr*. **1960**, *54*, 22560e.
38. Binder, D.; Noe, C. R.; Geisler, F.; Hillebrand, F. *Arch. Pharm. (Weinheim, Ger.)* Thiophene as a Structural Element of Physiologically Active Compounds IX: Thienopyrazine 1,4-Dioxides. **1981**, *314*, 564.
39. Outurquin, F.; Paulmier, C. Synthesis of 3,4-Diaminothiophene and some Derivatives. *Bull. Soc. Chim. Fr.* **1983**, *II*, 153.
40. Outurquin, F.; Paulmier, C. Synthèse de Nouveaux Systèmes Hétérocycliques Thiophéniques Azotés à Partir du Diamino-3,4-thiophène. *Bull. Soc. Chim. Fr.* **1983**, *II*, 159.
41. Pomerantz, M.; Chaloner-Gill, B.; Harding, L. O.; Tseng, J. J.; Pomerantz, W. J. Poly(2,3-dihexylthieno[3,4-*b*]pyrazine). A New Processable Low Bandgap Polyheterocycle. *J. Chem. Soc., Chem. Commun.* **1992**, 1672.
42. Kastner, J.; Kuzmany, H.; Vegh, D.; Landl, M.; Cuff, L.; Kertesz, M. Raman Spectra and Ground State of the New Low Bandgap Polymer Poly(thienopyrazine). *Synth. Met* **1995**, *69*, 593.
43. Kastner, J.; Kuzmany, H.; Vegh, D.; Landl, M.; Cuff, L.; Kertesz, M. Raman Spectra of Poly(2,3-R,R-thieno[3,4-*b*]pyrazine). A New Low-Bandgap Polymer. *Macromolecules* **1995**, *28*, 2922.
44. Kenning, D. D.; Mitchell, K. A.; Calhoun, T. R.; Funfar, M. R.; Sattler, D. J.; Rasmussen, S. C. Thieno[3,4-*b*]pyrazines: Synthesis, Structure, and Reactivity. *J. Org. Chem* **2002**, *67*, 9073.

45. Li, J.-C.; Hwang, M.-L.; Lee, E.-W.; Lee, S.-H.; Yu, S.-C.; Lee, Y.-S. Synthesis and Characterization of *N*-(2-Ethylhexyl)carbazole-2,3-Bis(4-fluorophenyl))thieno[3,4-*b*]pyrazine Copolymer. *Bull. Korean Chem. Soc.* **2010**, *31*, 2073.
46. Li, J.-C.; Beak, M.-J.; Kwon, J.-T.; Lee, E.-W.; Lee, S.-H.; Lee, Y.-S. Synthesis of Poly(3-Hexylthiophene-*alt*- 2,3-bis(4-fluorophenyl)thieno[3,4-*b*]pyrazine) for Polymer Photovoltaic Applications. *Macromolecular Research* **2010**, *18*, 1237.
47. Melaku, Y. Synthesis of Some Fluorene-Thiophene Copolymers. Project, Addis Ababa: Addis Ababa, Ethiopia, 2007.
48. Wen, L.; Rasmussen, S. C. Synthesis and Structural Characterization of 2,5-Dihalo-3,4-Dinitrothiophenes. *J. Chem. Crystallog.* **2007**, *37*, 387.
49. Wen, L.; Nietfeld, J. P.; Amb, C. M.; Rasmussen, S. C. Synthesis and Characterization of New 2,3-Disubstituted Thieno[3,4-*b*]pyrazines: Tunable Building Blocks for Low Bandgap Conjugated Materials. *J. Org. Chem* **2008**, *73*, 8529.
50. Lindgren, L. J.; Zhang, F.; Andersson, M.; Barrau, S.; Hellström, S.; Mammo, W.; Perzon, E.; Inganäs, O.; Andersson, M. R. Synthesis, Characterization, and Devices of a Series of Alternating Copolymers for Solar Cells. *Chem. Mater.* **2009**, *21*, 3491.
51. Gedefaw, D. A. Synthesis of Conjugated Polymers for Opto-Electronic Applications. Dissertation, Addis Ababa: Addis Ababa, Ethiopia, 2011.
52. Gedefaw, D. A.; Zhou, Y.; Ma, Z.; Genene, Z.; Hellström, S.; Zhang, F.; Mammo, W.; Inganäs, O.; Andersson, M. R. Conjugated Polymers with Polar Side Chains in Bulk Heterojunction Solar Cell Devices. *Polym Int* **2014**, *63*, 22.
53. Abdissa, Z. Synthesis and Characterization of Conjugated Polymers and Small Molecules for Organic Photovolatic Applications. Dissertation, Addis Ababa: Addis Ababa, Ethiopia, 2014.
54. Bathula, C.; Song, C. E.; Badgujar, S.; Hong, S.-J.; Park, S. Y.; Shin, W. S.; Lee, J.-C.; Cho, S.; Ahn, T.; Moon, S.-J.; Lee, S. K. Naphtho[1,2-*b*:5,6-*b'*]dithiophene-Based Copolymers for Applications to Polymer Solar Cells. *Polym. Chem* **2013**, *4*, 2132.
55. P. Morvillo; R. Diana,a; C. Fontanesi; R. Ricciardi; M. Lanzi; A. Mucci; F. Tassinari; L. Schenetti; C. Minarinia; F. Parenti. Low Bandgap Polymers for Application in Solar Cells: Synthesis and Characterization of Thienothiophene–thiophene Copolymers. *Polym. Chem.* **2014**, *5*, 2391.

56. Poduval, M. K.; Burrezo, P. M.; Casado, J.; Navarrete, J. T. L.; Ortiz, R. P.; Kim, T.-H. Novel Thiophene−Phenylene−Thiophene Fused Bislactam-Based Donor−Acceptor Type Conjugate Polymers: Synthesis by Direct Arylation and Properties. *Macromolecules* **2013**, *46*, 9220−9230.
57. Pron, A.; Gawrys, P.; Zagorska, M.; Djurado, D.; Demadrille, R. Electroactive Materials for Organic Electronics: Preparation Strategies, Structural Aspects and Characterization Techniques. *Chem. Soc. Rev* **2010**, *39*, 2577.
58. Chao, C.-Y.; Chao, C.-H.; Chen, L.-P.; Hung, Y.-C.; Lin, S.-T.; Su, W.-F.; Lin, C.-F. Band Structure Engineering for Low Bandgap Polymers Containing Thienopyrazine. *J. Mater. Chem* **2012**, *22*, 7331.

# 8. Appendices

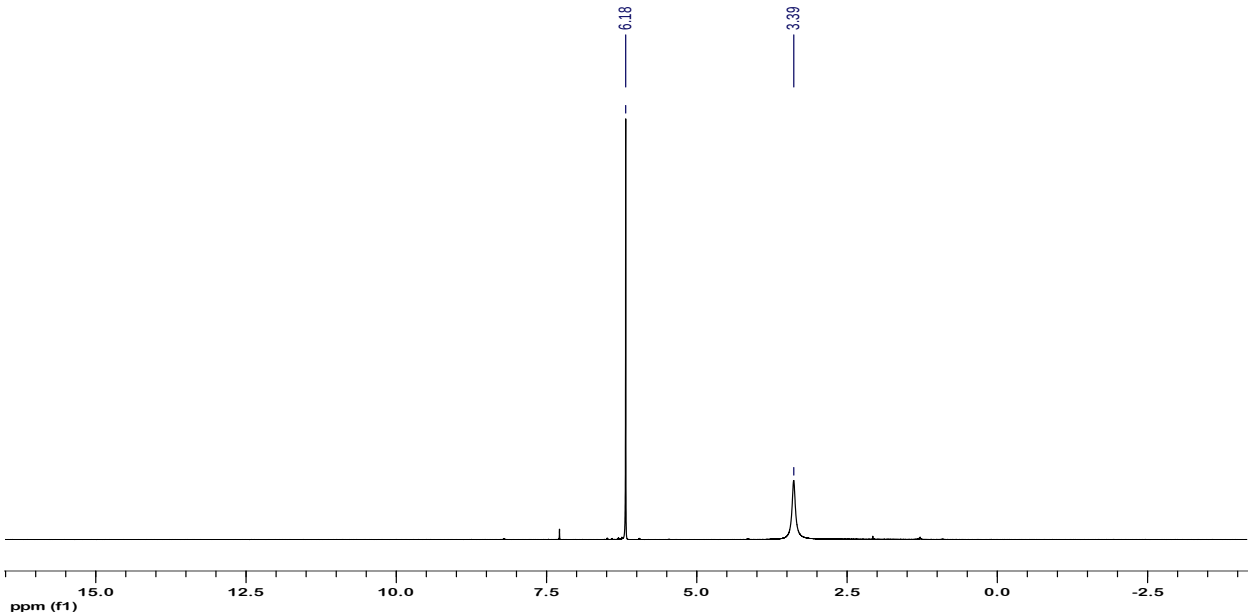


Appendix 1: $^{1}$H-NMR spectrum of 3,4-diaminothiophene (**13**).

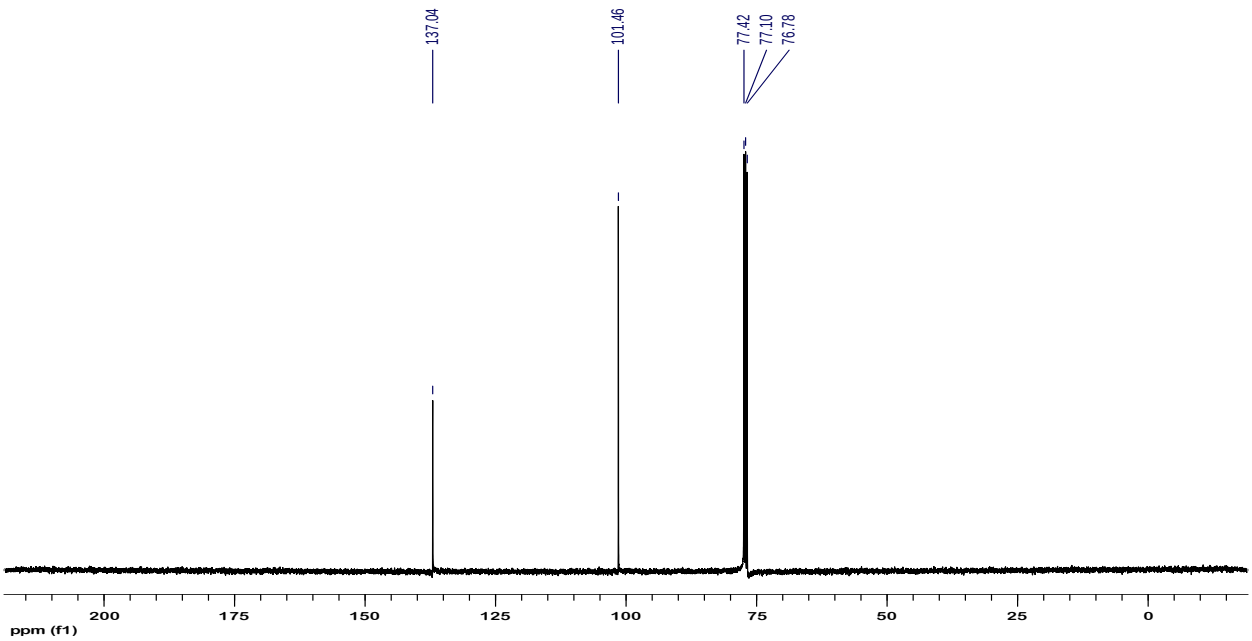


Appendix 2: $^{13}$C-NMR spectrum of 3,4-diaminothiophene (**13**).

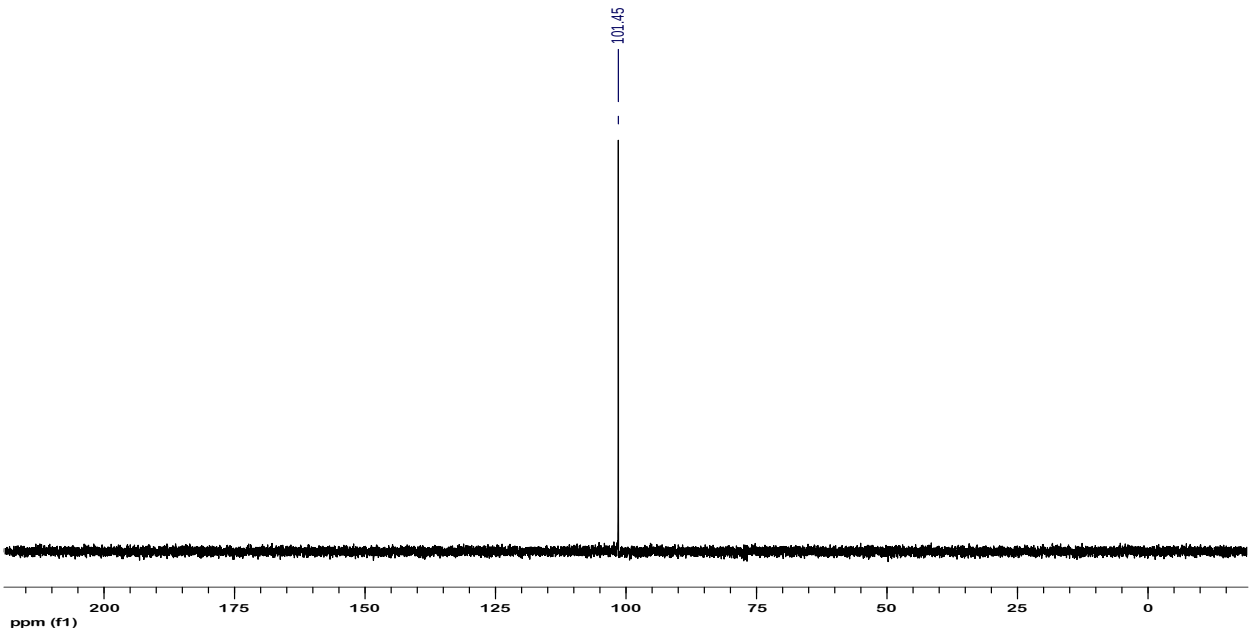


Appendix 3: DEPT-135 spectrum of 3,4-diaminothiophene (**13**).

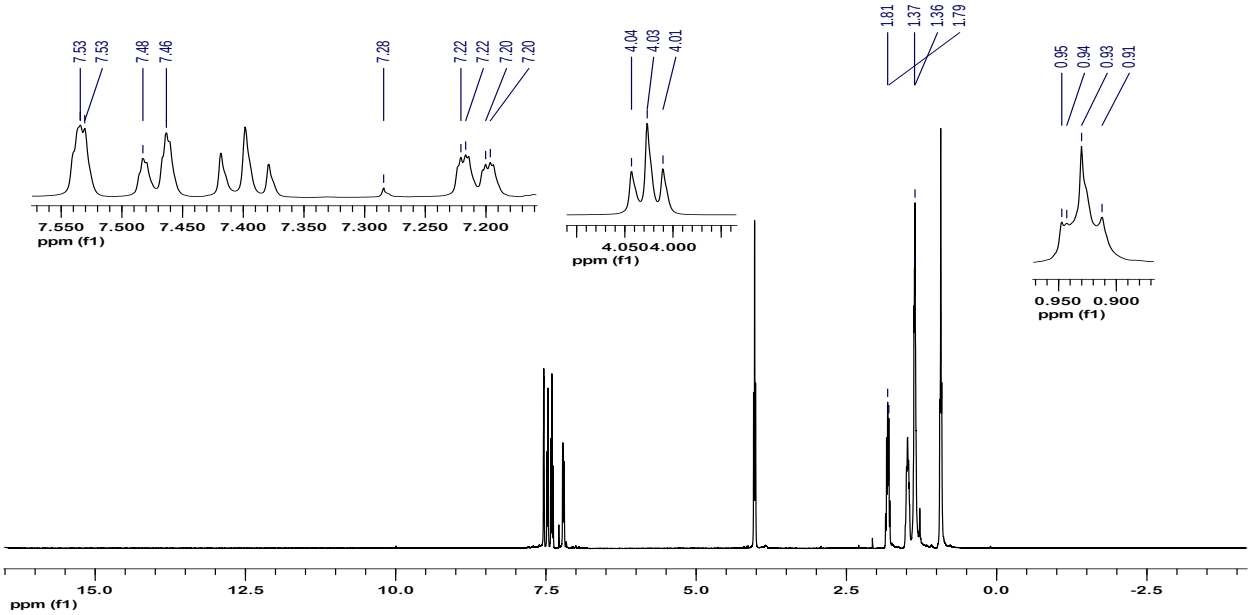


Appendix 4 : $^{1}$H-NMR spectrum of 1,2-bis(3-(hexyloxy)phenyl)ethane-1,2-dione (**43**).

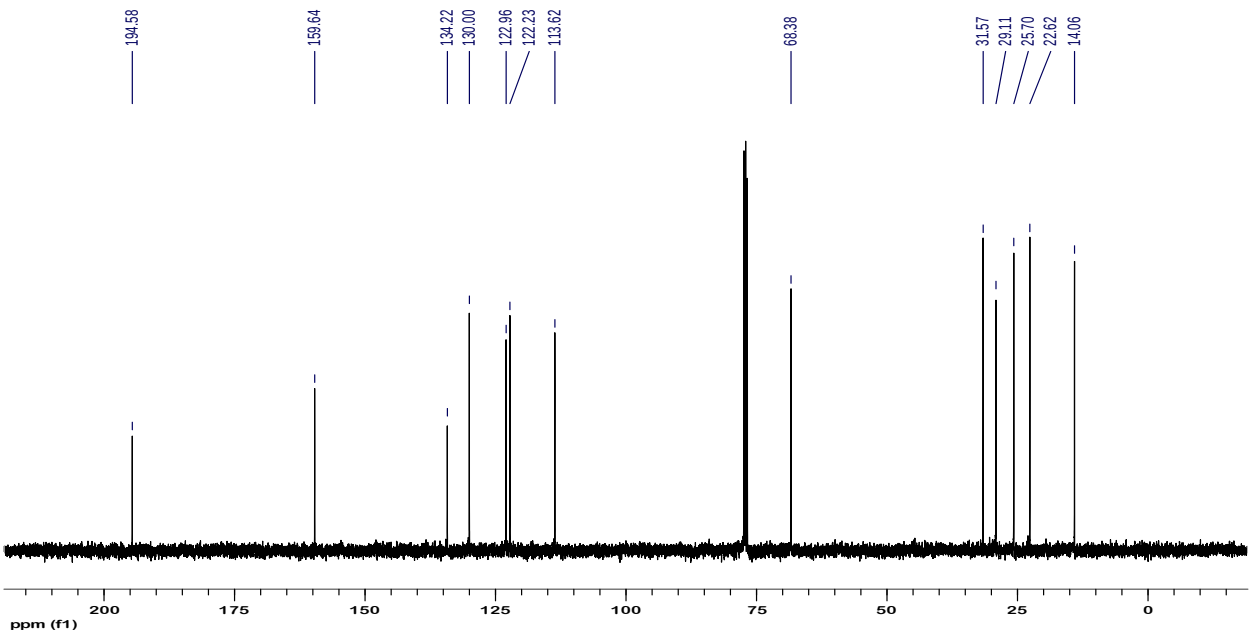


Appendix 5 : $^{13}$C-NMR spectrum of 1,2-bis(3-(hexyloxy)phenyl)ethane-1,2-dione (**43**).

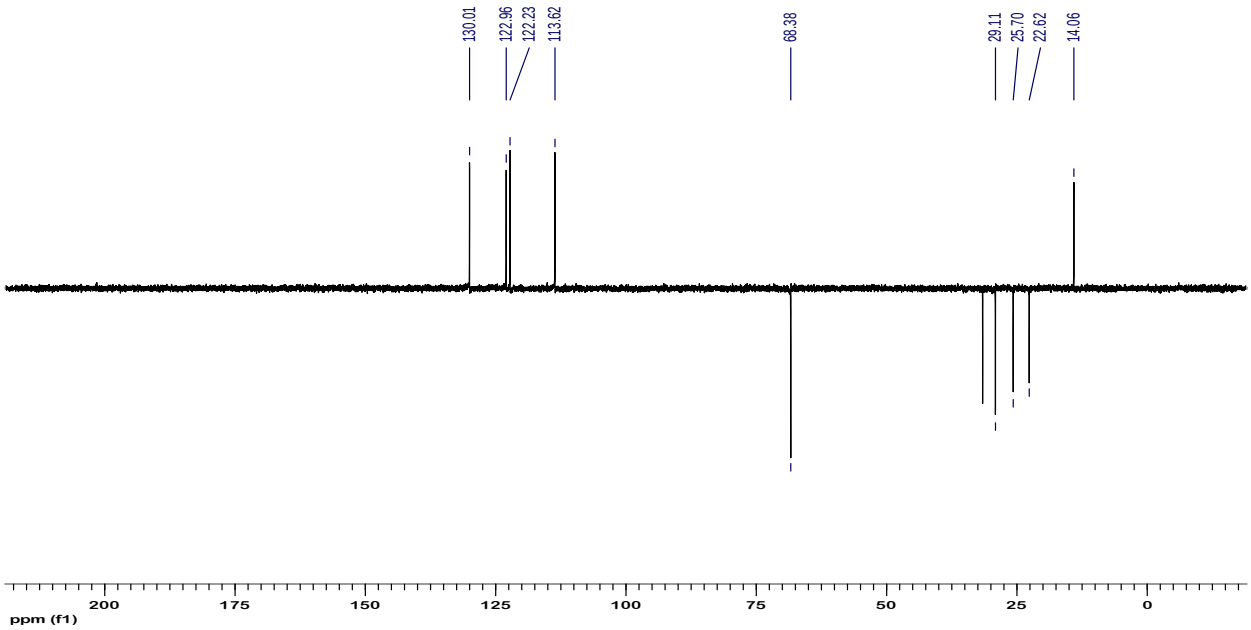


Appendix 6: DEPT-135 spectrum of 1,2-bis(3-(hexyloxy)phenyl)ethane-1,2-dione (**43**).

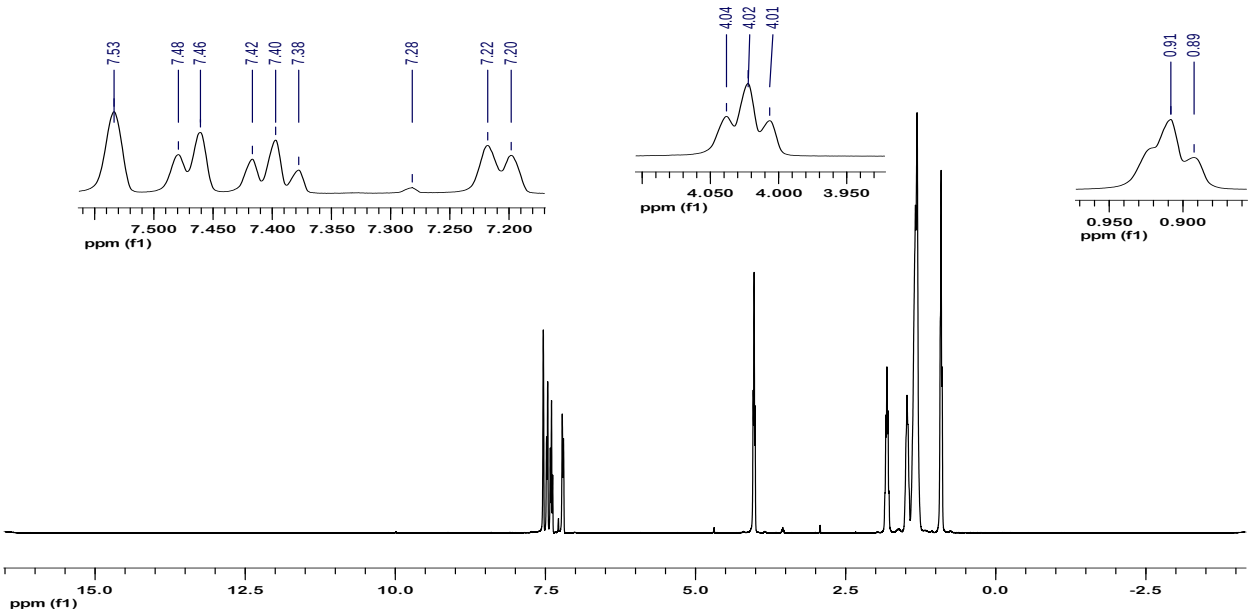


Appendix 7 : $^{1}$H-NMR spectrum of 1,2-bis(3-(octyloxy)phenyl)ethane-1,2-dione (**42**).

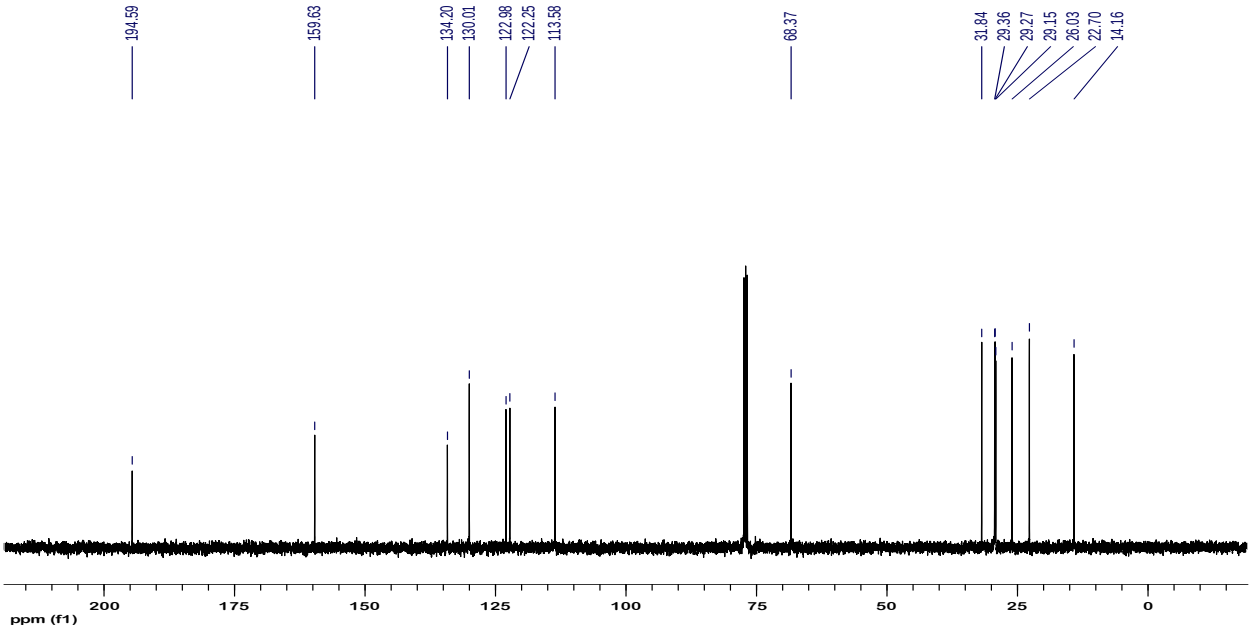


Appendix 8: $^{13}$C-NMR spectrum of 1,2-bis(3-(octyloxy)phenyl)ethane-1,2-dione (**42**).

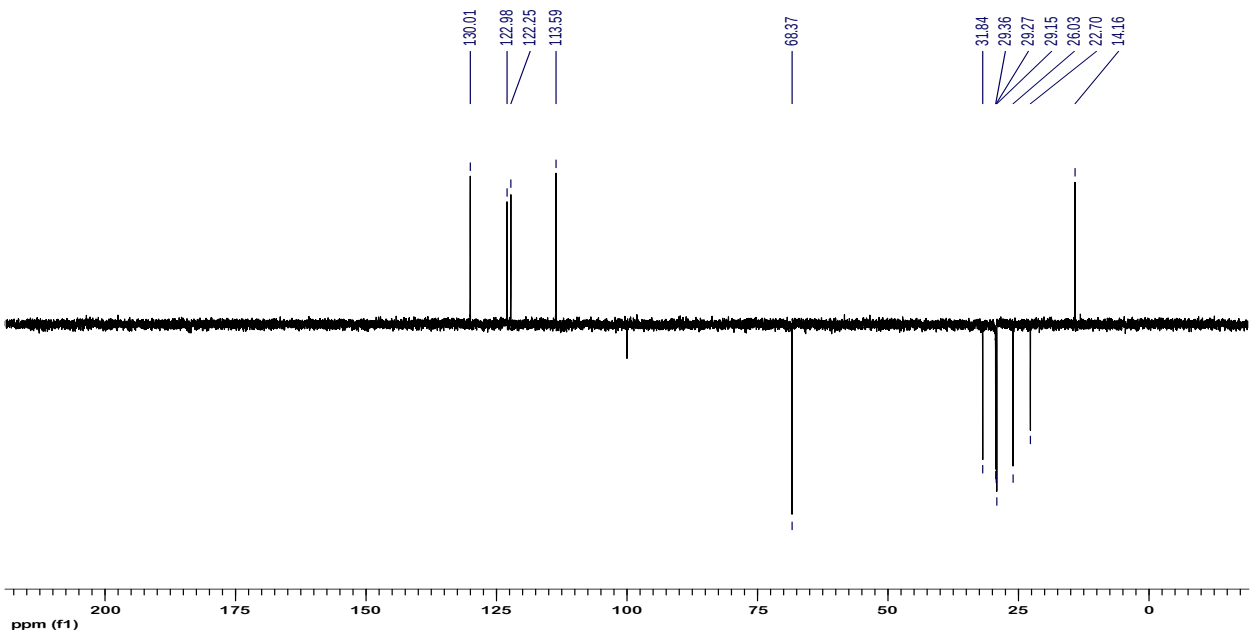


Appendix 9 : DEPT -135 spectrum of 1,2-bis(3-(octyloxy)phenyl)ethane-1,2-dione (**42**).

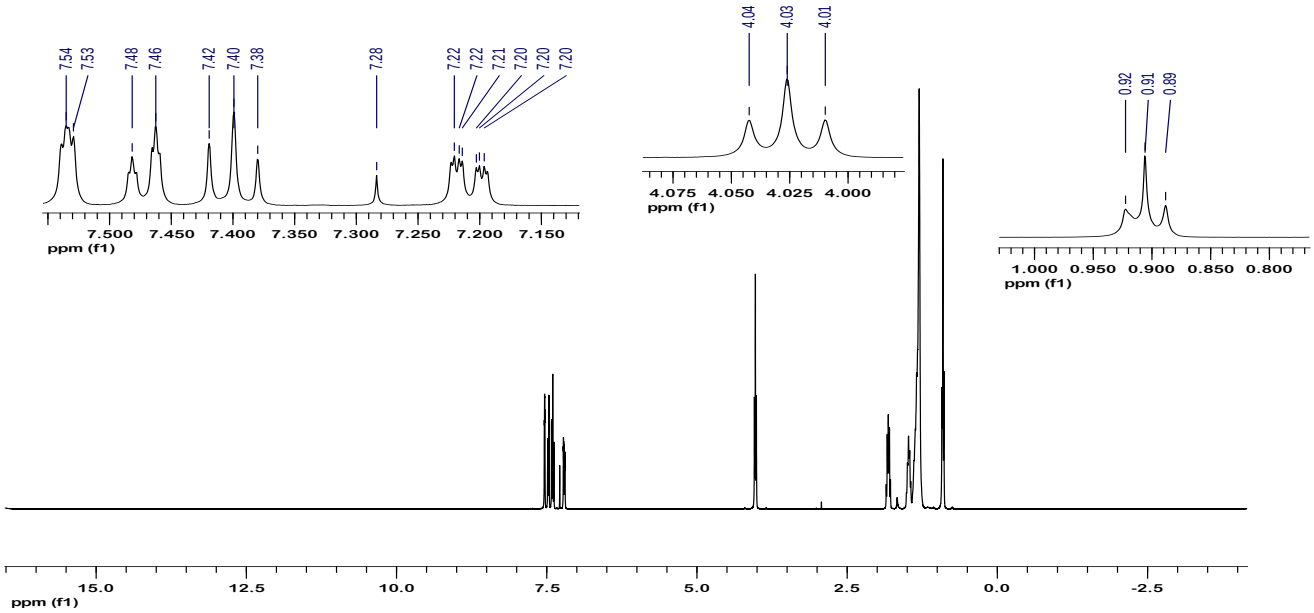


Appendix 10: $^{1}$H-NMR spectrum of 1,2-bis(3-(decyloxy)phenyl)ethane-1,2-dione (**41**).

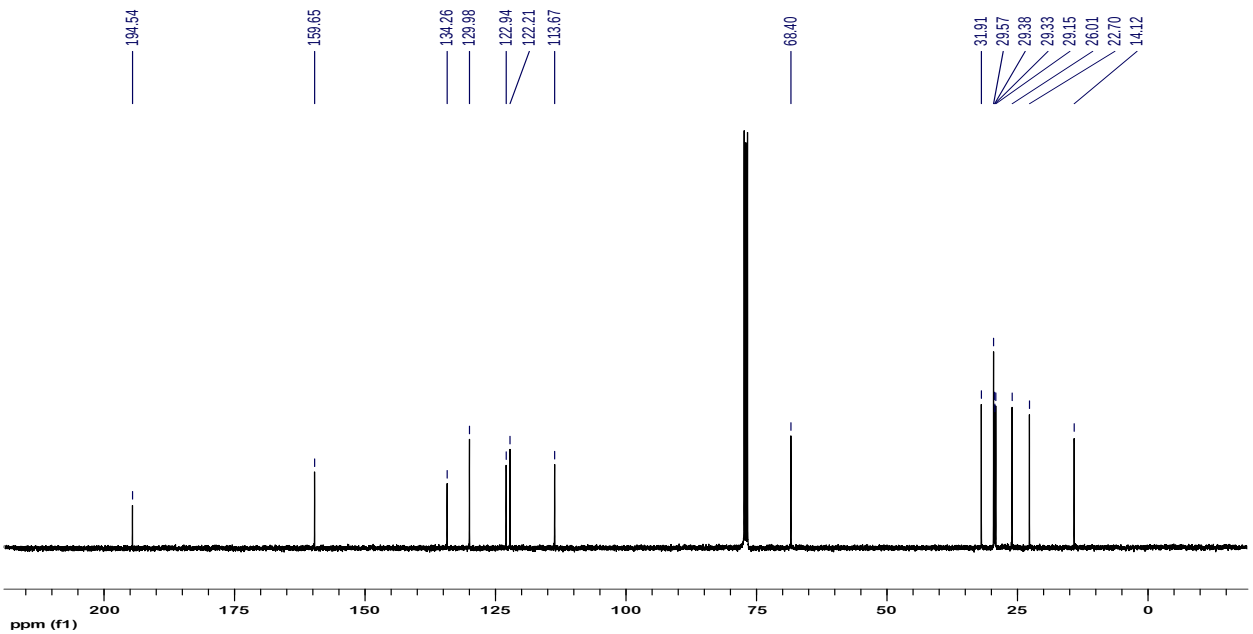


Appendix 11 : $^{13}$C-NMR spectrum of 1,2-bis(3-(decyloxy)phenyl)ethane-1,2-dione (**41**).

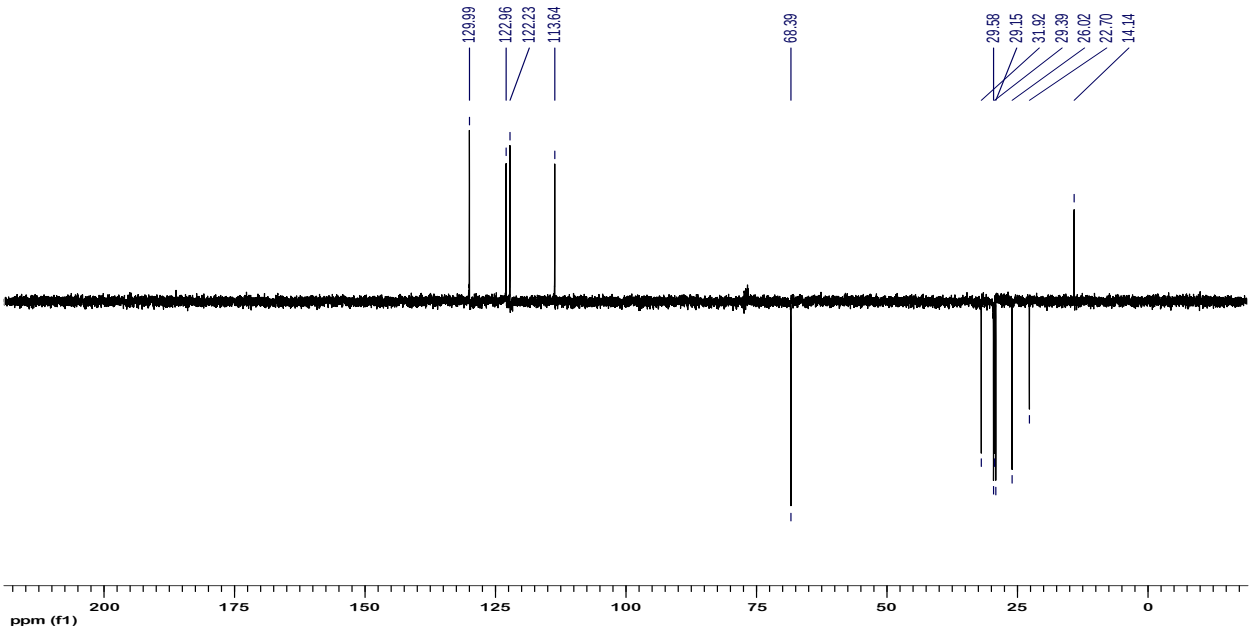


Appendix 12 : DEPT-135 spectra of 1,2-bis(3-(decyloxy)phenyl)ethane-1,2-dione (**41**).

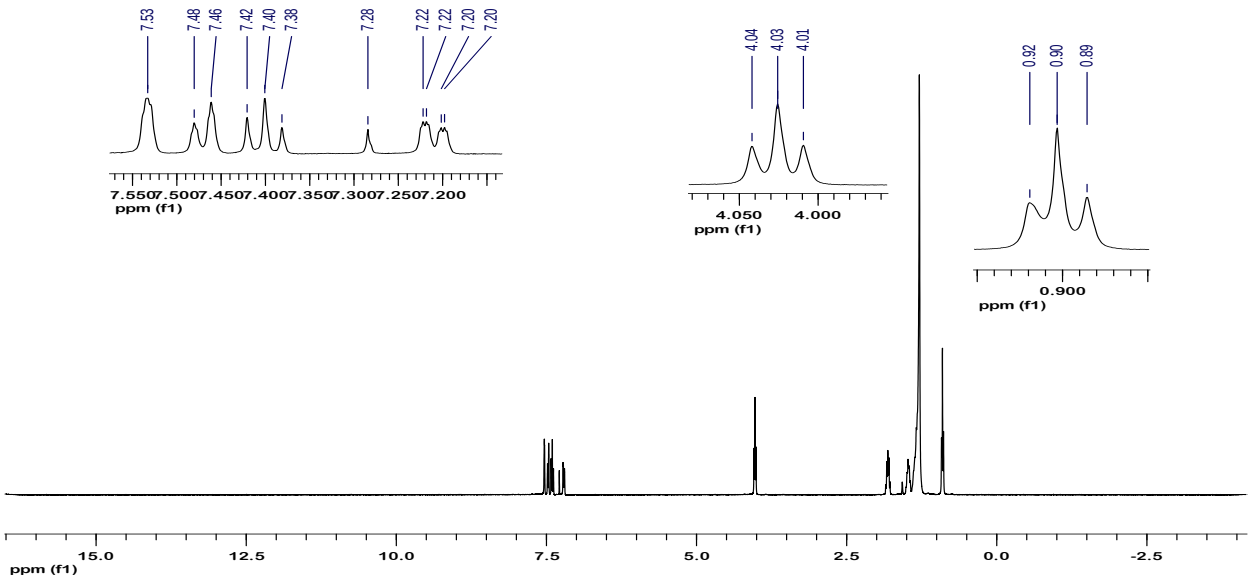


Appendix 13 : $^{1}$H-NMR spectrum of 1,2-bis(3-(dodecyloxy)phenyl)ethane-1,2-dione (**40**).

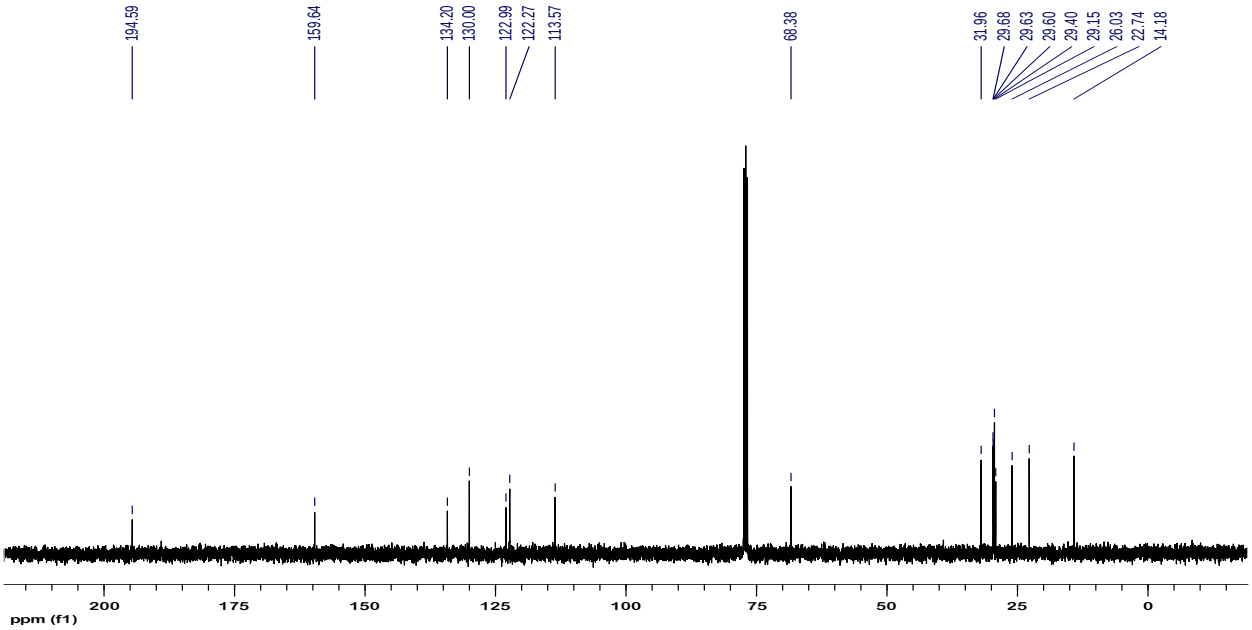


Appendix 14 : $^{13}$C-NMR spectrum of 1,2-bis(3-(dodecyloxy)phenyl)ethane-1,2-dione (**40**).

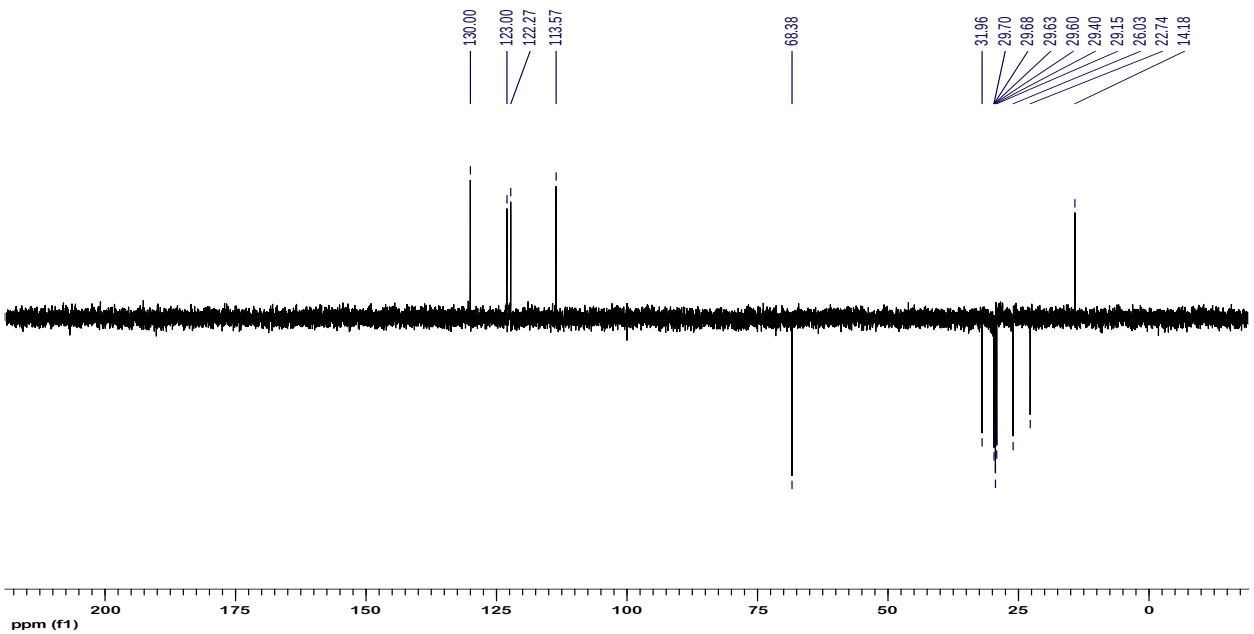


Appendix 15 : DEPT -135 spectrum of 1,2-bis(3-(dodecyloxy)phenyl)ethane-1,2-dione (**40**).

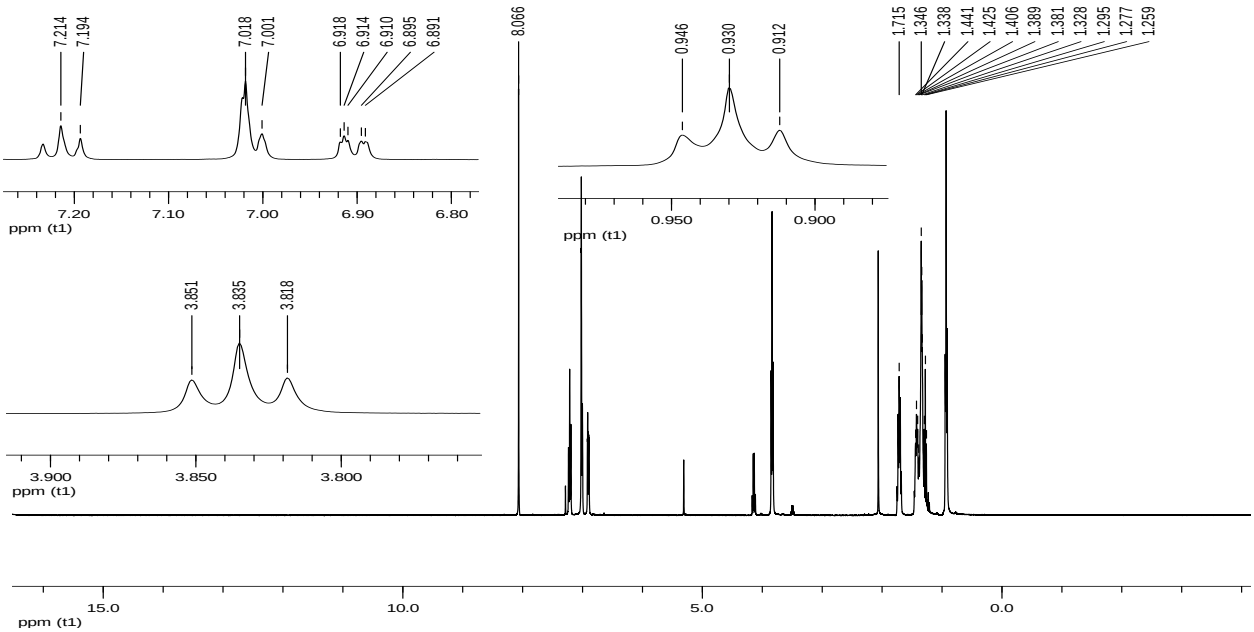


Appendix 16 : $^{1}$H-NMR spectrum of 2,3-bis(3-(hexyloxy)phenyl)thieno[3,4-*b*]pyrazine (**47**).

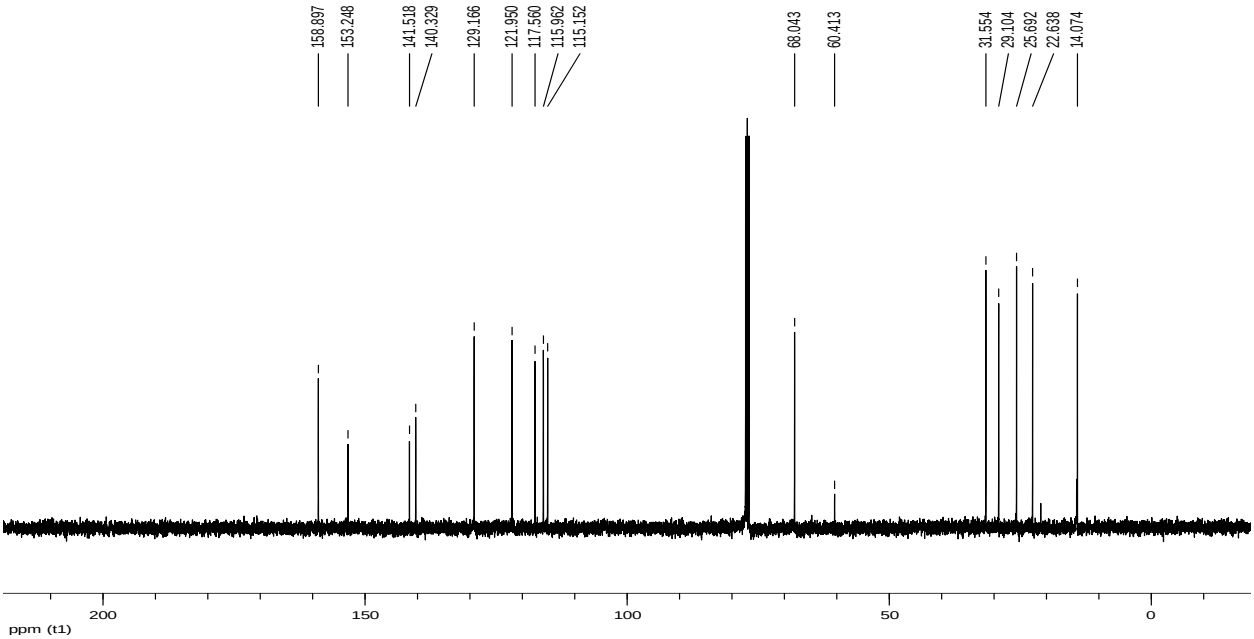


Appendix 17: $^{13}$C-NMR spectrum of 2,3-bis(3-(hexyloxy)phenyl)thieno[3,4-*b*]pyrazine (**47**).

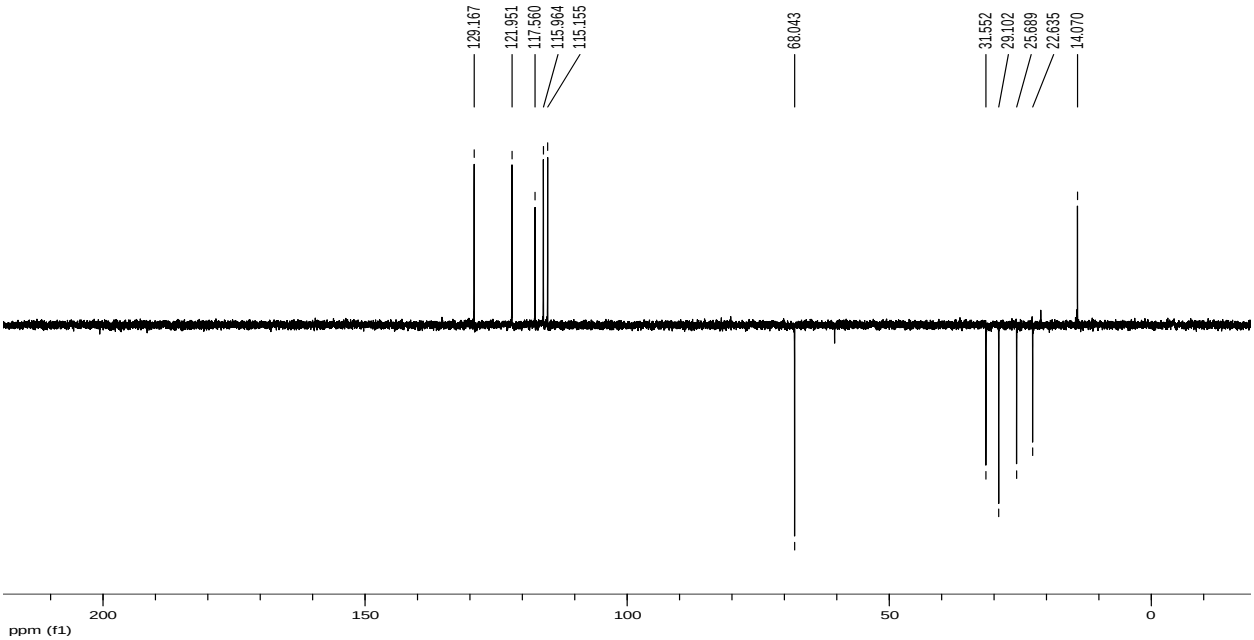

Appendix 18 : DEPT-135 spectrum of 2,3-bis(3-(hexyloxy)phenyl)thieno[3,4-*b*]pyrazine (**47**).

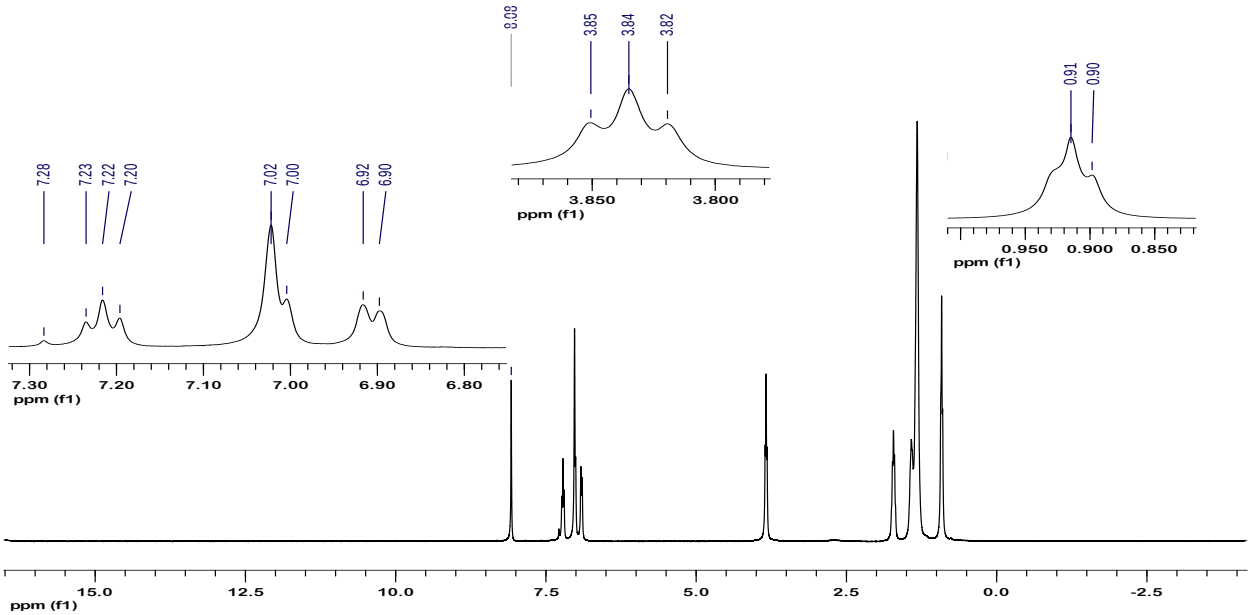


Appendix 19 : $^{1}$H-NMR spectrum of 2,3-bis(3-(octyloxy)phenyl)thieno[3,4-*b*]pyrazine (**46**).

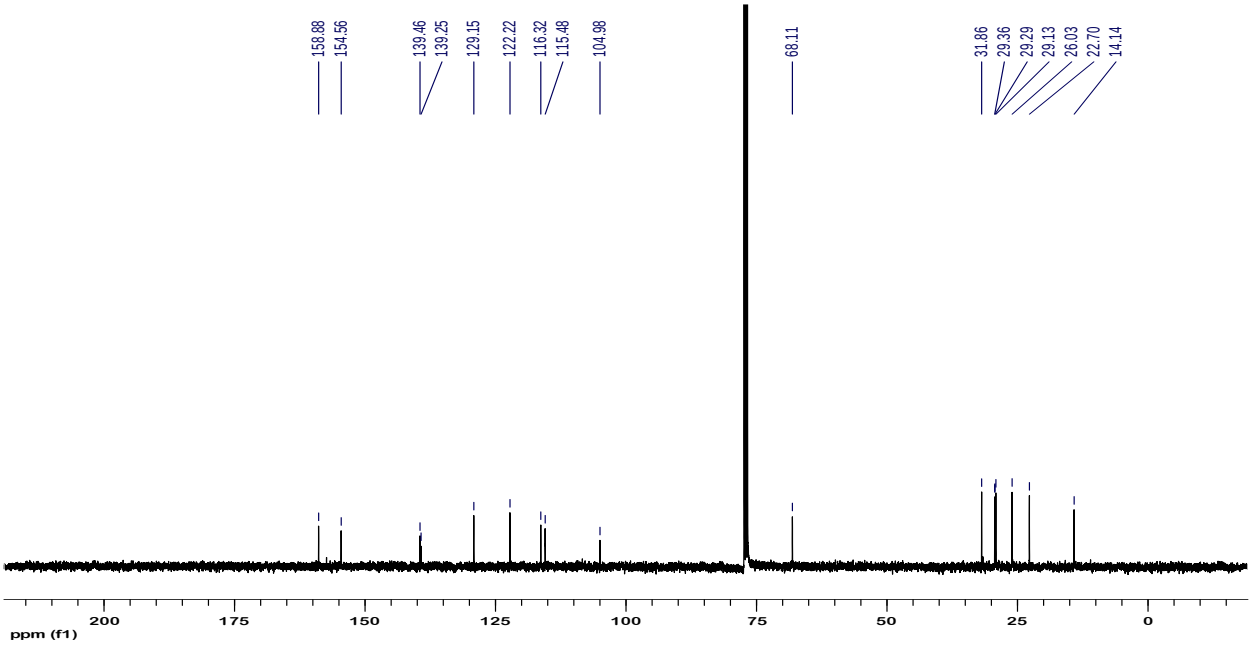


Appendix 20 : $^{13}$C-NMR spectrum of 2,3-bis(3-(octyloxy)phenyl)thieno[3,4-*b*]pyrazine (**46**).

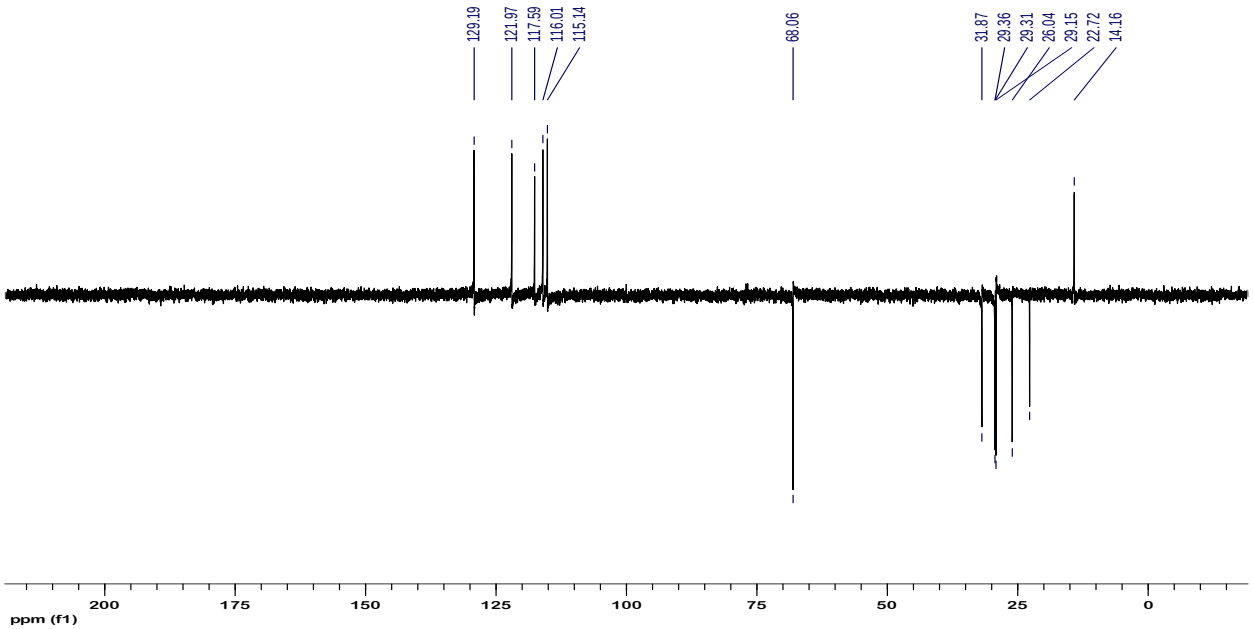


Appendix 21 : DEPT-135 spectrum of 2, 3-bis (3-(octyloxy)phenyl)thieno[3,4-*b*]pyrazine (**46**).

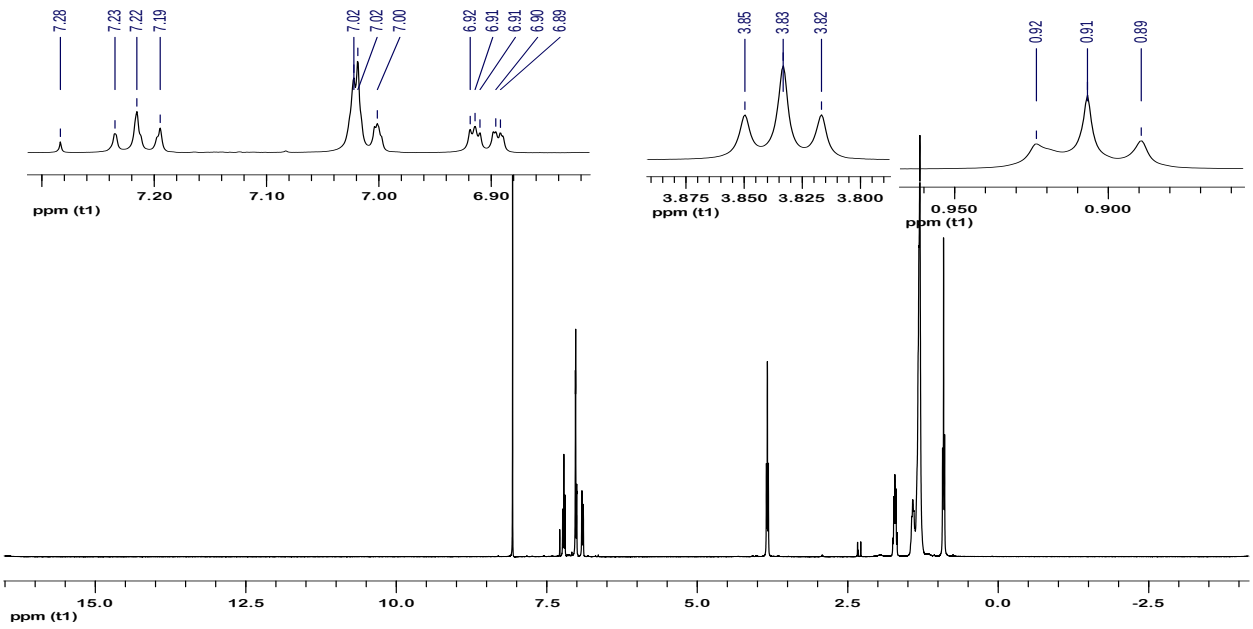


Appendix 22 : $^{1}$H-NMR spectrum of 2, 3-bis(3-(decyloxy)phenyl)thieno[3,4-*b*]pyrazine (**45**).

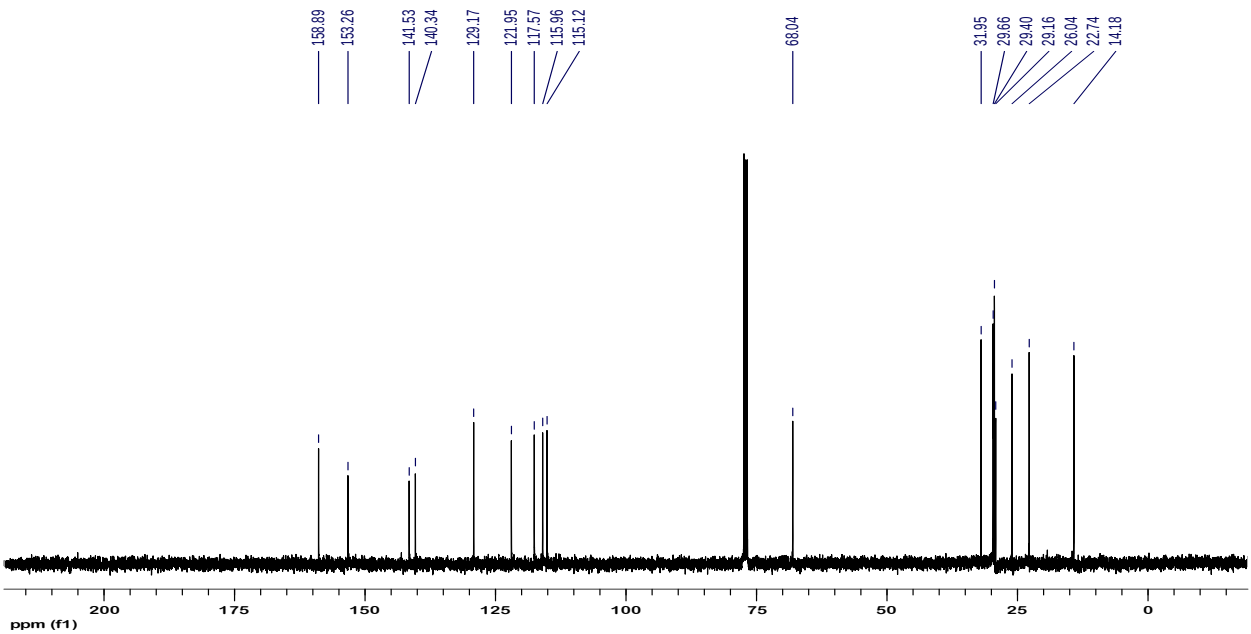


Appendix 23 : $^{13}$C-NMR spectrum of 2,3-bis(3-(decyloxy)phenyl)thieno[3,4-*b*]pyrazine (**45**).

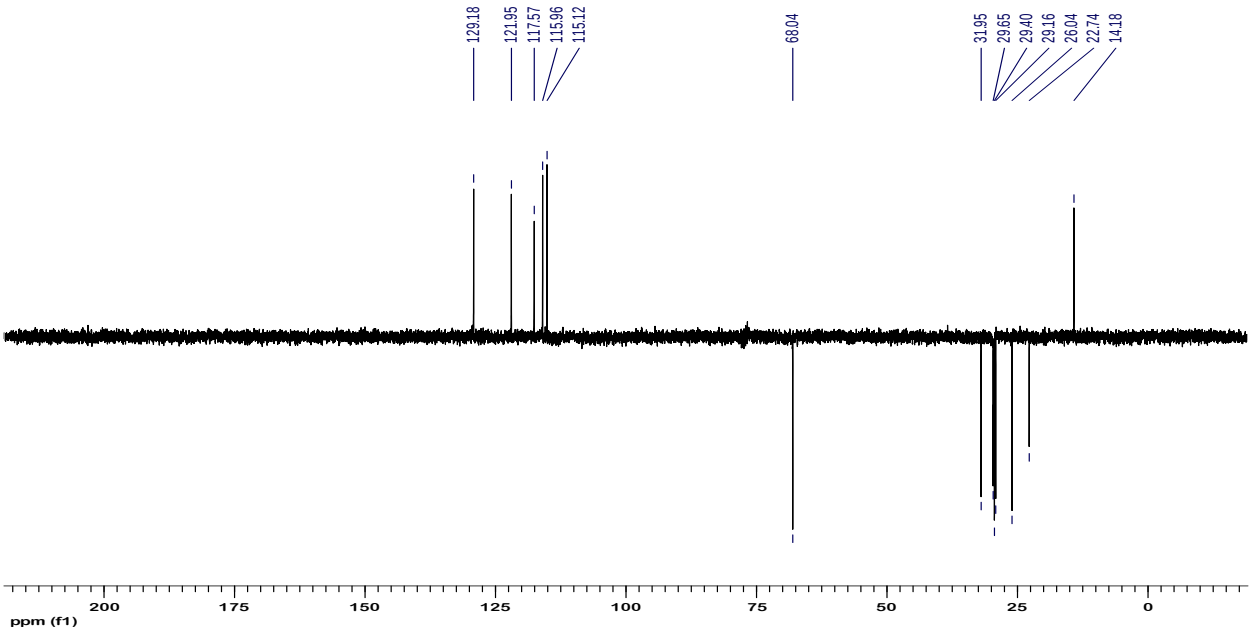


Appendix 24 : DEPT-135 spectrum of 2,3-bis(3-(decyloxy)phenyl)thieno[3,4-*b*]pyrazine (**45**).

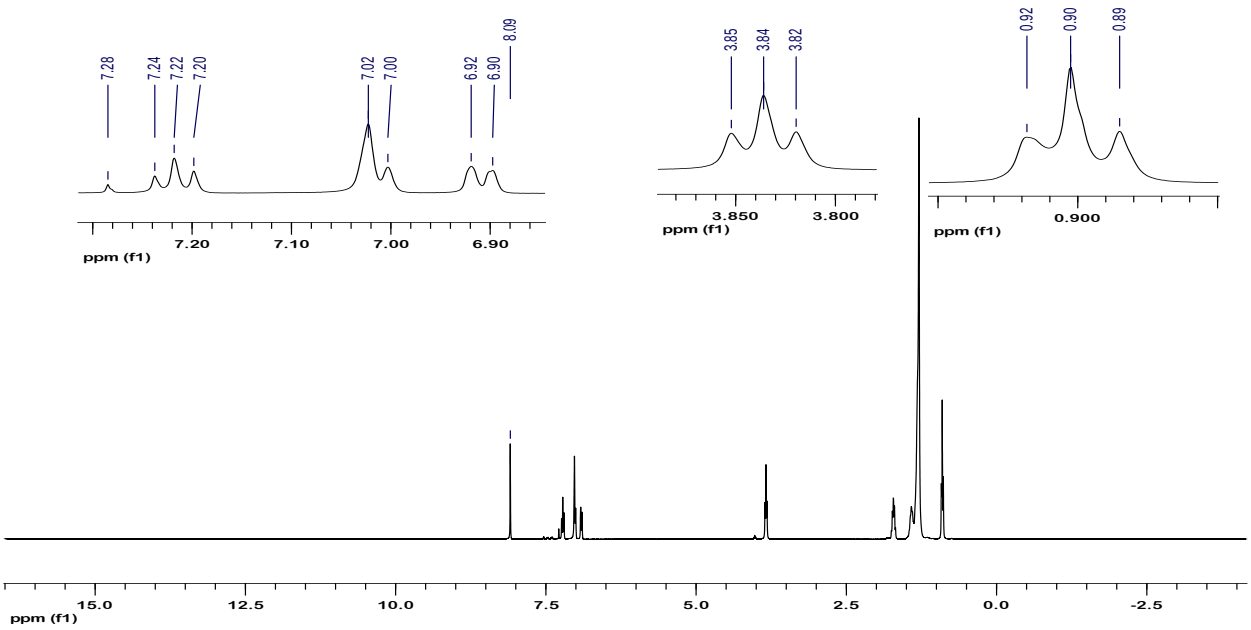


Appendix 25 : $^{1}$H-NMR spectrum of 2,3-bis(3-(dodecyloxy)phenyl)thieno[3,4-*b*]pyrazine (**44**).

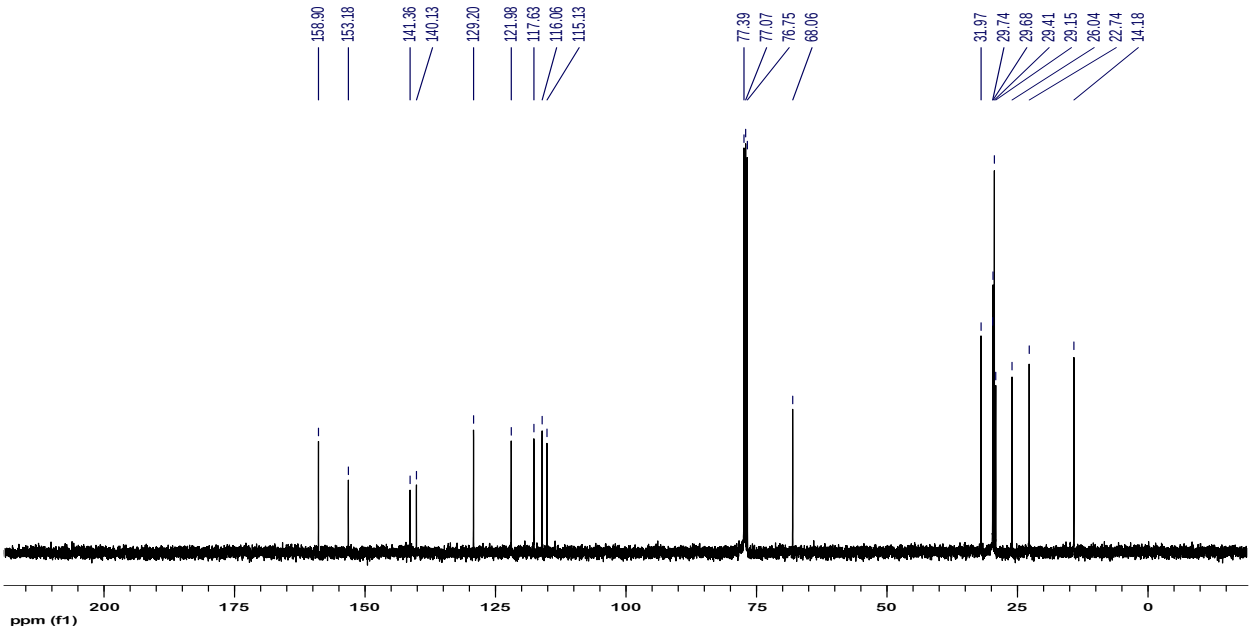


Appendix 26: $^{13}$C-NMR spectrum of 2, 3-bis(3-(dodecyloxy)phenyl)thieno[3,4-*b*]pyrazine (**44**).

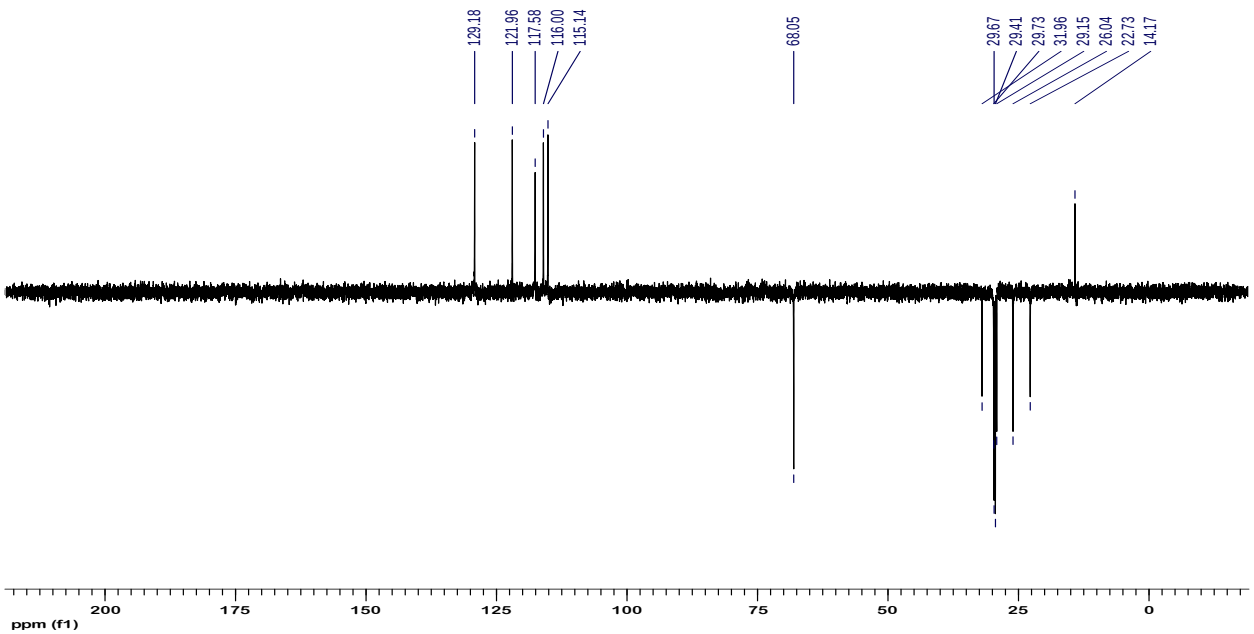


Appendix 27 : DEPT-135 spectrum of 2, 3-bis(3-(dodecyloxy)phenyl)thieno[3,4-*b*]pyrazine (**44**).

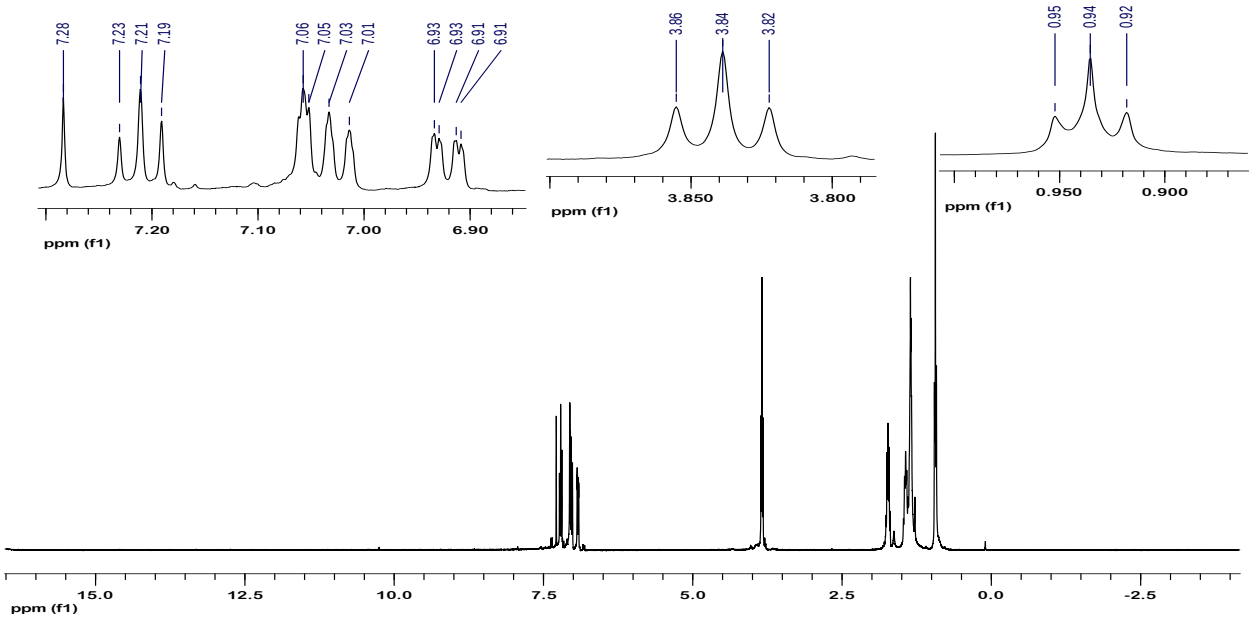


Appendix 28: $^{1}$H-NMR spectrum of 5,7-dibromo-2,3-bis(3-(hexyloxy)phenyl)thieno[3,4-*b*]pyrazine (**51**).

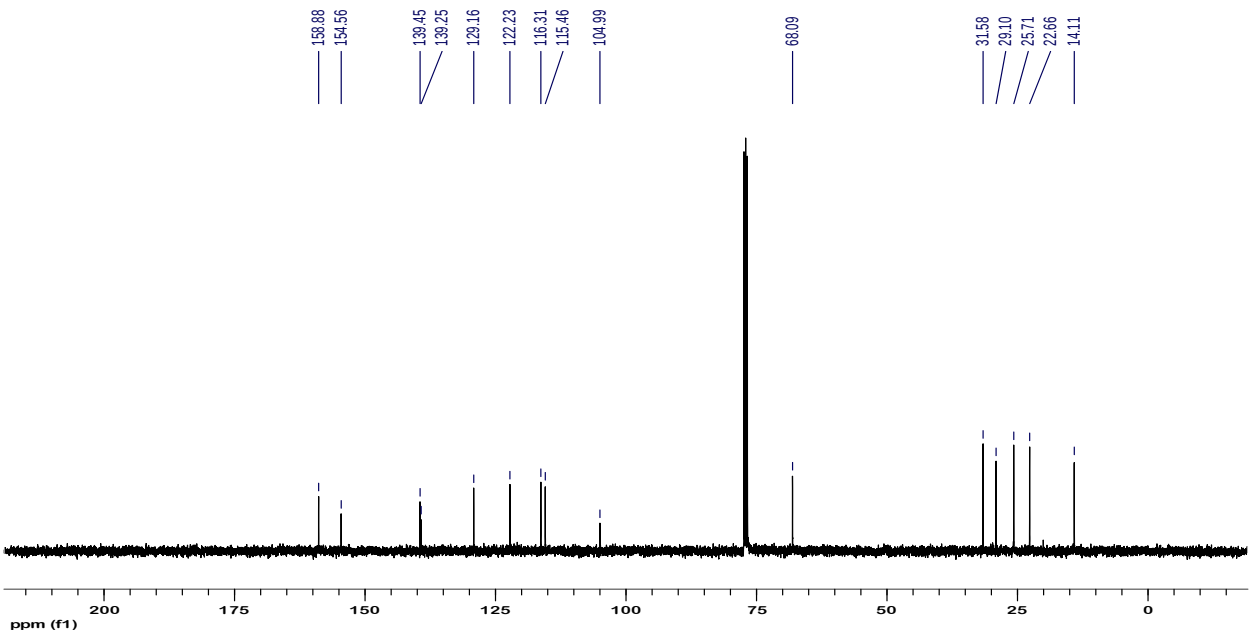


Appendix 29 : $^{13}$C-NMR spectrum of 5,7-dibromo-2,3-bis(3-(hexyloxy)phenyl)thieno[3,4-*b*]pyrazine (**51**).

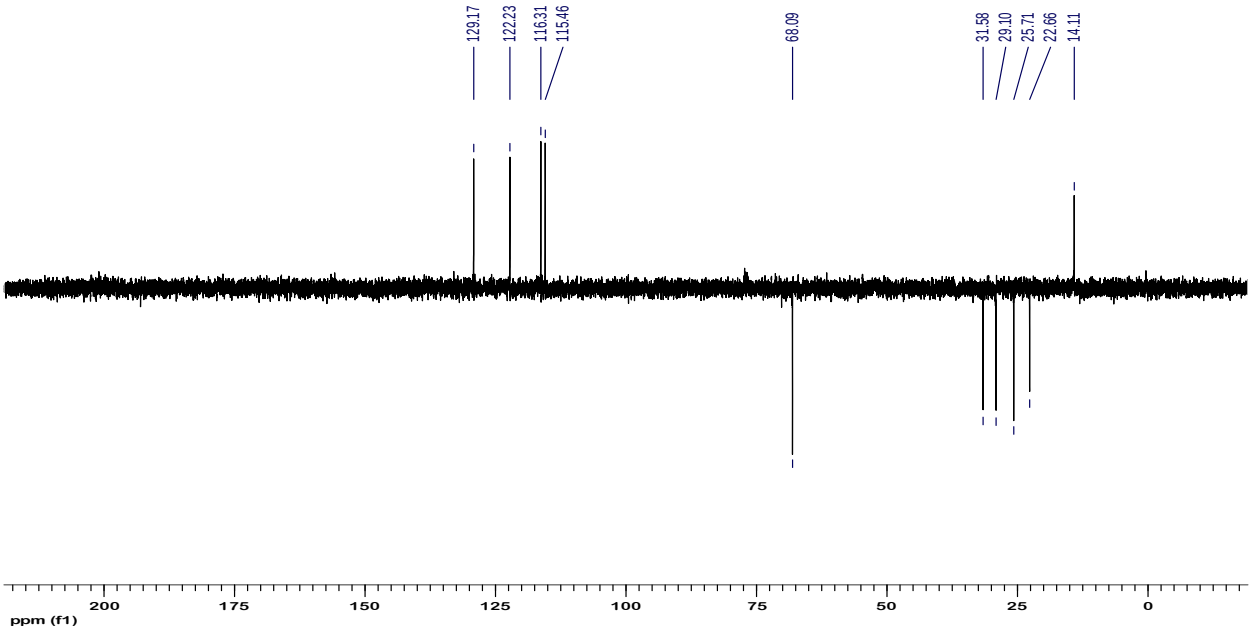


Appendix 30 : DEPT -135 spectrum of 5, 7-dibromo-2,3-bis(3-(hexyloxy)phenyl)thieno[3,4-*b*]pyrazine (**51**).

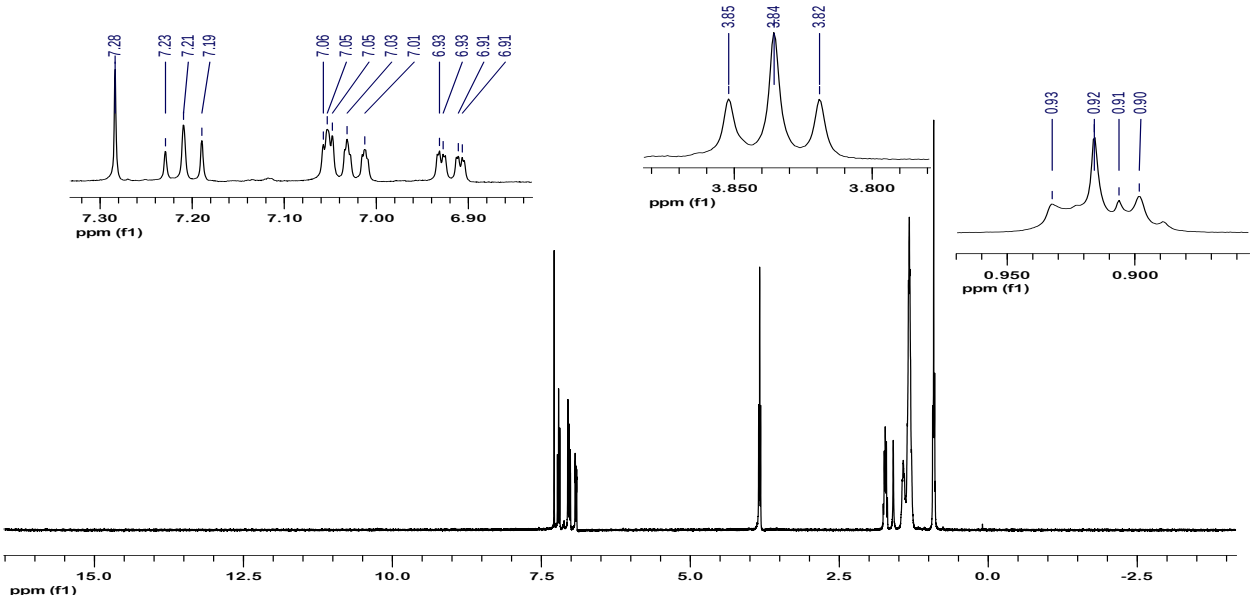


Appendix 31: $^{1}$H-NMR spectrum of 5,7-dibromo-2,3-bis(3-(octyloxy)phenyl)thieno[3,4-*b*]pyrazine (**50**).

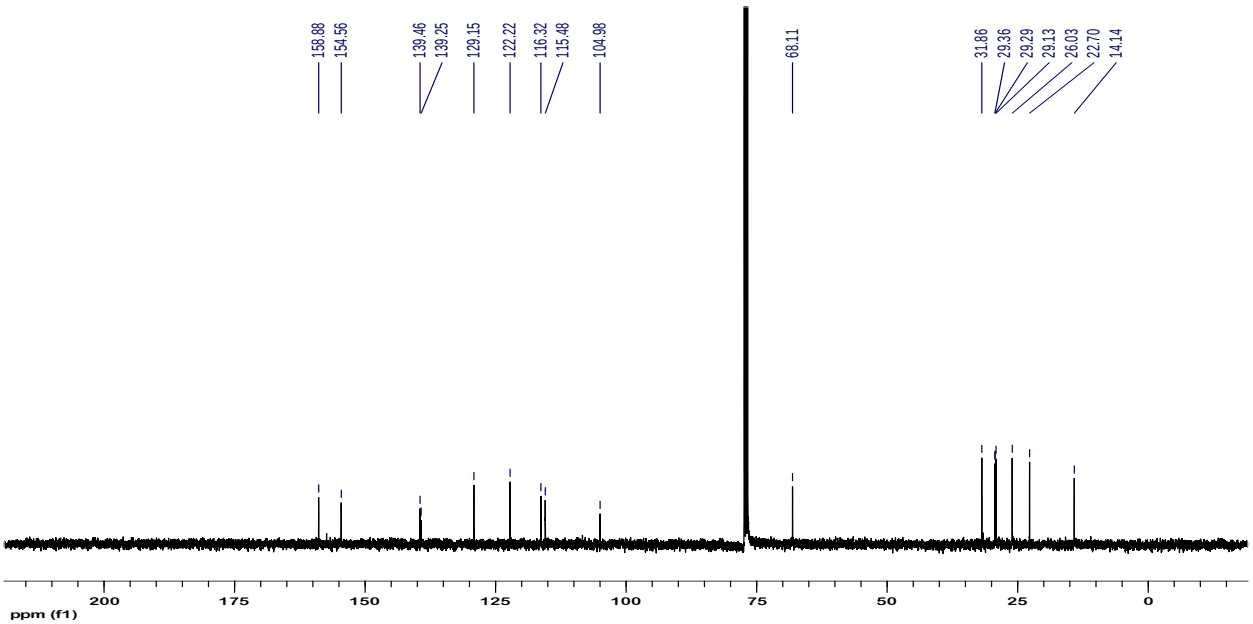


Appendix 32 : $^{13}$C-NMR spectrum of 5,7-dibromo-2,3-bis(3-(octyloxy)phenyl)thieno[3,4-*b*]pyrazine **(50).**

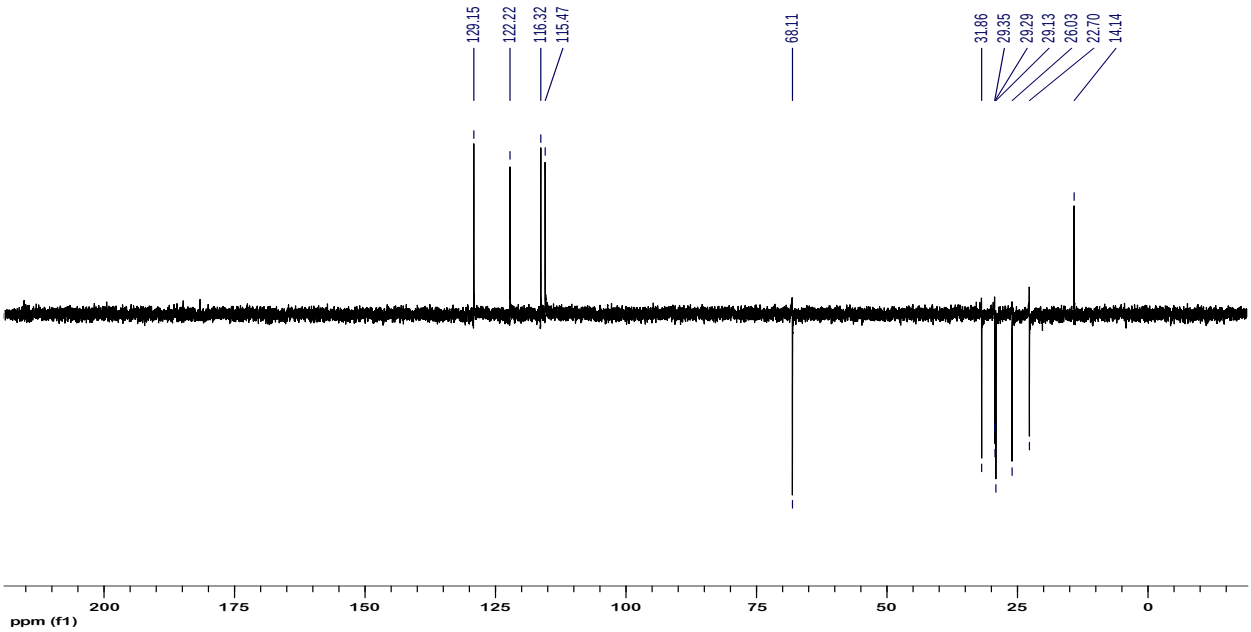


Appendix 33 **:** DEPT -135 spectrum of 5,7-dibromo-2,3-bis(3-(octyloxy)phenyl)thieno[3,4-*b*]pyrazine **(50).**

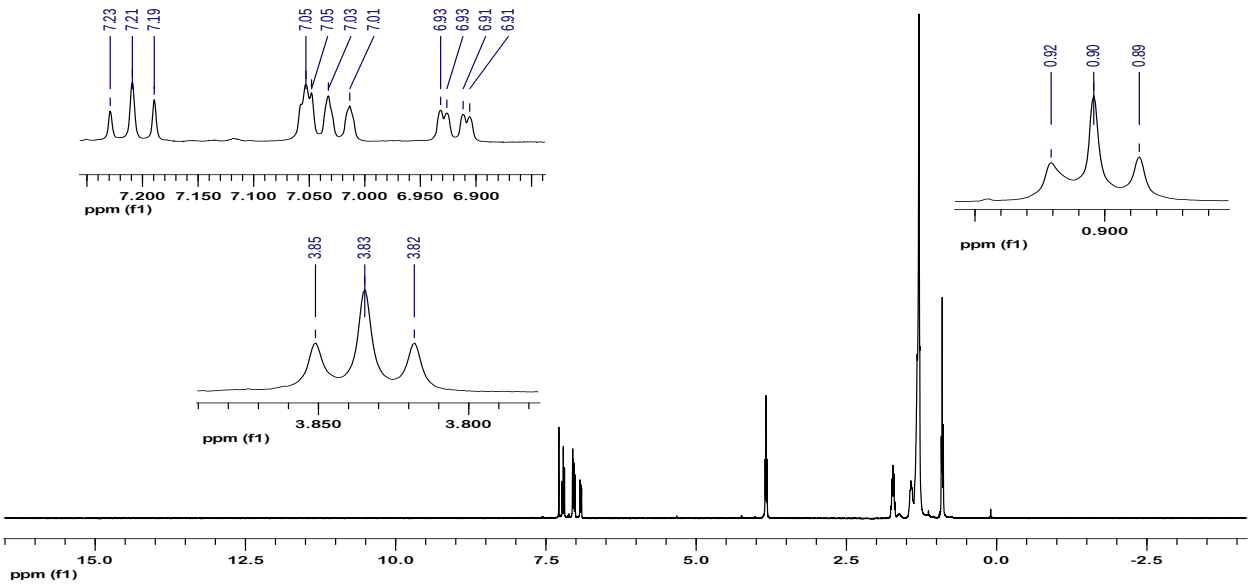


Appendix 34 : $^{1}$H-NMR spectrum of 5,7-dibromo-2,3-bis(3-(dodecyloxy)phenyl)thieno[3,4-*b*]pyrazine (**48**).

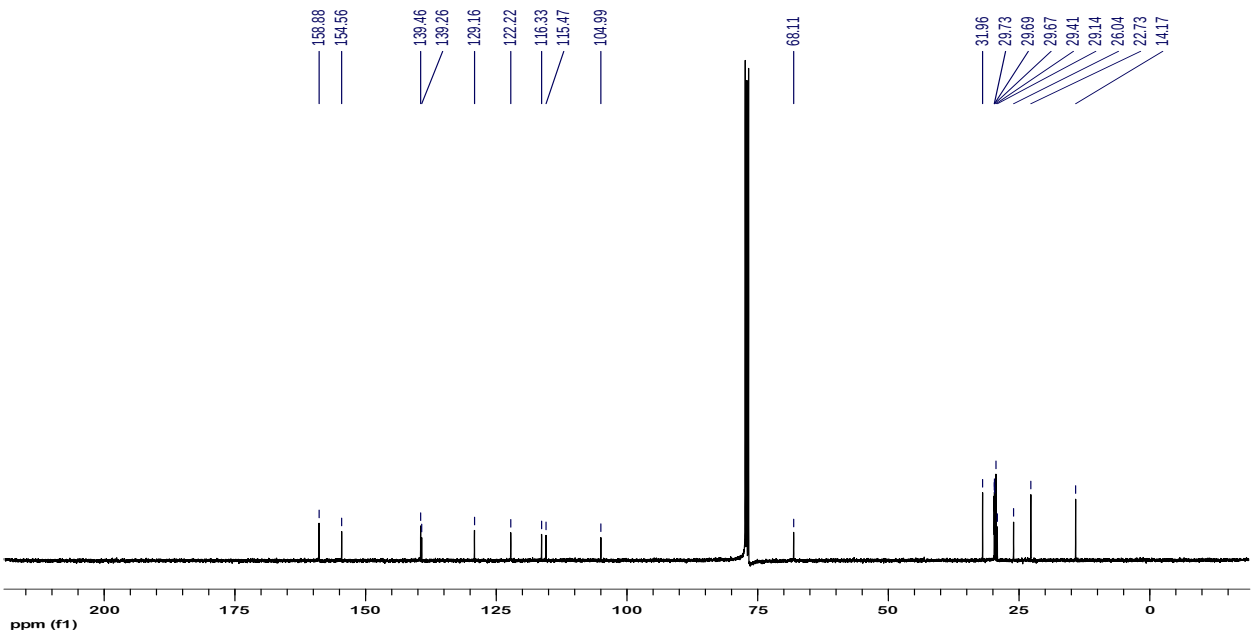


Appendix 35: $^{13}$C-NMR spectrum of 5,7-dibromo-2,3-bis(3-(dodecyloxy)phenyl)thieno[3,4-*b*]pyrazine (**48**).

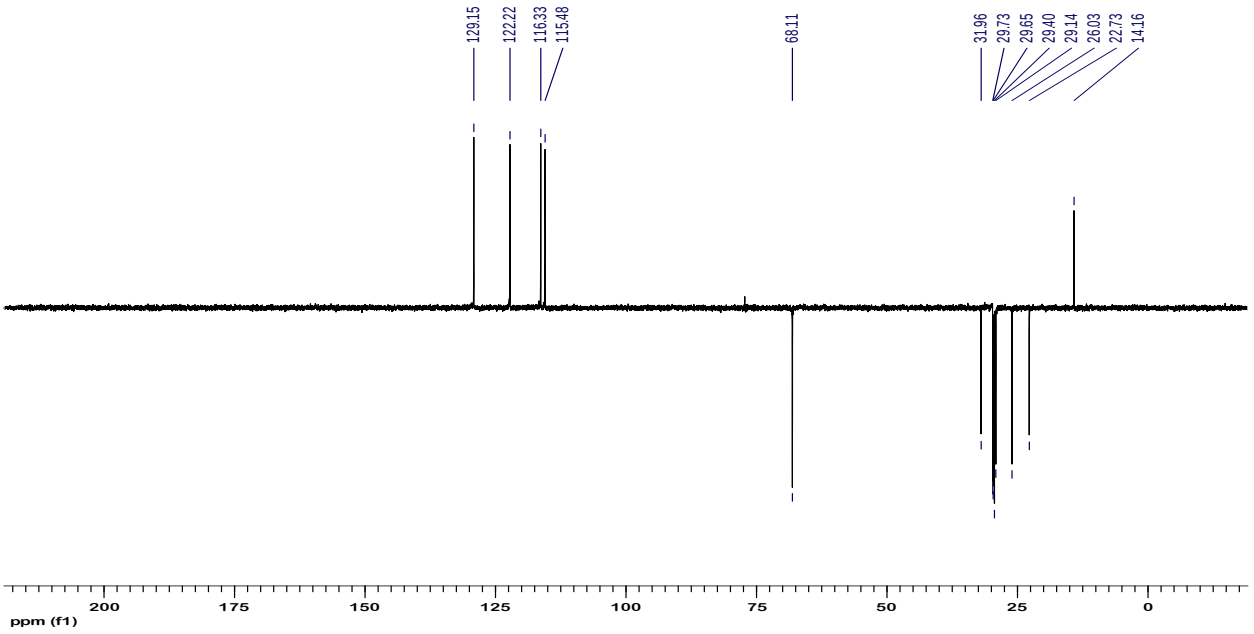


Appendix 36 : DEPT-135 spectrum of 5,7-dibromo-2,3-bis(3-(dodecyloxy)phenyl)thieno[3,4-*b*]pyrazine (**48**).

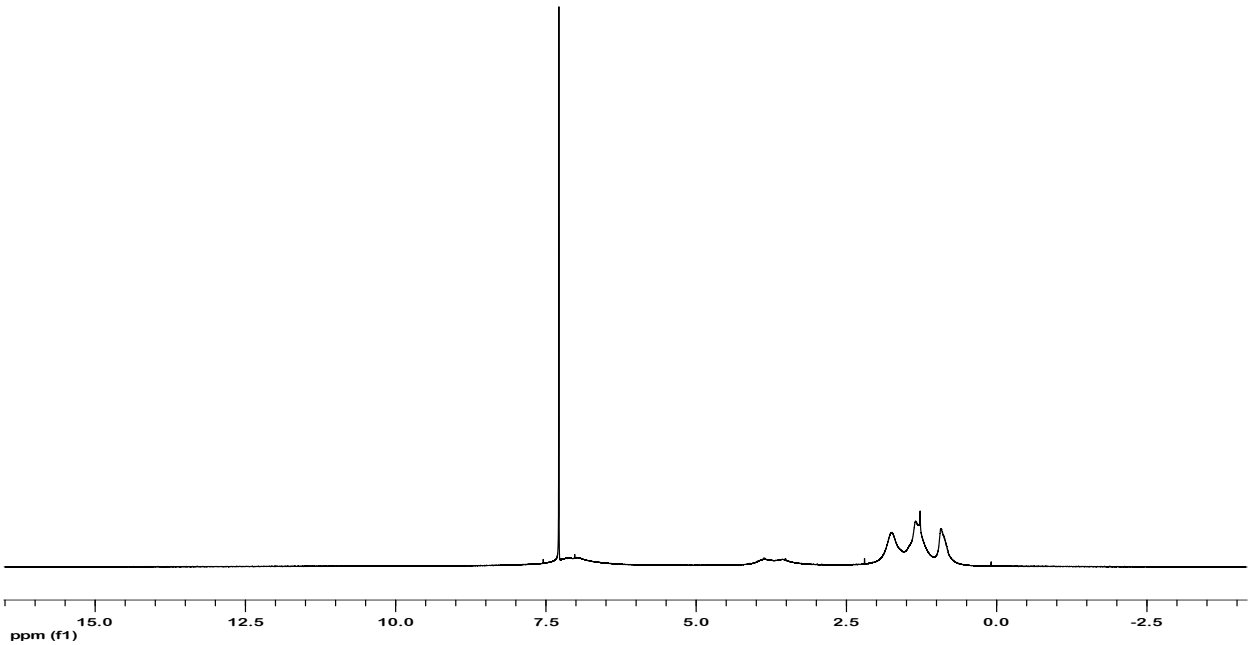


Appendix 37: $^{1}$H-NMR spectrum of poly[2,3-bis(3-(hexyloxy)phenyl)thieno[3,4-*b*]pyrazine -5,7-diyl-*alt*-thiophene-2,5-diyl] (**55**).

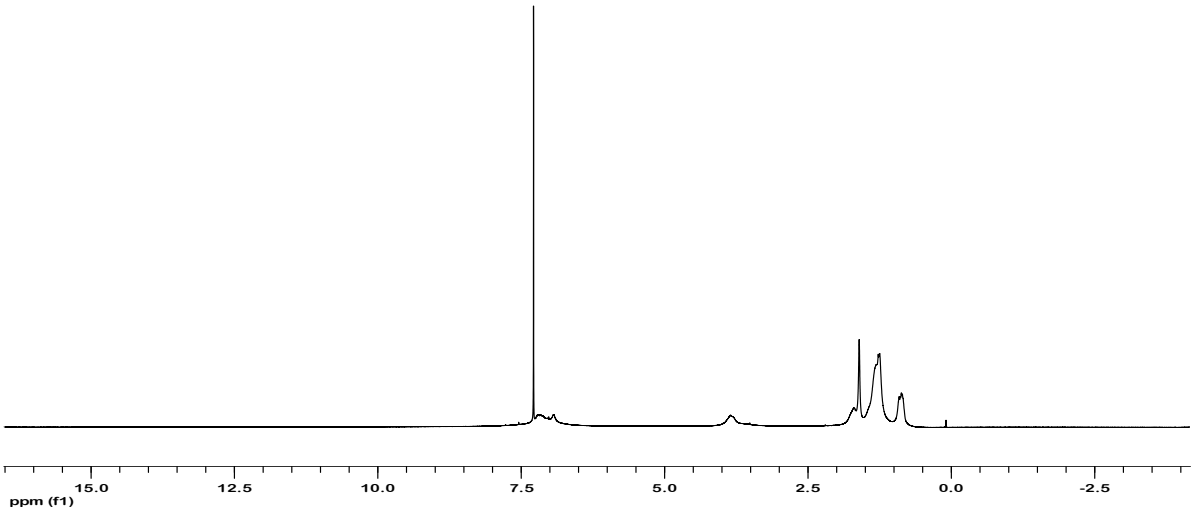


Appendix 38 : $^{1}$H-NMR spectrum of poly[2,3-bis(3-(octyloxy)phenyl)thieno[3,4-*b*]pyrazine-5,7-diyl-*alt*-thiophene-2,5-diyl] (**54**).

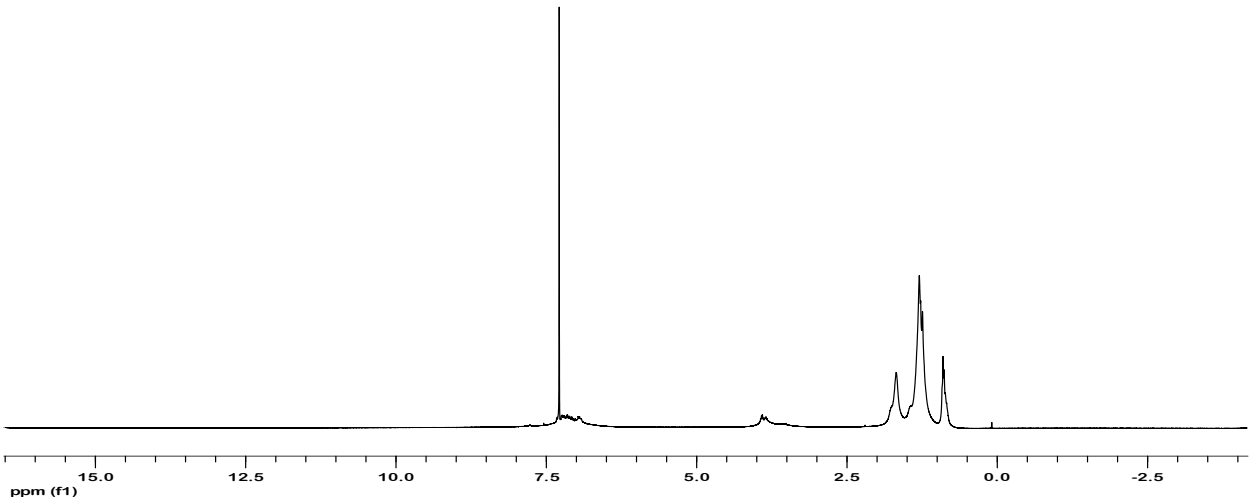


Appendix 39 : $^{1}$H-NMR spectrum of poly[2,3-bis(3-(decyloxy)phenyl)thieno[3,4-*b*]pyrazine-5,7-diyl-*alt*-thiophene-2,5-diyl] (**53**).

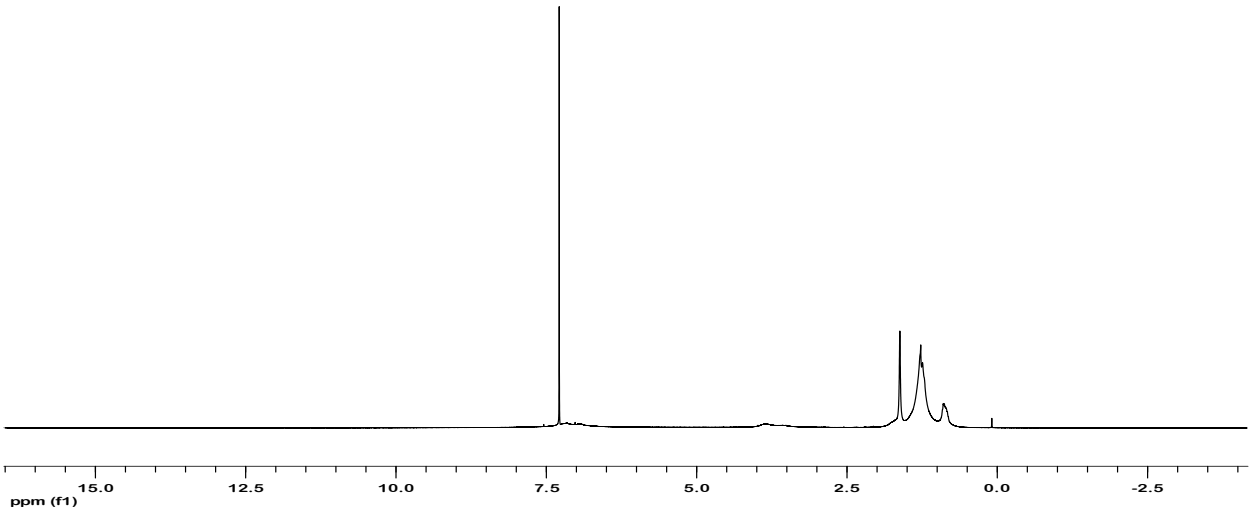


Appendix 40 : $^{1}$H-NMR spectrum of poly[2,3-bis(3-(dodecyloxy)phenyl)thieno[3,4-*b*]pyrazine -5,7-diyl-*alt*-thiophene-2,5-diyl] (**52**).

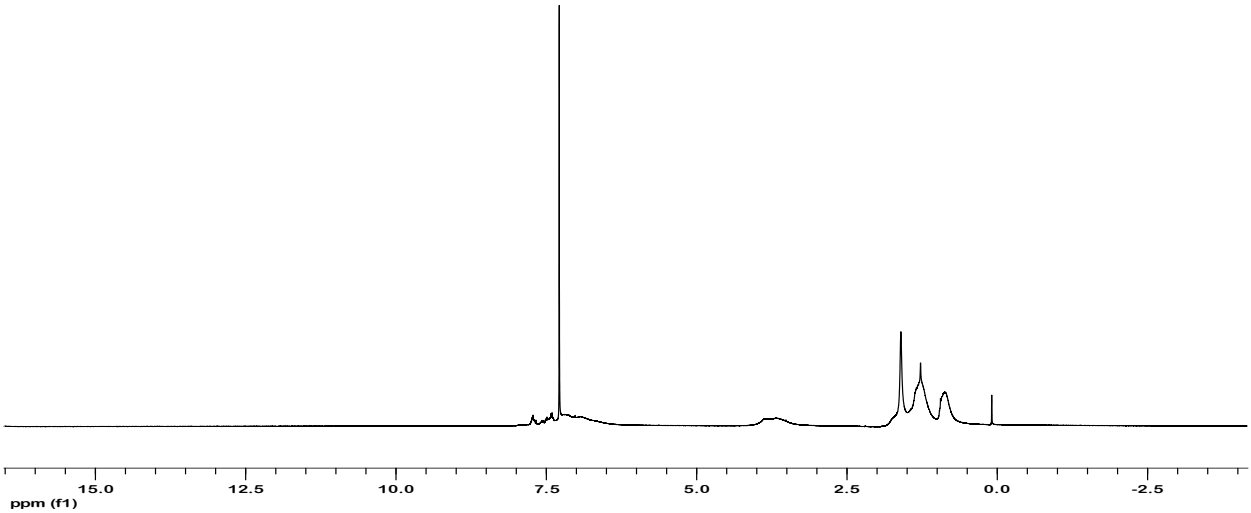


Appendix 41: $^{1}$H-NMR spectrum of poly[2,3-bis(3-(hexyloxy)phenyl)thieno[3,4-b]pyrazine -5,7-diyl-*alt*-thiophene-2,5-diyl] (**55'**).

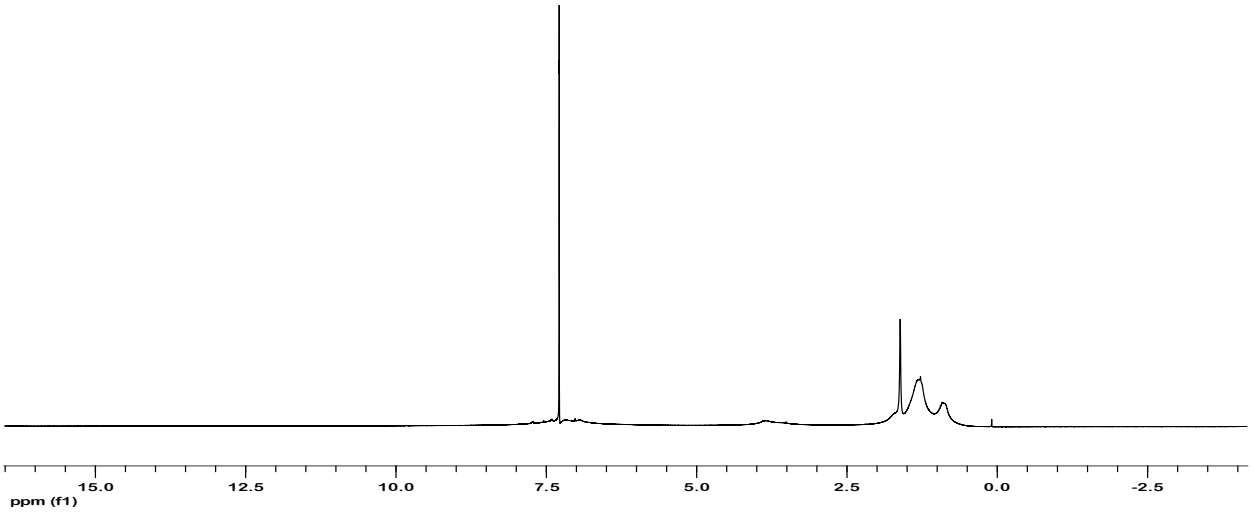


Appendix 42: $^{1}$H-NMR spectrum of poly[2,3-bis(3-(octyloxy)phenyl)thieno[3,4-*b*]pyrazine-5,7-diyl-*alt*-thiophene-2,5-diyl] (**54'**).

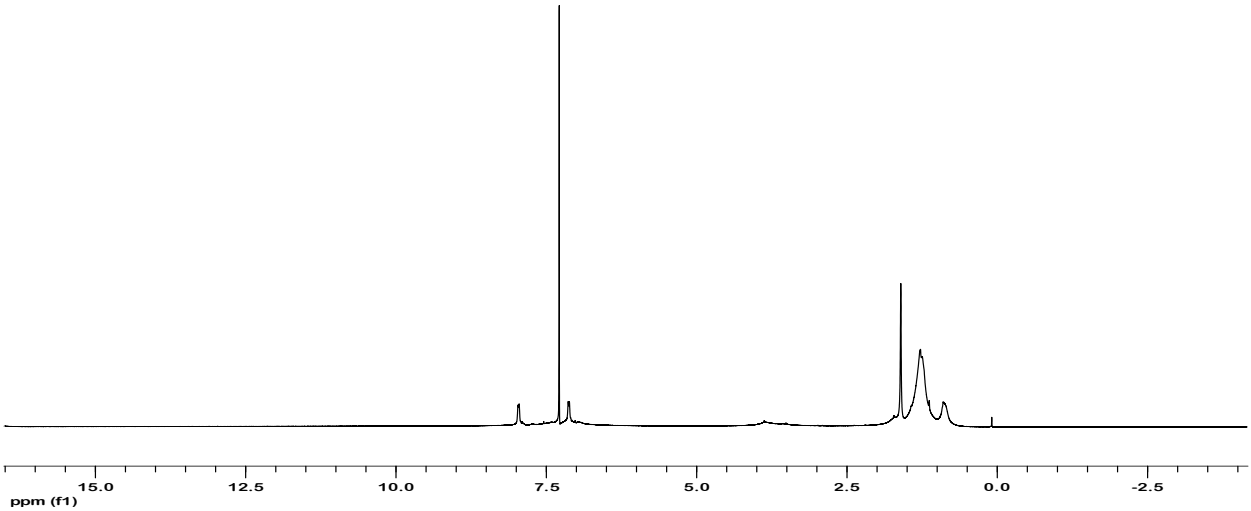


Appendix 43 : $^{1}$H-NMR spectrum of poly[2,3-bis(3-(dodecyloxy)phenyl)thieno[3,4-*b*]pyrazine-5,7-diyl-*alt*-thiophene-2,5-diyl] (**52'**).

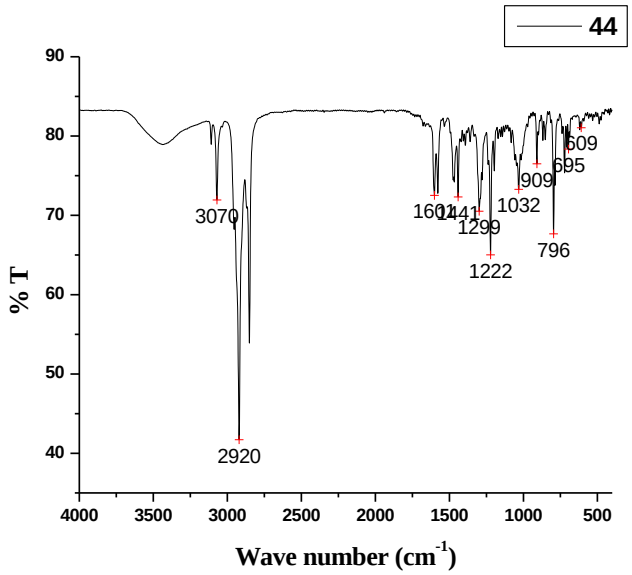


Appendix 44: IR spectrum of 2,3-bis(3-(dodecyloxy)phenyl)thieno[3,4-*b*]pyrazine (**44**).

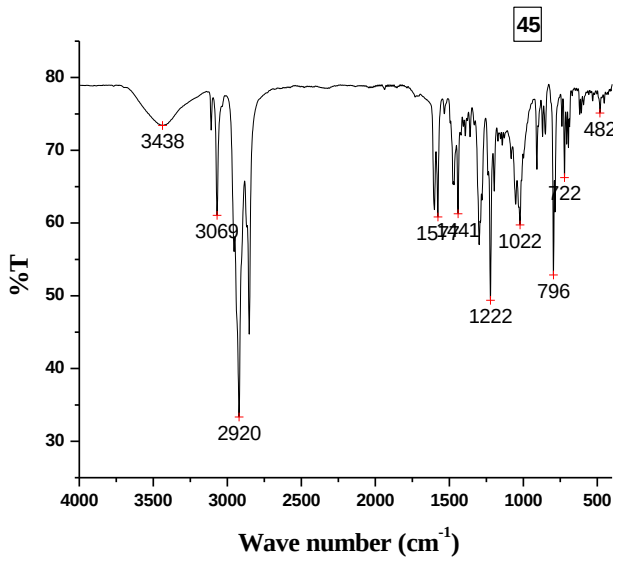


Appendix 45: IR spectrum of 2,3-bis(3-(decyloxy)phenyl)thieno[3,4-*b*]pyrazine (**45**).

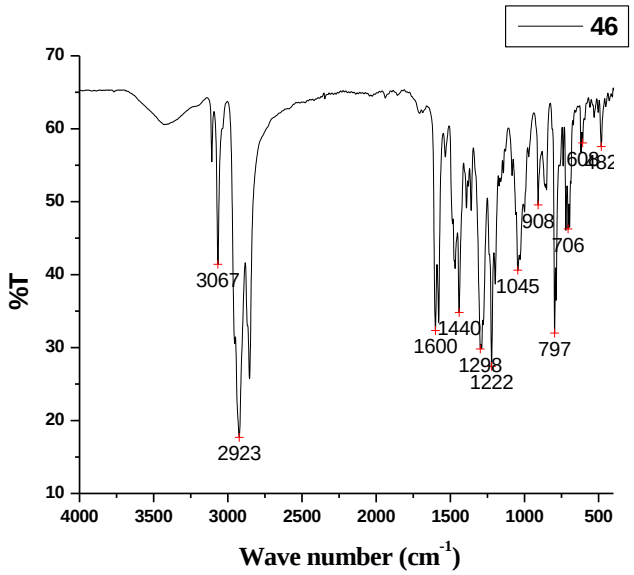


Appendix 46: IR spectrum of 2,3-bis (3-(octyloxy)phenyl)thieno[3,4-*b*]pyrazine (**46**).

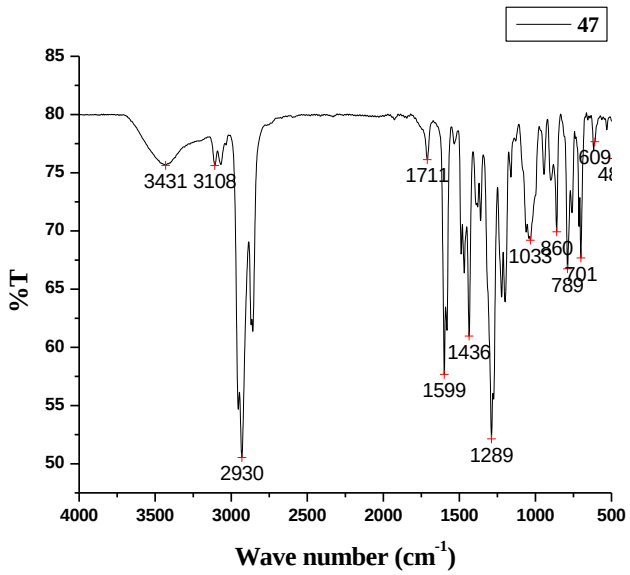


Appendix 47: IR spectrum of 2,3-bis(3-(hexyloxy)phenyl)thieno[3,4-*b*]pyrazine (**47**).

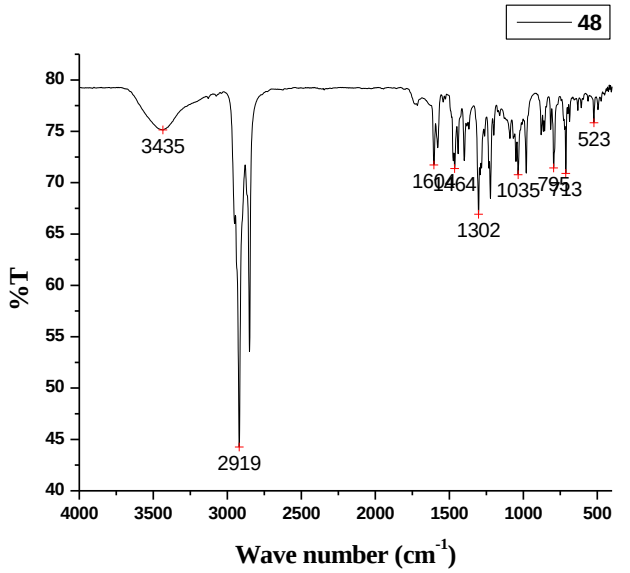


Appendix 48: IR spectrum of 5,7-dibromo-2,3-bis(3-(dodecyloxy)phenyl)thieno[3,4-*b*]pyrazine (**48**).

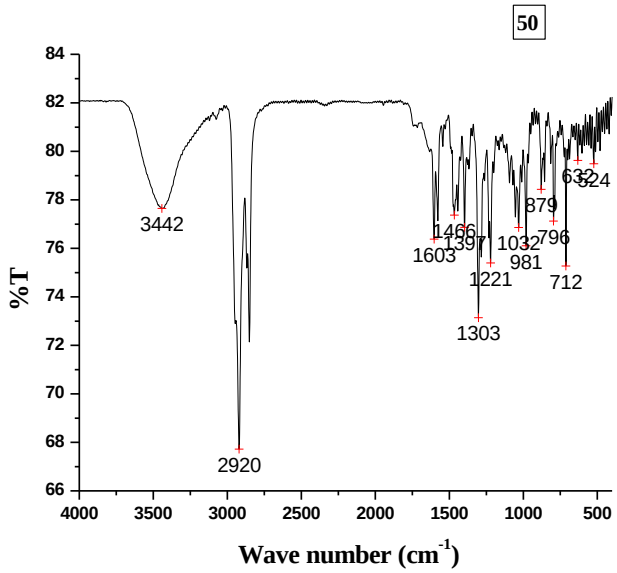


Appendix 49: IR spectrum of 5,7-dibromo-2,3-bis(3-(octyloxy)phenyl)thieno[3,4-*b*]pyrazine (**50**).

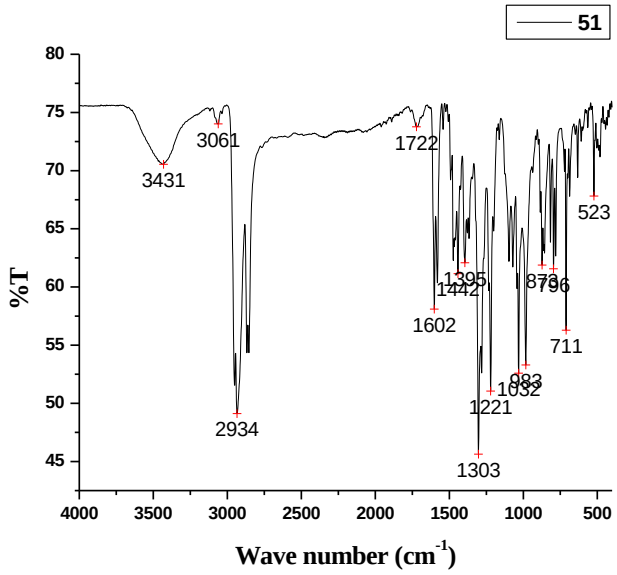


Appendix 50: IR spectrum of 5,7-dibromo-2,3-bis(3-(hexyloxy)phenyl)thieno[3,4-*b*]pyrazine (**51**).